

Structure and Dynamics of Hydrated Ions

Hitoshi Ohtaki*

Coordination Chemistry Laboratories, Institute for Molecular Science, Myodaiji-cho, Okazaki, 444 Japan

Tamás Radnai

Central Research Institute for Chemistry of the Hungarian Academy of Sciences, Budapest, P.O. Box 17, H-1525 Hungary

Received October 3, 1992 (Revised Manuscript Received January 9, 1993)

Contents

I. Introduction	1157	E. Rates of Water Substitution Reactions of Ions	1199
II. Methods for Determination of the Structure of Hydrated Ions	1158	V. Concluding Remarks	1199
A. Scattering Methods	1158	VI. References	1200
1. X-ray Diffraction (XD) Method	1159		
2. Neutron Diffraction (ND) Method	1160		
3. Electron Diffraction (ED) Method	1161		
4. Small-Angle X-ray (SAXS) and Neutron Scattering (SANS) Methods	1161		
5. Quasi-Elastic Neutron Scattering (QENS) Method	1161		
B. Spectroscopic Methods	1162		
1. Extended X-ray Absorption Fine Structure (EXAFS) and X-ray Absorption Near Edge Structure (XANES) Spectroscopies	1162		
2. Nuclear Magnetic Resonance (NMR) Spectroscopy	1163		
3. Mössbauer Spectroscopy	1165		
4. Infrared (IR), Raman, and Raleigh-Brillouin Spectroscopies	1165		
C. Computer Simulations	1165		
1. Molecular Dynamics Simulations (MD)	1166		
2. Monte Carlo Simulations (MC)	1167		
3. Molecular Mechanics Calculations	1168		
III. Structural Aspects of Ionic Hydration	1168		
A. First Hydration Shell of Ions	1169		
1. Monovalent Cations	1169		
2. Divalent Cations	1177		
3. Trivalent Cations	1181		
4. Tetravalent Cations	1186		
5. Halide Ions	1186		
6. Oxyanions	1188		
B. Second Hydration Shell of Ions	1189		
C. Influences of Ion-Pair and Complex Formation on Hydration of Ions	1193		
D. Influences of Temperature and Pressure on the Hydration Structure of Ions	1193		
IV. Dynamic Aspects of Ionic Hydration	1193		
A. Self-Diffusion Coefficients of Water Molecules and Ions	1193		
B. Rotational Correlation Time of Hydrated Water Molecules	1195		
C. Reorientational Time of Hydrated Water Molecules	1196		
D. Residence Time of Water Molecules in the First Hydration Shell of Ions	1197		

I. Introduction

Ionic hydration is one of the most attractive subjects to chemists, especially to those who are interested in reactions in aqueous solutions, and numerous studies on ionic hydration, i.e., the determination of hydration numbers of ions, rates of exchange of coordinated water molecules around ions, and interaction energies between ions and water molecules, have been carried out since Arrhenius.

In the time from the 1930s to the 1960s, various classical methods have been applied to investigate these problems. However, confusion in understandings of the structure of hydrated ions has been noticed in this period because of scattered data obtained by different methods and the lack of information of static and dynamic properties of water molecules coordinated to ions. When new methods were applied to the field of solution chemistry beginning in the 1970s, which became possible owing to the development of modern electronics and high-speed electronic computers, a steep increase in publication of interesting papers was seen in studies on the structures of hydrated ions, dynamics of coordinated water molecules, and interaction energetics of ions with water molecules.

A fairly large number of monographs¹⁻⁵ have so far been published concerning ionic hydration phenomena. Frequent reviews on hydration of ions have been published in various scientific journals. An excellent review on radii of ions in the hydrated species in solution by Marcus⁶ has appeared in this journal in 1988. Although some overlaps with Marcus' paper are not avoidable in the description of this review because the sizes of hydrated ions is the most fundamental element in studies of ionic hydration, we intend to pay more attention to other structural, as well as dynamic properties of hydrated ions. Most works quoted in this review were published in the last 10 years, but some important articles and monographs which were published in the last 2 decades are also referred to.

Since we focus our interest on the structure and dynamics of hydrated ions, results of thermodynamic measurements and quantum mechanical calculations for hydration of ions are generally not included in the discussion.



Hitoshi Ohtaki was born in Tokyo, Japan, in 1932. He graduated from Nagoya University in 1955 and obtained M.Sc. and Dr.Sc. degrees in 1957 and 1961, respectively, from Nagoya University. He became a Research Associate of the Tokyo Institute of Technology in 1959. He studied complex equilibria in solution under the supervision of Prof. L. G. Sillén, Royal Institute of Technology, Stockholm, Sweden, as a postdoctoral research fellow from 1961 to 1964. After returning to Japan, he was appointed Lecturer of Nagoya University in 1965 and promoted to Associate Professor in 1967. In 1970 he moved back to Tokyo Institute of Technology as an Associate Professor and then became a Full Professor in 1973. On the appointment in 1988 as Professor of the Institute for Molecular Science of the Okazaki National Research Institutes, he has served as the Director of the Coordination Chemistry Laboratories. He is also the Dean of the School of Mathematical and Physical Science of the Graduate University for Advanced Studies, of which the Institute for Molecular Science is one of the parent institutes. His research interests cover various areas of solution chemistry, especially structural chemistry of solution, including studies on structures of solvents, solvated ions and complexes existing in solution by means of X-ray diffraction; EXAFS and neutron diffraction methods have been occasionally employed as well. Thermodynamic studies on solution equilibria have long been another major area of his study. Molecular dynamics simulation studies on dissolution and nucleation processes of crystals have thrown a new sight for chemistry of ionic solvation and crystal growth from the dynamical viewpoint. He has published more than 170 research papers and a book on isotope chemistry (with H. Kakihana), on solution equilibria and kinetics (with M. Tanaka and S. Funahashi, which has been translated into Chinese) and one book on ionic hydration and two books on solution chemistry, all were written in Japanese. He was the editor of two English books and three Japanese books. He has translated two books (by V. Gutmann and by K. Burger) into Japanese. He was an author of chapters of more than 16 books. He has served as a visiting professor in Sweden, Austria, Thailand, and Philippines. His service has been extended on IUPAC bodies in various capacities since 1974. He is one of the three founders of Eurasia Conference on Chemical Sciences which was founded in 1988. He has received three awards: (Matsunaga Prize in 1976, Teijima Memorial Award in 1989 and Takei Prize in 1990).

II. Methods for Determination of the Structure of Hydrated Ions

The concept of the structure of hydrated ions largely depends on the methods of observation. We may classify the structure of hydrated ions into three categories depending on the methods of investigations as follows:

(1) Static structure, in which the structure is discussed on the time and space averaged ion-water interactions. Results obtained by X-ray and neutron diffraction methods are included in this category.

(2) Structure discussed on the basis of dynamic properties of coordinated water molecules. Results obtained by NMR measurements may be the typical case. When an ion is surrounded by coordinated water molecules which move much faster than the time of



Tamás Radnai was born in Budapest, Hungary, in 1949. He finished his university course in the Eötvös Loránd University, Budapest in 1973 with receiving an equivalent degree of M.Sc. He received Doctor University Degree (corresponding to Ph.D.) from the Eötvös Loránd University in 1977, and the academic title "Candidate for Chemical Science", a post-Ph.D. degree in 1991. He has held a continuous appointment at the Central Research Institute for Chemistry of the Hungarian Academy of Sciences in Budapest as a researcher. In the meantime, he was employed by the Ministry of Education, Science and Culture of Japan as a Research Associate, a Government Officer of Japan, from 1987 to 1989. He was invited to the Institute for Molecular Science as a Guest Foreign Associate Professor for one year from 1991. He has worked as a member of several international research groups in Italy and Germany. He is a senior fellow of the department of solution chemistry in the Central Research Institute for Chemistry of Hungarian Academy of Sciences. His main interest includes structural studies of electrolyte solutions by using diffraction methods, as well as computer simulations. He has published more than 40 research papers.

frequencies of the magnetic field employed in the NMR measurement, we observe that the ion has practically no hydrated water molecule in the coordination shell.

(3) Energetic considerations lead to the discrimination of strongly combined water molecules with ions from loosely interacting water molecules to ions. Spectroscopic investigations, including frequency measurements by Raman and IR spectroscopies and thermodynamic studies on ionic hydration give us information on water molecules strongly coordinated to ions. Information on water molecules weakly interacting to ions is always ambiguous. The borderline between coordinated and noncoordinated water molecules may be drawn on the basis of the kinetic energy kT or $2kT$ according to Bjerrum.⁷ However, it is obvious that the structure of hydrated ions discussed in terms of static and dynamic properties of water molecules coordinated also depends on interaction energies between ions and water molecules. Therefore, the classifications of the concept of ionic hydration is conventional.

A. Scattering Methods

The scattering methods may be separated into two. The one is the method to measure intensities of elastically scattered electrons, photons (X-ray), and neutrons by atoms and the other is the inelastic neutron scattering method. Since electrons and photons are so light, the quasi-elastic or inelastic scattering of them by atoms are not usually considered in the diffraction measurements as sources of structural information.

The former method provides the coordination number or frequency factor (n_{p-q}) of p-q atom pairs, the

distance between p and q atoms (r_{p-q}), and the temperature factor (b_{p-q}) of the atom pairs, which relates to the root mean square displacement (rmsd, l) of the atom pairs as $b = \langle l^2 \rangle / 2$, l being also obtainable from frequency measurements. The distance between atoms is a unique quantity obtained by the diffraction methods and it is hard to directly measure by other methods.

The electron scattering method is included in the elastic scattering method in the present classification. However, since electrons are easily absorbed by air, electron scattering measurements should be performed in vacuum, and liquid samples should be cooled to reduce the vapor pressure or kept in a cell with extremely thin windows. In most cases the former method is employed.

The hydrogen atom is not well detected by the electron and X-ray diffraction methods due to its small scattering power. Since the neutron diffraction method can provide the interatomic distances between an atom and hydrogen atoms (hydrogen atoms are replaced with deuterium atoms in usual cases), the determination of the average orientation of coordinated water molecules around the central ion is possible. The isotopic substitution method, applicable to cases in which suitable isotopes are available for the central ions in the measurements, provides detailed information on the structure of hydrated ions. The isomorphous substitution method in the X-ray diffraction measurements, in which ions with essentially the same size and charge but different atomic numbers are used, may be compared with the isotopic substitution method in the neutron diffraction measurements.

X-ray beams are scattered by electrons around atoms, while neutrons are diffracted by nuclei of atoms, and electron beams are scattered in the Coulombic field formed by both shell electrons and nuclei, and therefore, these methods are complementary.

It should be noted here that the distribution of electrons in an atom is not always spherical due to interatomic interactions. In the X-ray diffraction method a spherical electron cloud is assumed around a nucleus and the location of all electrons of an atom is considered to be at the center of the atom. The same assumptions are made in the electron diffraction measurement. However, the center of the nucleus of the atom due to interatomic interactions, and thus, interatomic distances of a given atom pair determined by these methods under similar experimental conditions are sometimes different.

The quasi-elastic and inelastic neutron scattering methods provide dynamic information predominantly of the translational motion of protons.

Brief descriptions for each method of measurements will be presented in the following sections.

1. X-ray Diffraction (XD) Method

Scattered intensities I are measured as a function of the momentum transfer, which is often denoted by k , s , q , or Q . In the X-ray diffraction method s is frequently used, where $s = (4\pi/\lambda)\sin \theta$ (2θ is the scattering angle and λ wavelength), and is also called a scattering variable or reciprocal space variable. However, in order to unify symbols with the same physical meaning, the letter k will be used for describing the quantity of the momentum transfer in all the scattering methods.

The intensities $I(k)$ are measured as a function of θ at a constant λ (the method is called as angular dispersive method) or as a function of λ or energy at a given θ (energy dispersive method). The former method is often used when the apparatus is equipped with a usual X-ray tube, from which a relatively strong characteristic X-ray is emitted. On the other hand, the latter is favorable when a strong white X-ray source such as synchrotron orbital radiation (SOR) is available. When sample solutions contain heavy atoms which emit fluorescence X-rays in the course of radiation with white X-rays, elimination of the fluorescence X-rays is sometimes difficult. X-rays emitted during the disturbing incoherent scattering process are more easily corrected in the former than in the latter. Therefore, for many electrolyte solutions which often contain atoms with various atomic numbers, the angular dispersive method is extensively employed. The energy dispersive method is used for the structural analysis of organic liquids in which atoms with relatively low atomic numbers are involved. Application of a multichannel detector tremendously shortens the measuring time in the energy dispersive method compared with the angular dispersive method.

Another way of classification is to separate the methods into the transmission method and the reflection method. The former allows the incident X-rays to pass through a sample cell, and the detector is placed behind the cell. On the other hand, reflected X-rays scattered at the surface of a liquid sample are measured in the latter technique. A free surface of liquids can be used as the reflection area in the latter method, so that corrections for a container of the sample are not necessary. On the other hand, the corrections are unavoidable in the former. The advantage of the transmission technique is that experimental conditions such as temperature and pressure can be changed over a much wider range than the reflection method can. Absorption, multiple scattering, and polarization of scattered X-rays should be corrected in both methods.

The scattering factor $f_M(k)$ of atom M is calculated from quantum mechanical theories.⁸ $f_M(0)$ is identical to the number of electrons in a given atom M . Sometimes an atomic group containing hydrogen atoms is regarded as one scattering unit with a group scattering factor $f_G(k)$. This treatment is convenient because it reduces the number of "atoms" in the system to be treated, but deviation from the assumed spherical distribution of electrons of the group should lead to errors in this treatment. For the X-ray analysis of pure water, however, the introduction of the group scattering factor for a water molecule does not result in significant errors in the structural information of intermolecular interactions of water.

The structure function $i(k)$ multiplied by k as a weight can be calculated from the observed intensities after subtraction of coherent and incoherent self-terms of scattering of atoms as follows:

$$ki(k) = k[I_{\text{abs}}(k) - \sum x_\alpha f_\alpha^2(k) - \sum x_\alpha I_\alpha^{\text{inc}}(k)] \quad (1)$$

where $I_{\text{abs}}(k)$ is the corrected intensity converted to the absolute unit, x_α the atomic fraction of atom or atom group α . $I_\alpha^{\text{inc}}(k)$ represents the intensity caused by the incoherent scattering by α . The summation extends over each α type independent scattering units in one stoichiometric volume. In practice the $ki(k)$ function

is often multiplied by an arbitrary chosen modification function or sharpening function $M(k)$ in order to minimize the truncation effect of the measured intensities at the Fourier transform of the intensity data.

The radial distribution function $D(r)$ is obtained by the Fourier transform of the structure function:

$$D(r) = 4\pi r^2 \rho_0 + 2r\pi^{-1} \int_0^{k_{\max}} ki(k)M(k) \sin(kr) dk \quad (2)$$

The function $D(r) - 4\pi r^2 \rho_0$ is conventionally used to emphasize peaks in the $D(r)$ function in the large r region.

Instead of the $D(r)$ function, the $G(r)$ and $H(r)$ functions are also often used:

$$G(r) = D(r)/(4\pi r^2 \rho_0) \quad (3)$$

$$H(r) = G(r) - 1 \quad (4)$$

Analysis of the structure function $ki(k)$ is usually carried out on the assumption of various models of molecular structures and molecular arrangements in a given system. In the space area constructed with short-range interatomic interactions, a discrete electron distribution can be reasonably assumed, while in the area of long-range interatomic interactions, ordering of atoms and molecules disappears and the region can be assumed to be constructed with a practically homogeneous electron distribution. Thus, the structure function may be separated into two parts, discrete $ki_d(k)$ and continuous $ki_c(k)$ parts:

$$ki(k) = ki_d(k) + ki_c(k) \quad (5)$$

The discrete part can be calculated by the formula derived by Debye:⁹

$$ki_d(k) = \sum x_\alpha \sum n_{\alpha\beta} f_\alpha(k) f_\beta(k) \Delta_0(kr_{\alpha\beta}, l_{\alpha\beta}) \quad (6)$$

and the continuous part can be formulated as

$$ki_c(k) = -4\pi\rho_0 \sum R_{\alpha\beta}^2 x_\alpha x_\beta f_\alpha(k) f_\beta(k) \Delta_1(kR_{\alpha\beta}, L_{\alpha\beta}) \quad (7)$$

where x_α and x_β represent the atomic fractions of α - and β -type particles, respectively, and Δ_m is associated with the $j_m(x)$ spherical Bessel function of the m th order

$$\Delta_m(x, y) = j_m(x) \exp\{-(y^2/2)k^2\} \quad (8)$$

The structure function includes three kinds of short-range structural parameters, the frequency factor or coordination number $n_{\alpha\beta}$, the average discrete interatomic distance $r_{\alpha\beta}$, and its root mean square deviation (rmsd) $l_{\alpha\beta}$ for the α - β atom pair, and moreover, two kinds of long-range parameters, $R_{\alpha\beta}$ for the boundary of the continuum distribution of electrons and $L_{\alpha\beta}$ for the sharpness at the boundary between discrete and continuum regions. Some authors prefer to use the temperature factors $b_{\alpha\beta} = l_{\alpha\beta}^2/2$ instead of $l_{\alpha\beta}$.

In the course of discussion of the hydration structure of ions, the values of $n_{\alpha\beta}$ and $r_{\alpha\beta}$ are most interesting. The $l_{\alpha\beta}$ values are important to consider the reliability of the estimated $n_{\alpha\beta}$ values, because the $n_{\alpha\beta}$ and $l_{\alpha\beta}$ values are strongly correlated. When we have information from frequency measurements by using Raman and IR spectroscopies, the $l_{\alpha\beta}$ values may be compared with the vibrational amplitude of a given α - β atom pair in the system. It should be noted here that the introduction of the continuum electron distribution for long-range interactions usually also improves the ac-

curacy of parameters in the short-range interactions, especially the $n_{\alpha\beta}$ values.

Interpretations of the radial distribution function and the structure function are usually started from a model of the first neighbors and the hydration number $n_{\alpha\beta}$ is estimated by eq 6 on the basis on the model proposed under the assumption that the shape of the peak in the radial distribution curve from which the $n_{\alpha\beta}$ value is evaluated is assumed to be Gaussian. This assumption is also applied to the data analysis in the neutron diffraction method.

The structural information for the second hydration shell is usually not clear when we directly analyze the radial distribution function and the structure function, because many interatomic interactions may overlap each other and it may be very difficult to extract the only peak due to the second hydration shell of ions.

In order to obtain more reliable structural information on the second hydration shell, the isomorphous substitution method is applied to some suitable systems, in which central metal ions with practically the same ionic radii but reasonably different atomic numbers are available. Details of the isomorphous substitution method will be given in the next section, because the method is compared with the isotopic substitution method in the neutron diffraction method.

2. Neutron Diffraction (ND) Method

The basic principles of the elastic neutron diffraction method are similar to those of the X-ray diffraction method except for some respects. One of the remarkable differences between the two methods is the difference in the scattering coefficients of atoms for X-rays and neutrons. In the former the scattering power of atoms is a function of k and depends on the number of electrons in the atom, i.e., the atomic number, and in the latter the scattering ability of atoms depends on the composition of the atomic nuclei and thus varied with isotopes of a given element.

Essentially two different techniques are employed for neutron scattering experiments. In one technique neutron beams emitted from a reactor are monochromatized by using the Bragg reflection. In the other pulsed neutrons are used and the time of flight after the production of pulsed neutrons is measured to determine energies of incident neutrons. The latter is called the "time-of-flight (TOF)" method.

An important advantage in the neutron diffraction method over the X-ray diffraction technique is the application of the isotopic substitution method, in which samples with the same atomic composition but different isotopes for a particular element are prepared and the difference in scattering intensities or $G(r)$ functions is used for the structural analysis of the sample solutions, in which no other interatomic pair correlations are included except for the functions related to the isotopic elements. For instance, in an MX aqueous solution the following 10 atomic pairs should be included in the $G(r)$ function:

$$G(r) = aG_{M-O}(r) + bG_{M-H}(r) + cG_{X-O}(r) + dG_{X-H}(r) + eG_{M-X}(r) + fG_{M-M}(r) + gG_{X-X}(r) + hG_{O-H}(r) + iG_{O-O}(r) + jG_{H-H}(r) \quad (9)$$

Coefficients a-j are either a function of scattering factors for X-rays or scattering lengths for neutrons. When

the isotopic substitution method is applied, the difference $G(r)$ function, $\Delta G(r)$, of two identical solutions except for the isotopic composition of, say, M includes the only terms containing atom pairs with M:

$$\Delta G(r) = (a - a')G_{M-O}(r) + (b - b')G_{M-H}(r) + (e - e')G_{M-X}(r) + (f - f')G_{M-M}(r) \quad (10)$$

In solutions where no polynuclear complex is formed, the last term drops in the structural analysis of ionic hydration in solution, and thus the $\Delta G(r)$ function contains only three terms. When one discusses the structure in the first coordination sphere in a solution in which M-X ion pairs do not practically exist, the $\Delta G(r)$ function becomes very simple.

Readers should notice that suitable isotopes available for measurements of difference radial distribution functions are rather limited, because the isotopes should have reasonably large differences in the scattering lengths among them. Combinations of ^1H - ^2H (D), ^6Li - ^7Li , ^{35}Cl - ^{37}Cl , ^{40}Ca - ^{44}Ca , ^{54}Fe - ^{56}Fe - ^{57}Fe , ^{58}Ni - ^{60}Ni - ^{62}Ni - ^{64}Ni isotopes are often employed, but for other elements the isotopic substitution method may be hardly applicable. For the ^1H and D atoms corrections for inelastic collisions between the atoms and neutrons must be done.

A similar method can be applied to the X-ray diffraction method by using ions with isomorphous structures for suitable cases. In this case the atoms have different atomic numbers, but the structure around the relevant atoms is expected or known to be the same, and then, the difference in the radial distribution functions between the two sample solutions is calculated to eliminate the contribution of other atom pairs except pairs related to the isomorphous elements. However, the application of the isomorphous substitution method in the X-ray diffraction method is much more limited than the isotopic substitution method as anticipated, because the atoms or ions should have practically the same radius or the difference in the radii should be less than 2 pm. The Y^{3+} - Er^{3+} pair has been used in the hydration structural analysis of the ions.^{10,11} Similarly, the CrO_4^{2-} - SeO_4^{2-} pair was recently applied in a combined study of X-ray with neutron methods.²⁶⁷ Some other pairs such as Pt(II) - Pd(II) , Pt(IV) - Pd(IV) , MoO_4^{2-} - WO_4^{2-} , etc. may be used, but less studies have been done so far.

Another advantage in neutron scattering measurements compared with X-ray scattering measurements is the ability to determine the M-H (or M-D) and X-H (or X-D) bond lengths. Since the M-O and X-O bond lengths are determinable by both X-ray and neutron diffraction measurements, the tilt angle of hydrated water molecules in the first coordination sphere can be measured by the neutron diffraction method.

Uncertainty of experimental intensity data in neutron diffraction measurements is usually more pronounced than that in the X-ray diffraction method.

Some reviews have previously been published for structural data obtained by the neutron diffraction method.^{5,6,12-14}

3. Electron Diffraction (ED) Method

Electrons are scattered both by electrons and nuclei of atoms due to Coulombic interactions. The accessible range in the momentum transfer in the course of electron scattering is usually much wider than that

achieved in the course of X-ray scattering measurements. For instance, 68 keV electron beams corresponding to the wavelength of 5 pm cover the maximum k range of 0.25–0.30 pm^{-1} , in contrast to the upper limit of $k_{\text{max}} = 0.10$ (when Cu $K\alpha$ line is used) to 0.17 pm^{-1} (Mo $K\alpha$) in the X-ray diffraction method and may be compared with that in the neutron diffraction method. A disadvantage in the electron diffraction method is that measurements must be carried out in vacuum, and this requirement is rather fatal for studies of liquids and solutions, although this serious problem may be partly avoided by using solutions with extremely low vapor pressure and by application of special techniques with short measuring times.

Since the scattering lengths of electrons, X-rays, and neutrons are different for a given atom, one can separate the total pair correlation function into contributions of each atom pair by combining electron, X-ray, and neutron diffraction methods for one sample.¹⁵

4. Small-Angle X-ray (SAXS) and Neutron Scattering (SANS) Methods

Small-angle scattering X-ray and neutron diffraction methods are essentially similar, in principle, to the scattering methods in the large-angle range described in previous sections, but they can provide information of the long-range structure of large molecules and clusters. Since the covered k range is very short ($k_{\text{max}} \approx$ several thousands per picometer), special measurement techniques are required. The SAXS-SANS techniques usually cover the region of distances well above 5–10 nm in the r space, and therefore, they should be distinguished from the "low-angle scattering", which has a somewhat confusing name and relates to distances comparable to those observed by the large-angle diffraction methods. In electrolyte solutions containing relatively simple ions and complexes, scattering data in a low-angle region (a small k range) sometimes show a small peak in the structure function. Some authors suggested that the peak position corresponds to the interionic distance arising from a quasi-lattice arrangement of ions in solution (super-arrangement).^{16,17} The distance between ions R_c is given approximately as

$$R_c = 7.73/k_m \quad (11)$$

where k_m denotes the k value of the position of the peak maximum. The distance thus calculated usually agrees with the size of the stoichiometric volume containing one cation in solution in which $[\text{MX}_n]^{(m-n)+}$ type complexes are formed. However, in aqueous solutions containing only hydrated ions, observation of such a peak in the $ki(k)$ function is not clear, and moreover, alternative explanations can also be given.

5. Quasi-Elastic Neutron Scattering (QENS) Method

Intensity measurements of incoherent scattering of neutrons with protons, which provide a good probe due to its largest incoherent scattering contribution to the total scattering pattern of an aqueous solution, can elucidate dynamic properties of protons in aqueous solutions.

Intensities of scattered neutrons over a wide range of energy or frequency of a neutron beam ω at various k 's are measured. Under a special condition where the time scale of interactions between neutrons and ions is long enough, i.e., both the frequency of neutrons ω and

k are small, the theory assumes that the translational and rotational diffusion can be decoupled. In this case the incoherent space-time correlation function for the hydrogen atoms, $G_{\text{H}}^{\text{s}}(r, t)$, can be expressed in terms of the translational diffusion coefficient D for the hydrogen atoms as

$$G_{\text{H}}^{\text{s}}(r, t) = (4Dt)^{-3/2} \exp(-r^2/4Dt) \quad (12)$$

and the corresponding scattering function $H_{\text{H}}^{\text{s}}(k, \omega)$ is described as

$$H_{\text{H}}^{\text{s}}(k, \omega) = \frac{1}{\pi} \frac{Dk^2}{(Dk^2)^2 + \omega^2} \quad (13)$$

The D value obtained from the above equations for hydrogen atoms in water corresponds to the average diffusion coefficient of hydrogen atoms provided that the exchange rate of protons around an ion is fast; in other words, the bonding time τ_{RES} (called also as mean lifetime or residence time) of the protons in the hydration shell of an ion is much smaller than the characteristic observation time τ_{meas} of neutron scattering experiment (approximately 5×10^{-9} s)

$$\tau_{\text{RES}} \ll \tau_{\text{meas}} \quad (14)$$

Equation 12 holds for many aqueous ionic solutions, and the diffusion coefficient of ions can thus be determined, the value being compared with those determined by usual diffusion methods.

In the slow exchange limit, however, the residence time of protons around an ion is much longer than the observation time τ_{RES}

$$\tau_{\text{RES}} \gg \tau_{\text{meas}} \quad (15)$$

and the scattering function can be decomposed into two Lorentzian type functions

$$H_{\text{H}}^{\text{s}}(k, \omega) = \frac{1}{\pi} \left[c_{\text{b}} \frac{D_{\text{b}} k^2}{(D_{\text{b}} k^2)^2 + \omega^2} + c_{\text{t}} \frac{D_{\text{t}} k^2}{(D_{\text{t}} k^2)^2 + \omega^2} \right] \quad (16)$$

where D_{b} and D_{t} are the diffusion coefficients of protons in the hydrated water molecules (bound) and in the bulk, respectively, and c_{b} and c_{t} are constants characterizing the ratio of the population of the two kinds of protons. The average diffusion coefficient D_{H} is thus obtained as

$$D_{\text{H}} = c_{\text{b}} D_{\text{b}} + c_{\text{t}} D_{\text{t}} \quad (17)$$

It is worth noting that the τ_{RES} value of oxygen atoms in water is usually the same order of magnitude as for the protons. Exceptions are observed for the Cr^{3+} and other inert cations.

The quasi-elastic neutron scattering method has recently been developed rather rapidly. However, only partial reviews of the results have been published until now.^{18,19}

B. Spectroscopic Methods

Various spectroscopic methods have been employed in studies of ionic hydration. Among them, X-ray absorption spectroscopies have been developed very quickly in recent decades. The extended X-ray absorption fine structure (EXAFS) method is used for the determination of short-range intermolecular interactions and the X-ray absorption near edge structure (XANES) method is often employed to discuss the

electronic structure of the relevant element. NMR measurements have been used for determining the hydration structure of various ions, as well as structures of complexes in solutions. The method is preferably used for studies on dynamic properties of ions and hydrated water molecules rather than the static structure of hydrated ions after the appearance of the X-ray diffraction and X-ray absorption methods. Infrared and Raman spectroscopies are the traditional methods which have still been widely used in aqueous and nonaqueous solutions. Application of the Mössbauer spectroscopy to structural measurements of solutions is restricted to some special cases which contain Mössbauer active elements, but it is useful for studies on ionic hydration in solids, because the method can show different spectra for one element with different oxidation states. However, the method is not applicable to usual solutions without settling them by quick freezing.

1. Extended X-ray Absorption Fine Structure (EXAFS) and X-ray Absorption Near Edge Structure (XANES) Spectroscopies

Both methods are connected with X-ray absorption by atoms which are affected by their environmental structures. Separation of the EXAFS part from the XANES one is rather arbitrary.

Both white X-rays and a monochromatized X-ray beam are used simultaneously. A detector scans the spectrum over a wide-angle range to cover a reasonable k range to the Fourier transform of the EXAFS spectra. The use of synchrotron orbital radiations (SOR) is the most effective for the measurements, but several laboratory-scale instruments have also been developed. The EXAFS method has a large advantage over a usual X-ray diffraction method because of its high selectivity of the central elements and its high sensitivity to be able to use sample solutions with fairly low concentrations which are not possible to measure by the X-ray diffraction method in which scattered intensities from solvents hide information from the solutes. Since long-range interatomic interactions are practically eliminated from EXAFS spectra, only the local structure around X-ray absorbing atoms can be determined. Disadvantages in the EXAFS method are the necessity for the phase-shift correction and less reliability for frequency factors (coordination numbers) because the latter ones strongly correlate to the Debye-Waller factor, which corresponds to the temperature factor in the X-ray diffraction method.

If the multiple scattering of back-scattered electrons from surrounding atoms of the X-ray absorbing central atom is neglected, the ratio $\chi(E)$ of the incident beam and the beam after passing through a sample at a given energy E is described as follows:

$$\chi(E) = [\mu(E) - \mu_0(E)] / \mu_0(E) \quad (18)$$

where μ and μ_0 denote the measured intensity and the intensity of the incident beam, respectively. The energy dependence of χ can be converted to the dependence on the photon wave vector k .

Under the plane-wave approximation, the EXAFS interference function for the photoexcitation of an atomic species α is given by a superposition of contributions from all back-scattering atoms β surrounding α , and each contribution is expressed in the sinusoidal

form with a frequency which is a function of the interatomic distance $r_{\alpha\beta}$, the number of interactions (atom pairs) $n_{\alpha\beta}$, and the total phase shift $\phi_{\alpha\beta}(k)$. The $\chi(E)$ function is related to the pair-correlation function $g_{\alpha\beta}(r)$ through eq 19 as follows:

$$k\chi(k) = 4\pi\rho_0 S_\alpha(k) \sum x_\alpha F_\alpha(k) g_{\alpha\beta}(r) \times \exp(-2r/\lambda) \sin[2kr + \phi_{\alpha\beta}(k)] dr \quad (19)$$

where the summation runs over each species present in the system. χ_α is the atomic fraction of the α -type atoms, ρ_0 the bulk electron density, $F_\alpha(k)$ the absolute value of the complex scattering amplitude of atom α , $\phi_{\alpha\beta}(k)$ the total phase shift, λ the mean free path of the photoelectrons at k , and $S_\alpha(k)$ a phenomenological term which accounts for inelastic scattering. Introducing structural parameters of interatomic distance $r_{\alpha\beta}$, the coordination number $n_{\alpha\beta}$, and the root mean square displacement $l_{\alpha\beta}$ into eq 19, we obtain

$$k\chi(k) = S_\alpha \sum F_\alpha(k) n_{\alpha\beta} r_{\alpha\beta}^{-2} \exp(-2r_{\alpha\beta}\lambda^{-1}) \times \exp(-2k^2 l_{\alpha\beta}^2) \sin[2kr_{\alpha\beta} + \phi_{\alpha\beta}(k)] \quad (20)$$

The parameter values are calculated by a least-squares fitting procedure. The values of S_α , F_α , and $\phi_{\alpha\beta}$ should be evaluated in advance by separate experiments or by an assumption. The value of $\mu_0(E)$ is also obtained in the course of the fitting process as an adjustable parameter. Therefore, we usually use a crystal with a known structure as a reference substance to determine some of the parameter values. When a central atom is coordinated with more than one kind of ligand atoms, the situation becomes more complicated.

The Fourier transferred EXAFS spectra usually contain many ripples arising from the truncation of the EXAFS k -space spectra at a finite value, and thus, a window function is usually introduced to cut off a main peak in the r space from Fourier transform (corresponding to the radial distribution curve), and the least-squares procedure is carried out for the extracted EXAFS k -space spectrum to obtain structural parameters related to the interatomic interactions.

The principles of the method are given in a review by Lee et al.²⁰ and some recent results are summarized by Magini et al.⁵

2. Nuclear Magnetic Resonance (NMR) Spectroscopy

NMR spectroscopy is a very useful method for both studying the static and dynamic structures of hydrated ions. However, explanations of NMR spectra in terms of structures of species in solution are not straightforward compared with those of radial distribution functions obtained by X-ray, neutron, and electron diffraction methods and EXAFS spectra except for simple cases. The time scale accessible in NMR measurements should be longer than 10^{-9} s, because we can use frequencies of the magnetic field of some 100 MHz. Several effects are included in chemical shifts, and the separation of these factors in order to extract structural or dynamic properties from the spectra are usually complicated, especially when we discuss the behavior of protons in aqueous solutions. The static and dynamic behavior of water molecules in the coordination sphere can be separated from that in the bulk when we measure the NMR spectra of oxygen atoms (^{17}O), but still deconvolution of a single peak into the components is

necessary except for limited cases containing inert ions such as Cr^{3+} .

Principles of NMR measurements for aqueous electrolyte solutions and results obtained have been reviewed by various authors.^{3,21-32}

Interactions between the total spin I of an atomic nucleus in a solution system and the outer magnetic field H_0 applied result in a magnetic resonance spectra in which $2I + 1$ different energy levels are separated by

$$h\omega_L = h\gamma H_0 \quad (21)$$

where γ represents the gyromagnetic ratio of the nucleus and ω_L stands for the Larmor frequency. In a solution there are many spins which interact with the local electric and magnetic fields generated by the nuclear spins and electric charges of the other atoms. The most important interactions are those between dipoles, between an outer electric field and an electric quadrupole of a nucleus, and between the spin of an atomic nucleus and the magnetic field generated by the rotation of an adjacent molecule. The Hamiltonian is given as the sum of the Zeeman Hamiltonians of the eigenstates and other types of "lattice" Hamiltonians. Finally, the Hamiltonian H_c is described as

$$H_c = - \sum \int d\mathbf{r} H(\mathbf{r}) \mu_\alpha^M \delta(\mathbf{r} - \mathbf{r}_\alpha) \quad (22)$$

where $H(\mathbf{r})$ is the external magnetic field and μ_α^M is the magnetic moment of an α type nucleus, and thus, eq 22 expresses the coupling between the applied magnetic field and the system. By using this Hamiltonian, the spectral densities and time-correlation functions can be calculated.

The experimental information is obtained from the position and the shape of the resonance maxima on NMR spectra. Moreover, the motion of molecules and ions can be monitored through the selection of the resonances characteristic to the nucleus in question. It is worth noting that the primary information is always the effect of the environment on the motion of the spins, and all other dynamic properties are deduced from it. The following properties are usually derived from NMR experiments:

(1) From the change in the *chemical shift* of peak positions, the change in the environment of the NMR nucleus, i.e., the coordination structure of the probe atom, can be estimated. In most cases the change in the coordination number causes a fairly large difference in the chemical shifts of a given central atom. A detailed analysis of chemical shifts of proton NMR spectra can elucidate ion-water interactions in solution in spite of proton exchange reactions much faster than water exchange reactions in aqueous solution on the NMR time scale. ^{17}O NMR spectra are often measured in order to discuss the structure and dynamic properties of hydrated water molecules.

(2) *Coordination numbers*, which are usually called *dynamic hydration numbers*, are determined under the area of the resonance peaks. In case of very inert ions such as Cr^{3+} , Be^{2+} , and Al^{3+} , two ^{17}O peaks, arising from the hydrated water and bulk water, can be separated and the areas under the two peaks are characteristic of the ratio of the two kinds of water molecules. Despite the fact that the accuracy of the area integration is sometimes very limited (a high concentration of electrolytes and good separation of the shifts are required), reasonable results can be obtained for the coordination

structure of hydrated ions. Various technical modifications have been applied to derive structural and dynamic properties from measurements of relevant NMR ions, protons, and ^{17}O atoms.³³⁻³⁵ Separation of peaks is usually tried by cooling down the sample solution to low temperatures by lowering the solvent substitution rate constants of the sample solutions. However, since we use aqueous solutions, only a limited range of temperature decrease is possible. Sometimes organic solvents are added to aqueous sample solutions assuming that the hydration structure is not varied by the addition of the organic solvents, but the freezing point of the solutions becomes low enough to separate the rate of solvent substitution reactions in the coordination sphere and in the bulk. Of course, preferential solvation of the relevant ions, if it occurs, can become a source of errors.

When dia- and paramagnetic ions are mixed, the residence time of surrounding molecules of the latter one is significantly shorter than that around the diamagnetic ion.

(3) *Spin-spin relaxation times and diffusion coefficients* can be derived because the width of the peaks in NMR spectra is a function of rates of molecular motions, and therefore, dynamic properties of the atom showing the NMR peak can be elucidated from the analysis of the peak shape.

In the case where the decay of the $C_{\mu\mu}(t)$ autocorrelation function with time is expressed in terms of an exponential function, the translational diffusion coefficient D_t and spin-spin relaxation times T_2 can be described by a Lorentzian law

$$C_{\mu\mu}(t) = C_{\mu\mu}(0) \exp\left[\frac{t}{T_2} - \frac{\gamma^2 g^2 D_t^3}{12}\right] \quad (23)$$

where g is a field gradient and γ the gyromagnetic ratio. Two measurements have to be carried out (with and without the presence of field gradient g), and from the comparison the diffusion coefficient can be determined. In most cases the so called spin-echo method is used.

In comparison between the spin-spin relaxation time measurement and quasi-elastic neutron diffraction measurements for investigating dynamic properties of ions and water molecules, the former has an advantage that the accessible diffusion coefficients are smaller than $10^{-9} \text{ cm}^2 \text{ s}^{-1}$. In the latter the limit of the diffusion coefficient measurable is in the order of $10^{-7} \text{ cm}^2 \text{ s}^{-1}$. The former method can cover the interaction time scale of $<10^{-4} \text{ s}$, much longer than $<10^{-9} \text{ s}$ in the latter. A drawback of the spin-spin relaxation method is that T_2 itself must not be too short, and therefore, only a limited set of nuclei with the spin of $1/2$ can be used (^1H , ^{19}F , ^{31}P , etc.). Moreover, the diffusion coefficient is determinable when the diffusion of the molecules or ions can be described in terms of a single translational coefficient.

(4) *Spin-lattice relaxation.* Another relaxation time T_1 can be assigned to the response for weakly interacting spins of a kind of nuclei in a solution with the "lattice" represented by the solution in a strong magnetic field. In the simplest case, the spin I is $1/2$ and the lattice is constructed from a random magnetic field, the corresponding autocorrelation function being exponential and the decay being characterized by the spin-lattice correlation time τ_c . The longitudinal magnetization decays, under some conditions, as an exponential

function of time with a characteristic T_1 spin-lattice relaxation time, which relates to the correlation time as

$$T_1^{-1} = 2\gamma^2 H_x^2 \tau_c \quad (24)$$

where H_x denotes the strength of the random magnetic field. When the spin is larger than $1/2$, the exponential function becomes a sum of exponential functions. In real solutions H_x is not expressed in terms of the random magnetic field and the quantity becomes more complicated, and therefore, the extraction of the parameter τ_c is difficult. Calculations with preliminary models and a series of measurements are usually required for data analyses. The relaxation mechanism is often separated into a few typical relaxation mechanisms of different types of molecular motions such as translational and rotational motions. However, the separation is not simple, especially in the case of proton spin-lattice relaxation measurements. The relaxation via quadrupole interactions gives information similar to that by the depolarized Raman scattering of light, and thus, it is sensitive to the rotational motions. An example of the application of this method is the determination of the anisotropic rotational diffusion with two different diffusion constants of parallel D_{\parallel} and perpendicular D_{\perp} to the symmetry axis.

The spin-lattice relaxation via spin-rotation mechanisms is also important for the determination of rotational motions of molecules. Since the rotational mechanism is different from that of the others discussed above, the relaxation time thus measured is different from the values determined by other methods. Moreover, the efficiency depends on the spin of nuclei. The ^{13}C nucleus has a large efficiency in this measurement. It may be worth noting that there are some other relaxation mechanisms, but they are not included here because they are less important for aqueous solutions.

(5) *Application of NMR measurement to the elucidation of solvent substitution reaction mechanisms.* Since water molecules bound to ions to form the hydration shell have different relaxation times from that in the bulk solvent, attempts have been made to extract information about kinetics of substitution reactions of water molecules between the hydrate shell and the bulk from NMR data.

The rate constants for the solvent substitution reactions between the hydration shell and the bulk are measured by using a high-pressure NMR technique at various temperatures and pressures. From the variation of the rates with temperature the entropy of activation ΔS^{\ddagger} as well as the enthalpy of activation ΔH^{\ddagger} of the reaction are determined. The activation volume ΔV^{\ddagger} is determined from the variation of the rates with pressure. A simple assumption has been introduced for the exchange mechanisms, i.e., the reaction occurs *associatively* when ΔS^{\ddagger} or ΔV^{\ddagger} is negative, while the mechanism of reactions with positive ΔS^{\ddagger} and ΔV^{\ddagger} is *dissociative*. The temperature variation for the reaction rates can be observed by usual methods at different temperatures, and thus, the entropy of activation ΔS^{\ddagger} can be measured by many other experimental methods. However, the specialists believe²⁴ that the determination of the sign of ΔV^{\ddagger} is more reliable than that of ΔS^{\ddagger} because a long extrapolation is needed in the latter.

The distinction of the reaction mechanisms upon the sign of the activation volume thus measured has been done under a very simple assumption that in the

associative mechanism a water molecule in the bulk enters in the coordination sphere so that the entropy in the activation state of the complex may decrease and the volume of the complex may be smaller than the sum of the volume of the original hydrated ion plus the volume of one water molecule in the bulk, provided that no significant bond length variation within the complex occurs at the activation process. It is obvious that the assumption is too simple to explain the reaction mechanism from the signs of ΔS^* and ΔV^* , because in the associative reaction mechanism the coordination number of the central ion increases, and thus, it is expected that the bond length between the central atom and the ligand atom increases which may cause the expansion of the volume of the activated complex, while the reverse may be true for the dissociation mechanism. Therefore, further discussions with more careful considerations about changes in the bond length in activated complexes, and thus, volume changes at the activation step, may be needed to interpret the thermodynamic quantities in the solvent substitution reactions, as well as any other ligand substitution reactions.

3. Mössbauer Spectroscopy

Mössbauer spectroscopy is based on a recoilless nuclear γ -ray resonance phenomenon of atomic nuclei. The formal description of the Mössbauer scattering is essentially the same as that for the X-ray scattering, provided that the scattering factor $f_a(k)$ is characteristic to the γ -scattering substitutes. The Mössbauer effect is mostly applied to systems containing ^{57}Fe and ^{119}Sn , and ^{99}Ru , ^{121}Sb , ^{125}Te , ^{127}I , ^{129}I , ^{129}Xe , ^{131}Xe , ^{151}Eu , ^{153}Eu , ^{191}Ir , ^{193}Ir , ^{197}Au , and ^{237}Np are also used for Mössbauer spectroscopic measurements.

Energy changes due to energy transitions are usually called the isomer shift, chemical isomer shift, or center shift, and they are influenced by the electron distribution around a nucleus, and thus, the local environment of the excited atom or ion. Moreover, since the size of the excited nucleus may be different in the excited state than in the ground state, the shift is related to the oxidation state of the ion. These two facts provide a sensitive tool for investigating the structural changes around an ion. However, the Mössbauer spectroscopy can be used only for solids where the whole crystal lattice absorbs the energy and the momentum of the recoil. Therefore, the use of this method is impossible, in principle, for liquids without quenching liquids and solutions. Some reports have been published that the Mössbauer effect is observable for solutions which are absorbed on porous glasses. However, a question remains if no structural change occurs when the bulk solution is absorbed on the glass, or if the quenched solution preserves its structure same as that at room temperature.

4. Infrared (IR), Raman, and Raleigh-Brillouin Spectroscopies

Infrared and Raman spectroscopies played a pioneering role in structural and dynamic investigations at an early stage of investigation of solutions and they became dominant in solution chemistry in the 1960s and 1970s. Even now their role in solution chemistry is very important, of course. Methods such as the Brillouin scattering spectroscopy can also be used for

investigating molecular coagulation in mixed solutions. Detailed studies and reviews on the results are referred to the literature.^{3,32,36}

The common feature of the spectroscopic methods of this group is that electromagnetic waves which are absorbed or scattered have a long wavelength compared to molecular dimensions. They interact with the electric field of ions and molecules and the interaction Hamiltonian can be written as

$$H_c = - \int d\mathbf{r} [E(\mathbf{r},t)\mu(\mathbf{r},t) + (1/2)E(\mathbf{r},t)a(\mathbf{r},t)E(\mathbf{r},t) + o(\mathbf{r},t)] \quad (25)$$

where $E(\mathbf{r},t)$ is the electric field vector of the incident electromagnetic field, $\mu(\mathbf{r})$ the dipole moment at position \mathbf{r} in the liquid, $a(\mathbf{r},t)$ the polarizability tensor, $a(\mathbf{r},t)E(\mathbf{r},t)$ the induced polarizability, and $o(\mathbf{r},t)$ the higher order terms, which can be ignored.

If we assume that only the permanent dipoles exist in the liquid, the dynamical variable may be given by

$$\mu(\mathbf{r}) = \sum \mu_\alpha \delta(\mathbf{r} - \mathbf{r}_\alpha) \quad (26)$$

where μ_α is the dipole moment of the α -type particle. The absorption of the electromagnetic radiation is proportional to the spectral density $C_{\mu\mu}(\omega)$, and the related autocorrelation function is

$$C_{\mu\mu}(t) = (1/N) \langle \sum \mu_\alpha(0) \mu_\beta(t) \rangle \quad (27)$$

If the electric field can be written in the form of $E_0 \cos \omega t$, then

$$\mu = \mu_0 + \sum \mu_n \cos \omega_n t \quad (28)$$

where ω_n are the normal frequencies. Dielectric absorption arises from the contribution of μ_0 , while IR absorption is originated from changes in μ brought by vibration or rotation. It can be shown that the second term of the right hand side of eq 28 is connected to the Raleigh-Brillouin and Raman scattering. In the simple case when the polarizability is scalar, the polarization P can be written as

$$P = E\alpha_0 \cos \omega t + (1/2)E_0 \sum \alpha_n [\cos(\omega - \omega_n)t + \cos(\omega + \omega_n)t] \quad (29)$$

where α_0 is the static polarizability. The first term of the right hand side of eq 29 corresponds to the origin of the Raleigh scattering, and the next two terms produce the Raman lines of the spectrum. The condition is that the rotation or vibration of a molecule changes the polarizability of the molecule. In case of Brillouin scattering, the situation is more complicated, because the normal frequencies are associated with acoustic phonons in the liquid.

C. Computer Simulations

Computer simulations are theoretical approaches to elucidate structure and dynamics of molecules and molecular ensembles in the condensed phases, as well as in the gas phase. The simulations may be classified into three categories: molecular dynamics (MD), Monte Carlo (MC) simulations, and molecular mechanics (MM) calculations. The first one can describe both structural and dynamic properties of a system, because the simulation includes time in the treatment, while the latter two have no time-dependent parameter in the course of the calculations, and thus, they give only

structural or energetic information. Molecular dynamics and Monte Carlo simulations are usually applied to systems containing a number of molecules, which may be assumed to be similar to bulk systems. Special techniques are usually used in the calculation, which include the periodical boundary condition, in which a small system containing a limited number of ions and molecules is repeatedly set up to build an infinite system. Such a periodical boundary condition is accepted in crystals, but an assumption that the condition is acceptable even in liquids and solutions, provided that the basic system (basic cell) is large enough in which long-range interatomic interactions are reasonably assumed to have no correlation, is introduced. On the other hand, the molecular mechanics simulation is a calculation usually applied to an isolated molecule. Combinations between MD or MC and MM in structural and dynamic calculations of liquid and solution systems have been examined in some solutions containing polyatomic solutes, although the computer program is still rather simple. Molecular dynamics simulations in combination with molecular orbital calculations have also been tried to treat some systems in order to correct effects of polarization of electrons in molecules on intermolecular interactions.

1. Molecular Dynamics Simulations (MD)

The basic assumption of MD simulations is that any kind of interatomic interactions can be described in terms of the sum of the interactions of the atomic pairs, and thus, the multibody problem is not taken into consideration in the course of the simulation procedures, except for a very limited cases.³⁷ An interatomic interaction is described in terms of a pair potential function and the total energy of the system calculated is reduced by changing positions of atoms in a given system until it reaches the minimum value, allowing fluctuations in energies due to thermal motions at a given temperature. Average dynamic properties of atoms and molecules of a system in the equilibrium state are deduced from the atomic and molecular motions around the minimum value of the total system. For a bulk system the periodic boundary condition is usually introduced, and long-range interatomic interactions such as Coulombic interactions which may affect the behavior of other atoms beyond the size of the cell are corrected by the application of the Ewald summation,³⁸ reaction field method,³⁹ or shifted force potential method.⁴⁰ Selection of a set of good pair-potential functions for each atom pair is an essential problem for the achievement of simulation calculations. If the potential functions are reasonable, acceptable reproduction of measurable properties should be done, and thus, other properties which have never been measured should also be predicted with reasonable certainties.

Statistical averages are taken over the ensemble of phase space points of the trajectories over a sufficient length of time in order to reproduce the structural and dynamical properties of the system. The most frequently used statistical ensemble is a modified microcanonical ensemble⁴¹ where the total momentum of the system is also fixed in addition to the (N, V, E) parameters.

Various types of models and potentials have been applied to describe behavior of ions and water molecules. Ions are usually characterized in terms of the point

charges and radii. Interionic interaction potentials are written in various ways. A Lennard-Jones-type function with suitable parameter values derived from some theories or experimental values in combination with the Coulombic interaction is often used. Other polynomials and exponential type functions are also used which are fitted to the potential functions obtained from molecular orbital calculations. The Fumi-Tosi potential is often used for describing ion-ion interactions in the alkali halide systems of rock salt type.⁴²

The potential function describing water-water intermolecular interactions has been a big subject in the development of simulation calculations. A first attempt was done by Bjerrum⁴³ who represented a water molecule as a regular tetrahedral structure with the oxygen atom centered between two hydrogen atoms and two lone with pair electrons at the apexes of the tetrahedron. Atom-atom and electron-atom distances were fixed in the model. The charges were distributed on the atoms and electrons to reproduce the permanent dipole moment of an isolated water molecule. The water model was too simple to describe the behavior of molecules in the bulk water, so then, various modifications were applied to describe structural and dynamic properties of water. Water models proposed by Ben-Naim-Stillinger (BNS model)⁴⁴ and Stillinger-Rahman (ST2 model)⁴⁵ are typical ones among the four-point charge models. The model proposed by Rowlinson⁴⁶ is a modified four-point charge model. Matsuoka-Clementi-Yoshimine's model⁴⁷ is a three-point charge model of the water molecule.

Besides these rigid models, flexible models have also been introduced, in which the bond length and bond angle between the hydrogen and oxygen atoms are changeable due to vibrations. Typical ones are the central force (CF) model⁴⁸ and its modifications proposed by Bopp-Jancsó-Heinzinger (BJH).⁴⁹ Other, less frequently used models were discussed by Bopp.⁵⁰

The recent progress of MD simulations applied to aqueous solutions have been reviewed by Heinzinger and his co-workers.⁵⁰⁻⁵²

MD simulations can derive the following properties of solutions:

(1) Since distances of all kinds of atom pairs in the basic cell of a given system are calculable, the radial distribution function is derived by MD simulations, which can be compared with those obtained by X-ray and neutron diffraction measurements. Any kind of partial structures and pair-correlation functions is derived from the results which are often hardly obtained by the diffraction methods, because many partial functions are overlapped in experimentally obtained functions.

(2) Angular distributions of water molecules around ions in the system are obtained. The values may be obtained by neutron diffraction measurements. In MD simulations an angular correlation function $P(\cos \theta)$ is obtainable, where θ denotes either the cation-oxygen-hydrogen or the anion-hydrogen-oxygen bond angle.

(3) The numbers of water molecules in the first and second hydration shells of each ion are obtained provided that a suitable definition of the hydration shells are set. By the diffraction methods only average hydration numbers are obtainable, which are often fractional numbers. However, the hydration numbers in the first and second hydration shells of individual

cations and anions in an electrolyte solution are determinable by MD simulations, and thus the average hydration numbers obtained by the diffraction measurements can be compared with the sum of the numbers of individual ions.

(4) The time evolution of interatomic distances and bond angles in the hydration shells is calculable, from which we can discuss the rigidity of the hydration shell and the symmetry of the hydration structure. If an extremely high-speed computer were available, the substitution reaction mechanism of the hydrating water molecules with bulk water molecules would be elucidated by computer simulations. However, unfortunately, the rates of water substitution reaction, as well as those of any kind of solvent substitution reactions, are too slow to compute by using presently existing computers.

(5) The time evolution of distances and angles in a specific atomic group can be seen, which cannot be determined by any kind of experimental techniques.

(6) The self-diffusion coefficient D can be derived from either mean square displacements

$$D = \lim_{t \rightarrow \infty} \frac{\langle [\mathbf{r}(t) - \mathbf{r}(0)]^2 \rangle}{6t} \quad (30)$$

or through the velocity autocorrelation function

$$D = \lim_{t \rightarrow \infty} \frac{1}{3} \int \langle v(0)v(t') \rangle dt' \quad (31)$$

The self-diffusion coefficient thus evaluated may be compared with those obtained by quasi-elastic neutron scattering and NMR measurements.

(7) Spectral densities of hindered translational motions of ions and water molecules are evaluated, which are obtained by the Fourier transform of the normalized velocity autocorrelation functions. From these spectra, important conclusions can be drawn directly for the collective motions of the ions and their hydrates.

(8) Flexible models allow the calculations of intramolecular vibrations, and the results are compared with infrared and Raman spectroscopic data. Information for the rotational spectra can be obtained even by rigid models.

It should be noted here that the hydration numbers $n_{\alpha\beta}$ determined by the diffraction methods and molecular dynamics simulations are not always the same even though the structure found in both methods are very similar. In the diffraction methods the hydration number (in more general, coordination number) is evaluated from the area under the relevant Gaussian-type peak. However, the concept of the coordination shell is not clear in MD, as well as MC, because no assumption is made in the simulations that all atoms in the nearest neighbor have the same interatomic distance from the central ion, and thus, the peak caused by the ion-water interactions in the nearest neighbor in the radial distribution curve drawn by the simulation calculations is not necessary to be a symmetrical Gaussian-type one. Of course, a similar shape of peaks may appear in the diffraction measurements and the asymmetrical peak shapes are analyzed under the assumption that two or more symmetrical peaks are involved in the peak. Since such an assumption is not made in the simulations, the first hydration shell is conventionally defined as the region from $r = 0$ up to

the first minimum $r_{1,\min}$ or r_1 at $g(r_1) = 1$ after passing the first maximum. In many cases, especially in cases where ion-water interactions are weak, observation of the first minimum ($r_{1,\min}$) is not clear, and thus, the second definition is preferably used. Therefore, the hydration numbers $n_{\alpha\beta}$ thus determined by the simulation calculations are sometimes larger or smaller than the value determined from the diffraction methods depending on the degree of asymmetry of the first peak. It is obvious that the hydration number thus estimated by the simulation methods are not necessarily integers. In systems in which ion-water interactions are strong, the peak shape calculated by the simulations become more symmetrical and the hydration number evaluated is close to an integer value. Such an asymmetrical distribution of coordinated ligand atoms reflect to the value of rmsd, $l_{\alpha\beta}$, in the diffraction methods.

2. Monte Carlo Simulations (MC)

Monte Carlo (MC) simulations differ basically from MD. In the former atomic configurations are created randomly, and thus, MC loses time-dependent information in the simulated system. Since the configurations are selected randomly, physically irrelevant configurations can also occur. The procedure distinguishes between acceptable and nonacceptable configurations which should be thrown away in the course of the calculations. The classical formulation of the method was given by Metropolis et al.⁵³ The criterion for the acceptance of a configuration is fixed, and the total energy of the system decreases along the line of the criterion. If the configuration yields in a lower energy, it is accepted. If not, it is accepted upon a prefixed probability criterion. The accepted configurations are then collected and stored for further analysis.

Since the acceptance criterion is fixed to the energy in the classical MC studies, the adoption of good interatomic potentials is very important to obtain reliable results. It is worth noting that although a very good reproduction of the bulk structural data is possible through the computation of the pair-correlation functions with a surprisingly small number of generated configurations, reasonable microscopic structures are sometimes hardly described in the MC simulations even after the generation of a huge number of configurations. A detailed review of the MC method has been given by Wood and Erpenbeck.⁴¹ Results on aqueous solutions are collected by Beveridge et al.⁵⁴

Recent MC techniques include significant modifications of the original MC procedures. One of such modifications is so-called reverse Monte Carlo (RMC) method, which has been invented by McGreevy and Pusztai.⁵⁵ In the RMC simulations pair potentials and energy criteria are completely omitted, and a new criterion is set for the fit between the $G(r)$ function calculated from the randomly generated configurations and that from a diffraction experiment. Although the method requires extensive calculations, the advantage is clear: the often dubious pair potentials are no longer needed and the set of accepted configurations reproduces the experimental pair correlation functions to an incredibly good extent. The RMC simulations have widely been used for many monoatomic liquid systems, but only one attempt has been made for the determination of the hydration structure of ions in solution.⁵⁶

3. Molecular Mechanics Calculations (MM)

The molecular mechanics (MM) calculation is usually applied to the calculation of the total energies and energies of interatomic interaction in a molecule with different configurations or some isolated systems with a very limited number of molecules which interact each other. However, some attempts have been made to calculate optimum configurations of a polyatomic molecule in water. In the treatment, interactions between the solute and surrounding water molecules are calculated in a way similar to MD simulations and the optimum configuration of the solute is stepwise improved with the change in the orientation of water molecules. Such examinations have only been tried on the laboratory level, and therefore not yet published in scientific journals. However, in the near future elaborated programs may appear.⁴¹⁶

III. Structural Aspects of Ionic Hydration

In this section the static structural features of the ionic hydration shells will be discussed. Since a partial structural survey of ionic hydration has been done by Marcus in this journal,⁶ we aim to summarize structural data which are important to the discussion of dynamic properties of ionic hydration which will be done in the next section, along with time- and space-averaged structural data. The static structural information obtained by the X-ray diffraction method is believed one of the most reliable data. EXAFS data may be less accurate than the X-ray diffraction data especially for the coordination number. However, the structural data obtained by the EXAFS method are generally better than those derived by NMR measurements and any other classical methods. We summarize the structural data for the first hydration shell of various cations and anions determined by the X-ray diffraction and EXAFS methods in Tables 1–7.

The neutron diffraction method provides similar structural information as obtained by the X-ray diffraction and EXAFS methods (which are also included in Tables 1–7), but information about the orientation of hydrated water molecules in the first coordination sphere is obtainable by the former method. These structural data are separately summarized in Table 8.

In concentrated electrolyte solutions, ion pairs and complexes are often formed, which still include water molecules in the first coordination shell of the central ions. The diffraction and EXAFS methods can determine the hydration number of ion pairs and metal complexes in solution under favorable conditions, and thus, we summarize the number of water molecules in the first coordination shell of metal complexes determined by the methods in Tables 9–11. The structural information is directly connected to the total coordination number of the central ions in the ion pairs and complexes. The hydration structure of anions in ion pairs and metal complexes is difficult to measure due to their weak hydration. The structures of ion pairs and metal complexes themselves are not discussed in this review.

In Tables 12–14 the structural parameters, determined from the radial distribution functions derived by computer simulations (MD and MC), are tabulated, which can be compared with those found by the diffraction and EXAFS data. MD simulations can give

hydration numbers of individual ions so as to be able to calculate the distribution of the hydration numbers of ions, which are never obtainable by usual experimental observations. The average hydration number calculated from the distribution weighted with hydration numbers of individual ions should be compared with the hydration numbers obtained by experimental methods. Such distribution of the hydration numbers may be relatively wide in weakly solvated cations and anions and may be sharp in high valent small cations. The parameters that represent the distribution are tabulated in Table 15.

Under favorable experimental conditions or by using special techniques, we can estimate hydration numbers in the second hydration shell by the X-ray and neutron diffraction methods. The EXAFS method is less suitable than the diffraction methods for determining the structure of the second hydration shell, because the method is rather insensitive to long-range interatomic interactions. The structural data for the second hydration shell are summarized in Table 16.

The structure of the second hydration shell can certainly be determined by computer simulations with a less arbitrary definition for the second shell. The data are included in Table 17.

Although the NMR method is now believed a less reliable technique than the diffraction methods to determine the hydration numbers of substitution labile ions, the method can still give us useful information especially for the discussion of the dynamic behavior of hydrated water molecules. The static hydration numbers of ions determined by the NMR method are summarized in Table 18, which may be discussed by comparing those with the diffraction data given in preceding tables.

Dynamic parameters of hydrated water molecules determined by various methods are tabulated in Tables 19–27.

The methods applied are abbreviated as follows: X, X-ray diffraction; N, neutron diffraction; EX, EXAFS; MD, molecular dynamics; MC, Monte Carlo; E, electron diffraction; S, method explained in the footnote.

Sometimes various (usually two) methods are combined to discuss the hydration structure of ions. In such cases the first letter in the column of "method" in the tables refers to the source of the data.

Various models are usually adopted to interpret radial distribution curves obtained by the diffraction methods. The models used are referred to by the following abbreviations:

FN1 (first neighbor model 1). A hydrated species is assumed to have a symmetrical structure such as an octahedron or a tetrahedron and the rest of the solution is assumed to have the bulk water structure, whose radial distribution function is separately measured by using pure water.

FN2 (first neighbor model 2). A hydration species is assumed to have a symmetry similar to FN1, but the water structure is also assumed to be describable in terms of some symmetrical molecular arrangement.

FN3 (first neighbor model 3). No symmetrical arrangement is a priori assumed for hydrated species and water structure.

SNM (second neighbor model). The structure of the second coordination shell is taken into account in the determination of structure of the cationic hydration

shells. Water structure is subtracted by using the bulk data or assumed to have some symmetrical molecular arrangement as those assumed in FN1 or FN2.

rdf. The structure is analyzed from the analysis of the radial distribution functions without least squares fitting.

iso. The isomorphous substitution method is applied by using ions with the same ionic charge and essentially the same ionic radii. The method is used for X-ray diffraction measurements.

fod (the first-order difference). The difference curve of two radial distribution functions obtained from isotopically substituted samples is analyzed. The method is only applicable to the neutron diffraction method.

Other abbreviations applicable to the tables are as follows: T, tetrahedral symmetry; O, octahedral symmetry; H, hexahedral (cubic) symmetry; L, linear configuration; Sp, special symmetry (explained in the footnote); n, no specific symmetry is assumed; n in the column "second shell" indicates that no second shell is found around the ion; i, the existence of the second hydration shell is indicated, but not analyzed; a, the structure of the second hydration is analyzed, and the structural parameters are shown in Table 16.

Most measurements were carried out at room temperature or at 25 °C, unless otherwise stated in the footnote.

In the tables of computer simulation data, the structural parameters are obtained by the direct evaluation of the $g(r)$ functions. Since significant differences can arise from the potential models applied to describe water-water intermolecular interactions, the types of the potential functions are indicated in the tables: ST2, Stillinger-Rahman model;⁴⁵ MCY, Matsuoaka-Clementi-Yoshimine model;⁴⁷ CF, central force model;⁴⁸ BJH, Bopp-Jancsó-Heinzinger model;⁴⁹ CI, configuration interaction model;⁵⁷ HF, potential functions derived from Hartree-Fock calculations are employed;⁵⁸ TIP4P, a version⁵⁹ of transferable interaction potential (TIP);⁶⁰ SPC-FP, an elastic potential for a water molecule with a harmonic oscillation of O-H bonds.⁶¹

Various potential functions have so far been applied to describe ion-water and ion-ion interactions. Since variations of potential functions employed are numerous and practically dependent on authors in each work, no notation for the potential functions is indicated in the tables. Readers who are interested in the description of potential functions should consult the relevant reference. The characteristics of distributions of coordination numbers (Table 15) are calculated from the original histograms.

All values of distances (r) and root mean square deviations (rmsd) (l) are given in the picometer (pm) unit. The angles are represented by the degree unit.

The rmsd value reflects the statistical character of the distribution of interatomic ion-water distances in the hydration shell. They are usually determined from the theoretical $ki(k)$ (eq 1) or $G(r)$ (eq 3) values on the basis of a geometrical model fitted to the experimentally obtained structural data and treated as an independent variable. Under an assumption of the Gaussian shape of a peak, the rmsd value is related to the full width at half height (FWHH):

$$\text{FWHH} = 2\sqrt{\ln 2} \times \text{rmsd} \quad (32)$$

In the EXAFS analysis, the term Debye-Waller factor, is preferably used instead of rmsd (see eq 20). When the peak shape is not approximated to be a Gaussian type, the rmsd value does not coincide with the value of the Debye-Waller factor. It is a general trend that an increase in the size for ions with the same charge results in the increase in the rmsd value of an ion-water distance because of weakening of the ion-water bond.

Coordination structures around ions are expected to have symmetrical polyhedra according to the knowledge of coordination chemistry. This expectation is acceptable when the central ion is a transition metal ion in which the direction of the metal-water bonds is subjected by the direction of the d orbitals. However, in the hydration sphere in which ion-water interactions are essentially electrostatic, and therefore no specific direction is expected for the ion-water bonds, a polyhedral hydration structure may barely be constructed, and the number of water molecules accommodated in the first coordination sphere, and probably as well as in the second shell, of an ion may be restricted by the surface area of the central ion. The ion-water bond length may not necessarily be the same for all the bonds. Therefore an asymmetric structure of the hydration shell may result, and the average hydration number of the ion may not be an integer.

In the case where ion-water interactions are not very strong and a spherical electrostatic field is expected, the number of water molecules around ions of a given kind is not always the same, due to the fluctuation of the water structure in the bulk caused by thermal disturbance. The cases seem to be realized for alkali metal ions. MD and MC simulations show a distribution of the hydration numbers around ions, which also becomes a reason why the hydration number of a given ions is not an integer. In Table 15 the ranges of the coordination numbers found in the simulation calculations are given, together with the most frequently appearing coordination number for the ion and maximum percentage of the frequency. If the hydration structure is definitely concrete, only one value of the coordination number should be obtained with 100% frequency.

The orientation of water molecules around an ion is experimentally determinable by the neutron diffraction method. The distribution of the tilt angles is calculable by the simulations.

A. First Hydration Shell of Ions

1. Monovalent Cations

The hydration structure of ions is described, during the first stage of approach, in terms of the first neighbor ion-water distances and the number of nearest neighbor water molecules around the ion. Much attention has been devoted to the most accurate determination of these quantities from various measurement. Since 1930s widely spread numbers have been reported for a given ion under similar conditions by various experimental techniques which have different definitions of the hydration sphere, and thus a big confusion in the concept of the hydration structure of ions has been seen. Development of the diffraction methods removed

Table 1. Structural Parameters of the Hydration Shell of Monovalent Cations Derived from Diffraction and EXAFS Measurements (See Section III for the Full Definitions of the Abbreviations)

salt	H ₂ O/salt molar ratio	<i>r</i> _{MO} , pm	<i>l</i> _{MO} , pm	<i>n</i> _{MO}	symmetry	second shell	method	model	ref
H₃O⁺									
HCl	38.8	280		4	T	n	X	rdf	62
HCl	4–96	252		4	T	n	X, N	FN1	63
DCl	55.6	288		4	T	n	N	FN3	64
DBr	55.6	288		4	T	n	N	FN3	64
HCl + CoCl ₂	4.3	244,290		3,1	Sp ^a	n	X	FN3	65
HCl + RhCl ₃	75.9	270	8	4	T	n	X	SNM	66
HCl + Rh(ClO ₄) ₃	20.5	275	10	4	T	n	X	SNM	66
HNO ₃	25	280		4	n	n	X	FN3	67
HClO ₄ + Rh(ClO ₄) ₃	52.3	276	10	4	T	n	X	SNM	68
NH₄⁺									
NH ₄ F	24,11	295		5.3	n	n	X	FN1	69
NH ₄ F	3.6	288	38	4	T ^b	n	X	FN1	70
NH ₄ Cl	8.5	280	14	4	T ^b	n	X	FN1	70
NH ₄ Br	7.6	282	19	4	T ^b	n	X	FN1	70
NH ₄ I	8.2	291	8	4	T ^b	n	X	FN1	70
NH ₄ Cl	25	306	22	8	T ^c	n	X, MD	FN2	71
NH ₄ Cl	11.1	300		10–11	n	n	N	fod	72
NH ₄ ClO ₄	37	304	12	8	H	n	X	FN3	73
(NH ₄) ₂ SO ₄	15.8	301	15	8	H	n	X	FN3	73
Li⁺									
LiCl	3–8.2	195–225	25–31	4	T	n	X, N	FN1	74
LiCl	4.4–24.5	210		4	n	n	X	FN1	75
LiCl	54.3	190		4	T	n	N	FN3	76
LiCl	13.9,27.8	208,217	51,25	4	T	n	X	FN2	77
LiCl	5.6,15.6	195,195		3,3,5,5	n	i	N	fod	78
LiCl	4.0	218		5	n	n	X, MD	FN3	79
LiCl + CoCl ₂	7.5	203	14	4	T	n	X	FN1	80
LiCl + CoCl ₂	8–17	195–207	13	4	T	n	X	FN1	81
LiI	25	210	12	6	O	a	X, MD	SNM	82
LiI	20,9.2	220,228	14	4	T	n	X	FN1	83
LiBr	8.4–25	215–225	25	4	T	n	X	FN1	84
LiBr	31.7	194		4.5	n	n	N	fod	85
Na⁺									
NaCl	10.2	241		6	O	n	X	FN1	86
NaCl	54.3	250		8	n	n	N	FN3	87
NaCl	13.9, 27.8	242,242	27,21	4	T	n	X	FN2	77
NaI	7	240	9	4	n	n	X	FN3	88
NaNO ₃ ^d	6.1–9.3	244–248	19–22	6	n	n	X	FN3	89
K⁺									
KOH	27.5–15.9	287,292		4	n	n	X	rdf	90
KOH	3.2	292		4 or 6	n	n	X	rdf	91
KOH	38.8	270		6	n	n	X	rdf	62
KF	13.3–27	295		5.3	n	n	X	rdf	69
KCl	38.8	270		6	n	n	X	rdf	62
KCl	10.1	292		4	n	n	X	rdf	90
KCl	53.7	270		8	n	n	N	FN3	87
KCl	13.9,27.8	280,280	19,17	6	O	n	X	FN2	77
KCl	12.5	260		weak	n	n	N	fod	92
KI	108.4,19.5	290		3,2,2,2	n	n	X	rdf	93
Cs⁺									
CsF	2.3–8.0	307–321		6	O ^e	n	X	FN3	94
CsCl	53.1	295		8	n	n	N	FN3	76
CsCl	13.9,27.8	315,309	27,14	6,8	O, H	n	X	FN2	77
Ag⁺									
AgNO ₃	14.2	245	9	2.45	L	a	X	FN3	95
AgNO ₃	16.6,5.5	236,234		3.9,2.6	n	n	EX	FN3	96
AgNO ₃	16.6,4.3	242,243	4,4	4	T	a	X	SNM	97
AgNO ₃ + AgI	2.7	246	4	4	T	a	X	SNM	97
AgClO ₄	16.8	231	8	2.9	n	n	EX	FN3	98
AgClO ₄	10.4	241	9	2	L	a	X	FN3	95
AgClO ₄	16.3,3.3	238,243	5,5	4	T	a	X	SNM	97
AgClO ₄ + AgI	3.2	248	5	4	T	a	X	SNM	97
AgClO ₄ + HClO ₄	10.6	241	17	3.9	T	i	N	FN3	99

^a Trigonal pyramid. ^b A water molecule in the tetrahedral water network is substituted with an NH₄⁺ ion. ^c Four water molecules are located at larger distances. ^d Outer-sphere ion pairs are formed. ^e A short-range order analogous to the crystal structure is assumed.

a major part of the confusion, because the coordination sphere is more clearly defined in terms of the radial distribution functions. Some of ambiguities that still

remained in the explanation of peaks in the radial distribution curves are explained with supports of MD and MC simulations.

Ion-water distances can be determined with the rather high accuracy of a few tens picometers, independent of the experimental methods. However, the variation of the ion-water distance is sometimes significant and strongly depends on the methods. An extreme may be seen for the Li^+ ion, the $r_{\text{Li-O}}$ distance reported varies between 194 and 228 pm as shown in Table 1. Another example may be the $\text{Ni}^{2+}\text{-OH}_2$ distance which converges in an 11-pm range from 204 to 215 pm (Table 2). On the other hand, the length for the $\text{Mg}^{2+}\text{-OH}_2$ bond distance varies within a 7.6-pm range, and four different measurements for the hydrated Al^{3+} ion reported the $r_{\text{Al-O}}$ distances varying only by 3 pm (Table 3).

The hydration structures of monovalent cations are summarized as follows:

H_3O^+ . The hydration number of H_3O^+ is 4.⁶²⁻⁶⁸ The hydrated species is reported to be the tetrahedral $[\text{H}_3\text{O}^+(\text{H}_2\text{O})_4]$ complex for most cases,^{62-64,66-68} but a trigonal-pyramidal structure with a very weak $\text{HOH}\cdots[\text{OH}_3^+(\text{H}_2\text{O})_3]$ interaction is also proposed, the structure being better fitted to the structure expected from molecular orbital calculations.⁶⁵ In the latter structure three short O-O bonds of 244 pm and a long and practically not interacting O-O bond of 290 pm are concluded. Thus, a proton has four water molecules, one of the water molecules forms H_3O^+ and the remaining three molecules form a planar triangle structure around the H_3O^+ ion.⁶⁵ However, all other works concluded that one H_3O^+ species is tetrahedrally surrounded by four water molecules, and thus, one proton has *five* water molecules including the core and the first coordination shell. The $\text{H}_3\text{O}^+\text{-H}_2\text{O}$ bond length in the species is reported to be close to the $\text{H}_2\text{O}\text{-H}_2\text{O}$ bond length in the bulk water, except for one case.⁶³ The hydration structure of H_3O^+ found by neutron diffraction experiments is also tetrahedral^{63,64} (see Table 8).

NH_4^+ . An ammonium ion is believed to be easily embedded in the bulk water structure because its molecular structure is similar to the hydrogen-bonded water structure. The reported hydration number of an NH_4^+ ion is widely spread from 4 to 11. The hydration number of 4 may be easily concluded from the expected structure of hydrogen-bonding interactions between each proton in the NH_4^+ ion and a water molecule. However, NH_4^+ is a structure-breaking ion and thus it may not form a strong hydration shell like Li^+ and Na^+ . A large hydration number and a long r_{MO} distance as reported in refs 71-73 may indicate weak $\text{NH}_4^+\text{-H}_2\text{O}$ interactions. Similar results are obtained from computer simulations.^{278,279} However, it should be noted that it is extremely difficult to distinguish between oxygen and nitrogen atoms by the X-ray diffraction method and the method is practically blind for the detection of protons around an atom. Neutron diffraction with isotopic substitution is more promising.⁷²

Li^+ . Since a water molecule is regarded as a hard ligand, the ion-water bond length is well approximated as the sum of a half of the size of water molecule plus the characteristic ionic radius of an ion. The definition of the size of molecules and ions is more or less arbitrary because the electron cloud diffuses without a sharp boundary. Nevertheless, the radius of a water molecule, which is conventionally assumed to be spherical, is about 140 pm which is estimated from the water-water bond length in the bulk water. The distance of a water

molecule from the central ion depends on the coordination number and the spin state of the ion according to Shannon.³⁴¹ The ion-water bond lengths in the first coordination sphere of most ions have been determined with deviations of $\pm(2-3)$ pm from the simply averaged measured values with various methods for ions with rather definite coordination structures.

However, the ion-water bond length in the first coordination shell is rather largely dispersed in alkali metal ions. As already mentioned above, the $\text{Li}^+\text{-H}_2\text{O}$ bond length has been reported to be 194-228 pm, the variation is certainly beyond the uncertainties of measurements.⁷⁴⁻⁸⁵ The bond length measured by the neutron diffraction method seems to be shorter than that by X-ray diffraction (see Table 1). An interpretation of the shorter bond is that the neutron diffraction method measures the distance between the nuclei of lithium and oxygen, while the X-ray diffraction method measures the distance between the centers of electron clouds of the atoms, which may be deformed due to polarization. An assumption of a point electron distribution at the center of an atom at the analysis of X-ray diffraction data may cause another error for such a largely polarized case of water molecules. Another and more probable reason why the $\text{Li}^+\text{-OH}_2$ bond length disperses by observers is the concentration dependence of the coordination numbers of the lithium ion, which causes the change in the bond length. It is generally accepted that the ion-ligand bond length in a complex with a higher coordination number is longer than that with a lower coordination number. As we see from MD and MC simulations (see Table 15), the hydration number of the lithium ion distributes over the range 3-7, and the most frequent coordination number estimated by the simulations depends on the case, probably on the concentration of the ions. As expected, the most frequently appearing coordination number (MFACN) of Li^+ is smaller (e.g., in systems with $\text{H}_2\text{O}/\text{salt}$ ratio of 4, the MFACN becomes 4-5) in a system with a high concentration than that with a low concentration (MFACN = 6). The concentration dependence of the hydration number of Li^+ is not clear from the data in Table 1, however. The average hydration number of Li^+ determined from the area of the first peak of the radial distribution function derived by computer simulations is also not conclusive, but the $\text{Li}^+\text{-H}_2\text{O}$ bond length seems to be converged in a range of 200-213 pm (see Table 12). The hydration number of Li^+ estimated from the chemical shift of proton NMR spectra was 3³¹³ (Table 18), and the value seems to be too small.

Na^+ . Sodium ions have various numbers of water molecules in the first hydration shell according to computer simulations^{60,281,300,301} (see Table 15), as seen in the case of Li^+ . The hydration number of Na^+ measured by the diffraction methods is distributed over the range 4-8.^{77,86-88} The average hydration number of Na^+ estimated from the area under the peak of the radial distribution function calculated by computer simulations is 6^{60,281-284,297,299} or close to 6.^{58,285,289,398,300-302} The $\text{Na}^+\text{-H}_2\text{O}$ bond length determined by the diffraction methods falls in a relatively narrow range of 240-250 pm.^{77,86-89} A shorter length of the $\text{Na}^+\text{-H}_2\text{O}$ bond of 230-240 pm^{57,58,60,280-285,289,295-302} is given in the estimation by computer simulations (Table 12).

Table 2. Structural Parameters of the Hydration Shell of Divalent Cations Derived from Diffraction and EXAFS Measurements (See Section III for Full Definitions to the Abbreviations)

salt	H ₂ O/salt molar ratio	<i>r</i> _{MO} , pm	<i>l</i> _{MO} , pm	<i>n</i> _{MO}	symmetry	second shell	method	model	ref
Be²⁺									
BeCl ₂	10	167	3.5	4	T	i	X, MD	FN2	100
Mg²⁺									
Mg ²⁺	55	206.6		6	n	i	X	iso	101
MgCl ₂	25	200		6	O	n	X	rdf	102
MgCl ₂	9.8–13.0	210		8.1–7.9	n	n	X	rdf	103
MgCl ₂	27.1–55.5	210–212	4–12	6	O	a	X	SNM	104
MgCl ₂	11.5	211	12	6	O	a	X	SNM	105
MgCl ₂	50	212	4	6	O	a	X, MD	SNM	106
MgCl ₂ + CaCl ₂	25	204.4	6	6	O	n	X	FN1	107
MgCl ₂ + KCl ^a	12.3,73.6	209.2	8.4	6	O	n	X	FN2	108
MgCl ₂ + CsCl ^b	13.2,41.5	208.1	9.3	6	O	n	X	FN2	108
Mg(NO ₃) ₂	10.8–24.8	211	11	6	O	a	X	SNM	109
Mg(ClO ₄) ₂	18	212	12.9	6	O	a	X	SNM	110
MgSO ₄	20.5	209.4	12	6	O	a	X	SNM	111
Mg(BF ₄) ₂	14–37	215		6.4–6.2	O	i	X	rdf	112
Ca²⁺									
Ca ²⁺	55	233		6	n	i	X	iso	101
CaCl ₂	38.8	240		6	n	n	X	rdf	62
CaCl ₂	12.3–55.8	241–242	13–15	6	O	n	X	FN1	113
CaCl ₂ + MgCl ₂	25	242.8	14	6	O	n	X	rdf	107
CaCl ₂ ^c	8.8	236,270	9	3 + 6	O	n	X	rdf	105
CaCl ₂	12.4	240		5.5	n	n	N	fod	114
CaCl ₂	55,20,12	246,239,241		10,7.2,6.4	n	n	N	fod	115
CaCl ₂	50	239	13	6.9	n	n	X	FN3	116
CaCl ₂	8.6	244		6.0	n	a	X	FN3	117
CaBr ₂	26,44.1	240,249	12,20	6.6	O	n	X	FN1	118
Sr²⁺									
SrCl ₂	21.5	260		7.9	n	n	X	rdf	103
SrCl ₂	26.5,34.6	264	12,14	8	Sp ^d	a	X	SNM	119
Sr(ClO ₄) ₂	18.5	265		15	n	n	N	fod	120
Ba²⁺									
BaCl ₂	36	290		9.5	n	n	X	rdf	103
V²⁺ e									
–	–	221		6	n	n	EX	FN3	344
Cr²⁺									
CrSO ₄	55	208 ^f		4 ^f	n	n	EX	FN3	344
Mn²⁺									
Mn(ClO ₄) ₂	25.4	220		6	O	n	X	rdf	121
Mn(ClO ₄) ₂	55.5	217.7	7.8	6	O	n	EX	FN3	122
MnSO ₄	20,50,100	220		6	n	n	X	rdf	123
Fe²⁺									
FeCl ₂	14–140	218		6	O	n	EX	rdf	124
FeCl ₂ + HCl	52.2	213	28	6	n	i	N	fod	125
Fe(ClO ₄) ₂	25.5	212		6	O	n	X	rdf	121
Fe(ClO ₄) ₂	55.5	209.5	8.1	6	O	n	EX	FN3	122
Fe(ClO ₄) ₂	55.5	228	12	6.1	O	n	X ^g	SNM	126
Co²⁺									
Co ²⁺	55	209		6	n	i	X	iso	101
CoBr ₂	17	211		5.9	n	n	X	rdf	127
Co(NO ₃) ₂	550	208			n	n	EX	rdf	128
Co(ClO ₄) ₂	25	208		6	O	n	X	rdf	121
Co(ClO ₄) ₂	15	210	12	6	O	a	X	SNM	129
CoSO ₄	25–100	215		6.1–6.3	n	n	X	rdf	130
Ni²⁺									
Ni ²⁺	55	206.5		6	n	i	X	iso	101
NiCl ₂	25	210		6	O	n	X	rdf	102
NiCl ₂	12.6	205		5.8	n	n	N	fod	131
NiCl ₂	12.6,27.4	205,206	10,13	6	O	n	X	FN1	132
NiCl ₂	12.6–64.5	207–210		5.8–6.8	n	n	N	fod	133
NiCl ₂	14,18	206,207	4,4	7,6.2	n	n	EX	FN3	134
NiCl ₂	28	206	12	6	O	a	X	SNM	105
NiCl ₂ ^h	14	206	13	6	O	a	X	SNM	105
NiCl ₂	13.8	205.9	7.4	6.4	n	n	EX	FN3	135
NiCl ₂	11.5	207	13	5.8	n	n	N	fod	136
NiCl ₂	28–550	206		5.9–5.4	n	n	N	fod	137
NiCl ₂ ⁱ	25	206		5.9	n	n	N	rdf	138
NiCl ₂ ^j	25	207		6.0	n	n	N	rdf	138
NiCl ₂ ^k	25	207		5.5	n	n	N	rdf	138
Ni(NO ₃) ₂	550	205			n	n	EX	rdf	139
Ni(NO ₃) ₂	13.8	205.5	6.7	6.6	n	n	EX	FN3	135
Ni(NO ₃) ₂	13–110	205–206		6.4–7.1	n	n	EX	FN3	140
Ni(ClO ₄) ₂	26.6	204		6	O	n	X	rdf	121
Ni(ClO ₄) ₂	14.6	207		5.8	n	n	N	fod	133
Ni(ClO ₄) ₂	15.0	205	10	6	O	a	X	SNM	129
NiSO ₄	25–100	215		6.15–6.32	n	n	X	rdf	130

Table 2. (Continued)

salt	H ₂ O/salt molar ratio	<i>r</i> _{MO} , pm	<i>l</i> _{MO} , pm	<i>n</i> _{MO}	symmetry	second shell	method	model	ref
Ni ²⁺									
NiSO ₄	27.5	206.3	14	6	O	a	X	SNM	111
NiSO ₄ ^b	28	207	9	5.1	O	a	X	SNM	141
NiSO ₄	27	205.9	14	6	O	a	X	SNM	142
NiSO ₄ + H ₂ SO ₄	48	212	12	6	O	a	X	SNM	111
NiSO ₄ + Li ₂ SO ₄	37	205.9	11	6	O	a	X	SNM	142
Cu ²⁺									
Cu(NO ₃) ₂	55.5	196		4	O	n	N	fod	143
Cu(NO ₃) ₂ ^m	280	{ 204 229	{ 7 7	{ 4 2	O ⁿ	n	EX	FN3	144
Cu(ClO ₄) ₂	19.7	{ 194 243	{ 6 9	{ 4 2	O ⁿ	n	X	FN3	145
Cu(ClO ₄) ₂	55.5	{ 195.5 260	{ 3.6 12	{ 4 2	O ⁿ	n	EX	FN3	122
Cu(ClO ₄) ₂ ⁿ	14.6	197		6	O	n	N	fod	146
Cu(ClO ₄) ₂	15.4,25.1	{ 198 239,234	{ 7.5 12,6	{ 4 2	O ⁿ	a	X	SNM	147
Cu(ClO ₄) ₂	200–14.6	{ 196 228	{ 6–7 12–16	{ 4 2	O ⁿ	n	EX	FN3	148
Cu(ClO ₄) ₂ ^p	200–14.6	{ 196 229	{ 5–6 10–14	{ 4 2	O ⁿ	n	EX	FN3	148
Cu(ClO ₄) ₂	27.8	196	15	4.1	O	n	N	fod	143
CuSO ₄	48,100	{ 215 250		{ 5.2 5.0	n	n	X	rdf	123
CuSO ₄	75,160	{ 210 230		{ 4.1 2.2	O ⁿ	n	X	rdf	149
CuSO ₄	43.2	{ 194 238	{ 6 9	{ 4 2	O ⁿ	n	X	FN3	121
CuSO ₄	40.4	{ 201 233	{ 9 23	{ 4 2	O ⁿ	a	X	SNM	150
CuSO ₄ ^q	185,47	{ 198 –		{ 4.25,4.13 –	O ⁿ	n	EX	FN3	151
CuSO ₄ ^m	110,43	{ 200 227	{ 10,11 10,11	{ 4 2	O ⁿ	n	EX	FN3	144
Zn ²⁺									
Zn ²⁺	55	209.3		6	O	i	X	iso	101
ZnCl ₂	56.6,19.5	210,215		5.7,6.2	n	n	S ^q	rdf	152
Zn(NO ₃) ₂	9.0	217	27	6.6	n	a	X	SNM	153
Zn(ClO ₄) ₂	23.4	208	9	5.9	O	n	X	FN3	121
ZnSO ₄	31,50,100	215		6	O	n	X	rdf	123
ZnSO ₄	23.2	208		6	O	n	X	rdf	121
ZnSO ₄	27.1	210.7	10.2	6	O	a	X	SNM	154
ZnSO ₄	100–16.9	211–214	9–11	6	O	a	X	SNM	155
Zn(CF ₃ SO ₃) ₂	27.8	209	13	5.3	n	n	N	fod	156
Zn(gly) ₂ ^r	22.1	208	8	6	O	n	X	FN3	157
Zn(α-ala) ₂ ^s	43.8	208	8	6	O	n	X	FN3	158
Cd ²⁺									
Cd ²⁺	55	228.9		6	O	i	X	iso	101
Cd(ClO ₄) ₂	26.6	231	6	6	O	n	X	rdf	159
Cd(ClO ₄) ₂	23.0	229	10	6	O	a	X	SNM	160
Hg ²⁺									
Hg(ClO ₄) ₂	19.7	234	19.5	7	O	a	X	SNM	161
Hg(ClO ₄) ₂	15.8	241	23	6	O	n	X	FN3	162
Hg(BF ₄) ₂	27	233		6	O	n	X	rdf	163
Sn ²⁺									
Sn(ClO ₄) ₂ ^t	16.8	234,290	6,10	3.6,3	n	a	X	SNM	164
Sn(ClO ₄) ₂	16.8	221	10	3.8	n	n	EX	rdf	164
Sn(ClO ₄) ₂ ^t	12.0	233,283	6,10	2.4,3	n	n	X	FN3	165

^a KCl ion pairs are formed. ^b CsCl ion pairs are formed. ^c The short-range order analogous to the crystalline hydrate structure is assumed. ^d Square antiprism. ^e Composition of the salt used is not reported. No detail information is given in the literature except for the bond length. ^f Axial Cr²⁺–OH₂ bond length is not observable. ^g Mössbauer spectra of frozen solutions are also investigated. ^h Outer-sphere complex formation occurs. ⁱ In H₂O. ^j In D₂O. ^k In “null mixture” of H₂O and D₂O. ^l Numbers in the upper and lower lines indicate the parameters values of the equatorial and axial bonds, respectively, in the distorted octahedral structure. ^m Ab initio calculations and IR spectroscopy are also applied. ⁿ Distorted (elongated) octahedron. ^o Jahn–Teller effect is not found. ^p Anomalous X-ray scattering investigation. ^q In the glassy state. ^r Parameters refer to the hydrated Zn²⁺ ion. The structural parameters of hydrated water molecules of the mono(glycinato)zinc(II) and bis(glycinato)zincate(II) complexes are given in Table 11. The structural parameters of the tris(glycinato)zincate(II) complex is also given in the same reference. ^s Parameters refer to the hydrated Zn²⁺ ion. The structural parameters of hydrated water molecules of the mono(α-alaninato)zinc(II) and bis(α-alaninato)zincate(II) complexes are given in Table 11. The structural parameters of the tris(α-alaninato)zincate complex are also given in the same reference. ^t Two different M–OH₂ bond lengths are reported.

K⁺. The potassium ion is one of the most difficult ions to determine the hydration structure by the X-ray and neutron diffraction methods, because the ionic size of K⁺ is evaluated to be 152 pm for the case of CN = 6 and 165 pm for CN = 8,³⁴¹ and thus, the length of the

K⁺–H₂O bond is very close to that of the H₂O–H₂O bond in the bulk. Therefore, the hydration number of K⁺ is not possibly determined by the diffraction methods without an assumption for the water structure, and thus, the hydration number estimated by the

Table 3. Structural Parameters of the Hydration Shell of Trivalent Cations Derived from Diffraction and EXAFS Measurements (See Section III for Full Definitions of Abbreviations)

salt	H ₂ O/salt molar ratio	<i>r</i> _{MO} , pm	<i>l</i> _{MO} , pm	<i>n</i> _{MO}	symmetry	second shell	method	model	ref
Al³⁺									
AlCl ₃	23.8,54.0	188,190	9,4	6,6	O	a	X	SNM	173
Al(NO ₃) ₃	14.5	187	15	6	O	a	X	SNM	174
Al(NO ₃) ₃	100	190		6	n	a	X	rdf	169
Cr³⁺									
CrCl ₃	23.4	199	7	6	O	a	X	SNM	166
CrCl ₃	55	199.7	4	6	O	a	X	SNM	167
CrCl ₃	110	190		6	O	n	X	rdf	168
Cr(NO ₃) ₃	100	198		6	n	a	X	rdf	169
Cr(NO ₃) ₃	55,27	200,199.8	10,7	6	O	a	X	SNM	167
Cr(NO ₃) ₃	24.5–50.8	203	8	6	O	a	X	SNM	170
Cr(ClO ₄) ₃ ^a	55.5	198.5	6.5	6	O	n	EX	FN3	122
Cr(ClO ₄) ₃	55.5	196.6		6	n	n	EX	rdf	171
Cr(ClO ₄) ₃ ^b	25–27	198	27	5	n	n	N	fod	172
Fe³⁺									
FeCl ₃	52.2	201	32	6	n	i	N	fod	125
FeCl ₃ ^c	28.5	202	15	5.9	O	n	X	FN3	175
Fe(NO ₃) ₃	6.6–32.5	203	4–6	5.5–6.1	O	i	X	rdf	176
Fe(NO ₃) ₃	22.2,34.7,69	204–205	8–9	6	O	a	X	SNM	177
Fe(NO ₃) ₃ ^d	29.9,25.5	201,202		6,4.9	O	i	N	fod	178
Fe(ClO ₄) ₃	21.3–29.7	200.8		6	O	n	X	SNM	179
Fe(ClO ₄) ₃	55.5	199.0	5.5	6	O	n	EX	FN3	122
Fe(ClO ₄) ₃	20.1	201		6.3	O	i	N	fod	178
Y³⁺									
Y(ClO ₄) ₃	40,12.4	237	6,8	8.0	n	a	X	SNM	10
Y(ClO ₄) ₃	18–55	236	8	8.0	n	n	X	FN3	180
Rh³⁺									
Rh(ClO ₄) ₃ + HClO ₄	145	204	10	6	O	a	X	SNM	68
Rh(ClO ₄) ₃ + HCl	277	206	8	6	O	a	X	SNM	66
In³⁺									
In(ClO ₄) ₃	11.3	215	8	6	O	n	X	rdf	181
Tl³⁺									
Tl(ClO ₄) ₃	42.3	222.7		6	O	n	X	FN3	182
Tl(ClO ₄) ₃	42.3,17.8	223.6	10,9	5	n	n	X	FN3	183

^a Four equatorial H₂O molecules at 198.5 pm and two axial ones at 230 pm are also proposed. ^b Three different isotopic mixtures were used. ^c Highly hydrolyzed solution. ^d The second sample is heated to 90 °C during the preparation.

diffraction methods is not very reliable, although the K⁺–H₂O bond length may be determinable by the diffraction method within a reasonable uncertainties. The length of the K⁺–H₂O bond is reported to be 260–295 pm^{62,87,90–93} (Table 1). On the other hand, computer simulations can evaluate the K⁺–H₂O bond length and the average hydration number of the K⁺ ion without an assumption of the bulk water structure. The results summarized in Table 12 show that the K⁺–H₂O bond length is 271–286 pm^{57,58,280–284,285,303} except for one case (265 pm²⁹⁵) and the hydration number of K⁺ is 6.3–7.8.^{57,281–285,303} The distribution of hydration numbers around individual K⁺ ions in water shifts toward larger numbers (4–8)²⁸¹ (see Table 15) than that for Li⁺ and Na⁺ as expected from the larger size of the K⁺ ion than Li⁺ and Na⁺ ions. However, since the K⁺–H₂O interactions are weaker than the Na⁺–H₂O interactions, the hydration number of the K⁺ ion estimated by NMR measurements is smaller than that of Na⁺³¹³ (Table 18).

Rb⁺. The rubidium ion has not been investigated by means of X-ray diffraction, because it emits strong fluorescent X-rays upon irradiation of X-ray beams on samples by the most frequently used Mo characteristic wavelength. Since no diffraction data are available, no computer simulation has been carried out because of the lack of data to be compared with the results. An NMR measurement shows the hydration number of

Rb⁺ to be 3.5,³¹³ but the result has no reason to be believed.

Cs⁺. There are some results for the hydration structure of Cs⁺. The diffraction methods show a hydration number of either 6 or 8 for Cs⁺ and the Cs⁺–H₂O bond length of 295–321 pm^{76,77,94} (Tables 1 and 8). The results by computer simulations show a spread of values for the average hydration number of 5.3–8.2^{289,304,305} (Table 12). The Cs⁺–H₂O bond length estimated from the peak position of the radial distribution curve determined by computer simulations is 303–320 pm, which is close to the value determined by the diffraction methods.

Ag⁺. The hydration structure of Ag⁺ is interesting from the viewpoint of coordination chemistry, because the ion can form both 4- and 2-coordination structures. The final conclusion is that the Ag⁺ ion has a regular tetrahedral structure with the Ag⁺–H₂O distance of 238–248 pm^{97,99} (Table 1).

Orientation of water molecules in the first hydration shell has been investigated by means of neutron diffraction and computer simulations. Molecular orbital calculations of hydrated ions in the gas phase show that the hydrated water molecules are oriented so as to direct their dipoles toward the central ion, i.e., the M⁺–O–H angle is close to 127° and the ion, oxygen and two hydrogen atoms in a hydrated water molecule lay in one plane with the tilt angle $\theta = 0^\circ$ ³⁴² (see figure in

Table 4. Structural Parameters of the Hydration Shell of Rare Earth Ions Derived from Diffraction and EXAFS Measurements (See Section III for the Full Definition of the Abbreviations)

salt	H ₂ O/salt molar ratio	<i>r</i> _{MO} , pm	<i>l</i> _{MO} , pm	<i>n</i> _{MO}	symmetry	second shell	method	model	ref
LaCl ₃ ^a	20.8–31.9	248		8.0	H	n	X	FN3	184
LaCl ₃ ^a	14.6	258		9.1	n	n	X	rdf	185
LaBr ₃ ^a	20.9–18.8	248		8.0–7.9	n	n	X	rdf	186
La(ClO ₄) ₃	12.0	257.0	8.9	8.0	n	a	X	SNM	10
PrCl ₃	14.6	254		9.2	n	n	X	rdf	185
PrCl ₃	14.6	248		10	n	n	N	iso	187
NdCl ₃	32	241		8.0	H	n	X	rdf	188
NdCl ₃	16.5	251		8.9	n	n	X	rdf	185
NdCl ₃	17.5	248		8.5	n	n	N	rdf	189
NdCl ₃	17.5	248	9	8.4	n	n	N	fod	190
NdCl ₃	14.6	248		10	n	n	N	iso	187
Nd(ClO ₄) ₃ ^a	28	251	9.1 ^b	9.5	n	n	EX	rdf	191
Nd(ClO ₄) ₃ ^c	28	251	5.0 ^b	9.6	n	n	EX	rdf	191
Nd(ClO ₄) ₃	55,165	250,252	30,28 ^d	8.9,8.8	n	n	N	fod	192
SmCl ₃ ^a	17.2	247		8.8	n	n	X	rdf	193
Sm(ClO ₄)	15.2	245.5	8.9	8.0	n	n	X	SNM	10
Sm(ClO ₄) ₃	28	245	7.7 ^b	9.3	n	n	EX	rdf	191
Sm(ClO ₄) ₃ ^c	28	245	6.0 ^b	8.6	n	n	EX	rdf	191
Sm(ClO ₄) ₃	55	246	31 ^d	8.5	n	n	N	fod	192
EuCl ₃ ^a	17.2	245		8.3	n	n	X	rdf	193
Eu(ClO ₄) ₃	28	243	7.4 ^b	8.6	n	n	EX	rdf	191
Eu(ClO ₄) ₃ ^c	28	243	5.7 ^b	8.9	n	n	EX	rdf	191
GdCl ₃	26.8	240		9.9	n	n	X		194
GdCl ₃	30	237		8.0	H	n	X	rdf	195
Gd(ClO ₄) ₃	28	241	6.6 ^b	7.6	n	n	EX	rdf	191
Gd(ClO ₄) ₃ ^c	28	241	5.5 ^b	7.5	n	n	EX	rdf	191
TbCl ₃	15.9	241		8.2	n	n	X	rdf	196
TbCl ₃	18.4	239		9	n	n	N	iso	187
Tb(ClO ₄) ₃	39.4,13.7	240	7.7,10	8.0	n	n	X	SNM	10
Tb(ClO ₄) ₃	13.7	240		8.0	n	n	X	iso	180
Tb(ClO ₄) ₃	28	239	6.6 ^b	3.9	n	n	EX	rdf	191
Tb(ClO ₄) ₃ ^c	28	238	7.5 ^b	8.0	n	n	EX	rdf	191
DyCl ₃	6.9	240		7.9	n	n	X	rdf	196
DyCl ₃	21.0	237	15	7.4	n	n	N	fod	197
DyCl ₃	18.4	239		9	n	n	N	iso	187
DyCl ₃	55,165	238	25 ^d	7.8	n	n	N	iso	198
Dy(ClO ₄) ₃	28	237	6.8 ^b	8.1	n	n	EX	rdf	191
Dy(ClO ₄) ₃ ^c	28	237	4.2 ^b	6.8	n	n	EX	rdf	191
Dy(ClO ₄) ₃	55	239	25 ^d	7.9	n	n	N	iso	198
ErCl ₃ ^a	58.5–18.2	230		6.3–6.5	H	i	X	rdf	199
ErCl ₃	15.7	237		8.2	n	n	X	rdf	196
ErCl ₃	53.9	235	9.5	8.0	n	a	X	SNM	11
ErBr ₃	52.9	235	9.5	8.1	n	a	X	SNM	11
ErI ₃ ^a	41.7	230		6.3	H	i	X	rdf	199
Er(ClO ₄) ₃	12.1	236	10	8.0	n	n	X	SNM	10
Er(ClO ₄) ₃	12.1	236		8.0	n	n	X	rdf	180
Er(ClO ₄) ₃	28	234	6.4 ^b	7.8	n	n	EX	rdf	191
Er(ClO ₄) ₃ ^c	28	234	4.3 ^b	7.5	n	n	EX	rdf	191
Er(ClO ₄) ₃ ^e	49.2–12.2	235–236	9	8.0–7.9	n	a	X	SNM	11
TmCl ₃	15.3	236		8.2	n	n	X	rdf	196
TmCl ₃	15.6	233		8	n	n	N	iso	187
Tm(ClO ₄) ₃	28	233	6.6 ^b	8.0	n	n	EX	rdf	191
Tm(ClO ₄) ₃ ^c	28	233	4.2 ^b	7.3	n	n	EX	rdf	191
YbCl ₃	15.6	233		8	n	n	N	iso	187
Yb(ClO ₄) ₃	55	232	24 ^d	7.8	n	n	N	iso	198
LuCl ₃	15.3	234		8.0	n	n	X	rdf	196
Lu(ClO ₄) ₃	28	231	6.4 ^b	7.7	n	n	EX	rdf	191
Lu(ClO ₄) ₃ ^c	28	231	4.5 ^b	6.8	n	n	EX	rdf	191

^a The formation of outer-sphere complexes is probable. ^b Debye–Waller factor. ^c Quenched to the glassy state at a liquid nitrogen temperature. ^d The value of the full width of half height (FWHH). ^e Complex formation is not excluded at higher concentrations.

Table 5. Structural Parameters of the Hydration Shell of Tetravalent Cations Derived from X-ray Diffraction Measurements (See Section III for the Full Definitions of the Abbreviations)

salt	H ₂ O/salt molar ratio	<i>r</i> _{MO} , pm	<i>l</i> _{MO} , pm	<i>n</i> _{MO}	symmetry	second shell	method	model	ref
Th ⁴⁺									
Th(NO ₃) ₄ ^a	70.8,57.0	255		5.5,7	T	n	X	rdf	200
Th(ClO ₄) ₄	42.7–13.0	248.6	8	7.9–8.1	n	i	X	FN3	201
U ⁴⁺									
U(ClO ₄) ₄ ^a	35.7,31.2	250,251	10,13	7.9,9.2	Sp ^b	a	X	FN3	202

^a The formation of hydrolyzed species is reported. ^b Square antiprism is probable.

Table 6. Structural Parameters of the Hydration Shell of Halide Ions (X^-) Derived from Diffraction and EXAFS Measurements (See Section III for the Full Definitions of the Abbreviations)

salt	H ₂ O/salt molar ratio	r_{XO} , pm	l_{XO} , pm	n_{XO}	symmetry	method	model	ref
F⁻								
NH ₄ F	3.6	269	10	6	O	X	FN1	70
NH ₄ F	24,11	262		4.5	n	X	FN1	69
KF	13.3-27	262		4.5	n	X	rdf	69
CsF	2.3-8.0	292		4-6	n	X	FN3	94
Cl⁻								
HCl	8-27	320-325			n	X	rdf	204
HCl	62.7-33.6	325		8	n	X	rdf	205
HCl	4-96	313		4	T	X, N	FN1	63
DCl	55.6	310		6	n	N	FN3	64
HCl + CoCl ₂	4.3	313		4.98	n	X	FN3	65
HCl + RhCl ₃	75.9	323	14	6	O	X	SNM	66
HCl + Rh(ClO ₄) ₃	78.1	319	17	6	O	X	SNM	66
LiCl	3-8.2	319-310	19-20	6	O	X, N	FN1	74
LiCl	54.3	310		6	n	N	FN3	76
LiCl	13.9,27.8	315,308	19,19	6	O	X	FN2	77
LiCl	5.6,15.6	329		5.3,5.9	n	N	fod	78
LiCl	5.6,15.6	329,334		5.3,5.9	n	N	fod	206
LiCl	4.0	319		8	n	X, MD	FN3	79
LiCl	6.0	320		5.4	n	N	fod	207
LiCl ^a	6.0	317.5		5.4	n	N	fod	207
LiCl + CoCl ₂	7.5	316	20	6	O	X	FN1	80
LiCl + CoCl ₂	8-17	314-318	20	6	O	X	FN1	81
NaCl	54.3	310		6	n	N	FN3	87
NaCl	13.9,27.8	314,314	16,17	6	O	X	FN2	77
NaCl	10.4	320		5.5	n	N	fod	206
KCl	53.7	310		6	n	N	FN3	87
KCl	13.9,27.8	314,314	17,17	6	O	X	FN2	77
RbCl	12.7	320		5.8	n	N	fod	206
CsCl	53.1	310		6	n	N	FN3	76
CsCl	13.9,27.8	309,316	14,14	6	O	X	FN2	77
MgCl ₂	9.8-13.0	320		8.2-8.9	n	X	rdf	103
MgCl ₂	27.1-55.5	311-314	20-23	6	O	X	FN1	104
MgCl ₂	50	315	14	5.9	n	X, MD	FN3	106
MgCl ₂ + CaCl ₂	25	313	24	6	O	X	FN1	107
MgCl ₂ + KCl ^b	12.3,73.6	314.5	21	6.1	O	X	FN2	108
MgCl ₂ + CsCl ^c	13.2,41.5	316.4	26.5	6.0	O	X	FN2	108
CaCl ₂	12.3-55.8	314-315	21-23	6	O	X	FN1	113
CaCl ₂	12.4	325		5.8	n	N	fod	114
CaCl ₂	12.4	325		5.7	n	N	fod	206
CaCl ₂	50	312	22	8.2	n	X	FN3	116
SrCl ₂	21.5	320		8.2-8.9	n	X	rdf	103
SrCl ₂	26.5,34.6	318,319	19,13	6	O	X	SNM	119
BaCl ₂	36	320		8.2-8.9	n	X	rdf	103
BaCl ₂	50.5	326		6.2	n	N	fod	206
NiCl ₂	12.6	320		5.5	n	N	fod	131
NiCl ₂	12.6,27.4	313,314	21,28	6	O	X	FN1	132
NiCl ₂	14,28	313	18,21	6	O	X	SNM	105
NiCl ₂	12.7,18.5	320,325		5.7,5.5	n	N	fod	206
NiCl ₂	11.5	320		5.7	n	N	fod	136
ZnCl ₂	226-13.9	340-365			n	N	fod	208
CrCl ₃	23.4	314	23	6	O	X	SNM	166
CrCl ₃	55	308	25	6	O	X	SNM	167
CrCl ₃	17.9,26.5	317,316	28,24	6,6	O	X	SNM	209
CrCl ₃ + HCl	24.5	317	23	6	O	X	SNM	209
AlCl ₃	23.8,54.0	311,314	21,20	6,6	O	X	SNM	173
FeCl ₃	6-21.5	316-324	3-10	1.2-4.8	n	X	SNM	210
FeCl ₃	12-6.7	329,331	18,20	6	O	X	FN3	211
InCl ₃	8.8	320	13	8	H	X	SNM	212
NdCl ₃	19.5	345		3.9	n	N	fod	213
ErCl ₃	58.5-18.2	320		5.4-5.9	n	X	rdf	199
Br⁻								
DBr	55.6	321		6	O	N	FN3	64
NH ₄ Br	7.6	336	22	6	O	X	FN1	70
LiBr	8.4-25	329	23-26	6	O	X	FN1	84
CaBr ₂	26,44.1	334,332	23,26	6,6	O	X	FN1	118
SrBr ₂	15.8,158	340			n	EX	rdf	132
NiBr ₂	9.6-16.5	340		6	n	X	FN3	214
NiBr ₂	24.7	312	20	6	O	X	SNM	215
NiBr ₂	11.9,24.7	333,335	20,21	6	O	X	FN1	216
CuBr ₂	>1000	317-332			n	EX	rdf	217
ZnBr ₂ + 3LiBr ^d	38.4	349	20	4.36	n	E	FN3	218
ZnBr ₂ + 3LiBr ^d	38.4	345	25	4.20	n	X	FN3	218
ZnBr ₂ ^e	10.1	333-337	14-20	5.0-6.5	n	X	SNM	219

Table 6. (Continued)

salt	H ₂ O/salt molar ratio	<i>r</i> _{XO} , pm	<i>l</i> _{XO} , pm	<i>n</i> _{XO}	symmetry	method	model	ref
Br ⁻								
ZnBr ₂	7.57–1.0	385–340	12–6	2.9–8.0	n	X	SNM	220
InBr ₃	9.2	320	13	8	H	X	SNM	212
I ⁻								
NH ₄ I	8.2	361	24	6	O	X	FN1	70
LiI	129.6	370		4.2	n	X	rdf	93
LiI	10	370		9.6	n	X	rdf	93
LiI	25	363	36	6.9	n	X, MD	SNM	82
LiI	20,9.2	358,358	30,26	8.3,7.7	n	X	FN1	83
LiI ^c	20,9.2	355,359	19,18	5.6,4.7	n	X	FN1	83
NaI	7	360	22	6.4	n	X	FN3	88
KI	108,19.5	370		4.2	n	X	rdf	93
KI	8.4	370		9.6	n	X	rdf	93
ZnI ₂ ^e	18–55	355–363	4–29	3.4–0.8	n	X	SNM	221
ZnI ₃ ^h	5,10	356,357	13,17	4,5.6	n	X	FN3	222
ZnI ₂ ^{h,i}	5	360	17	6	n	X	FN3	222
ZnI ₂ ^{h,j}	5,10	357,354	14,17	5,6	n	X	FN3	222
ErI ₃	41.7	360		6.3–7.0	n	X	rdf	199

^a In the glassy state at –148 °C. ^b KCl ion pairs are formed. ^c CsCl ion pairs are formed. ^d 25 % [Zn(H₂O)₆]²⁺, 25 % [Zn(H₂O)₅Br]⁺, 35 % [Zn(H₂O)Br₃]⁻, and 15 % [ZnBr₄]²⁻ complexes coexist. ^e Parameters at –40, 25, 40, 80, and 100 °C are given. ^f At 70 °C. ^g LiI ion pairs are formed. ^h [ZnI_{*n*}]^{(2–*n*)⁺ complexes are formed. ⁱ Supercooled at –5 °C. ^j In the glassy state at –20 °C.}

Table 8). In the solution phase where the hydrated ions are surrounded by water molecules in the second coordination shell and in the bulk, on the other hand, the water molecules in the first hydration sphere are hydrogen bonded with water molecules outside the sphere, and thus, the water molecules in the first hydration sphere have the tilt angle θ of 30–70° (Tables 8 and 12).

2. Divalent Cations

Be²⁺. The beryllium ion is unique among the cations in the 2 group due to its high charge and small ionic size. Different from other ions, the beryllium ion has only four water molecules in the first coordination sphere according to the results of the X-ray diffraction measurements.¹⁰⁰ The same structure has been confirmed by MO calculations.³⁴³ MD simulations with modified potential functions, in which charge transfer from water molecules to the beryllium ion is more or less taken into consideration, show the hydration number of the beryllium ion to be 4³⁰⁶ instead of 6.¹⁰⁰ The conclusion may be obvious for most coordination chemists, because the coordination number of beryllium ions in many complexes is 4, and no 6-coordinated beryllium complex has been found. The Be²⁺–OH₂ bond length has been determined to be 169 pm by the solution X-ray diffraction method,¹⁰⁰ which is close to the sum of the reported ionic radius of the beryllium ion³⁴¹ and the size of a water molecule. The bond length evaluated by molecular dynamic simulations^{100,306} is slightly longer than the experimental value, probably due to a weaker Be²⁺–H₂O interaction in the simulation calculations than the real one in spite of the modification of the potential function³⁰⁶ from the original one.¹⁰⁰ NMR data also tell us the hydration number of 4 for the beryllium ion as expected^{35,315–317} (Table 18).

Mg²⁺. The magnesium ion is one of the most widely investigated ions by the X-ray diffraction method and computer simulations, and their results agree fairly well each other.^{101–112,132,136} The Mg²⁺–OH₂ bond length is evaluated to be 200–215 pm by the X-ray diffraction method, and many values fall in the range of 200–212 pm.^{103–106,109,110} An MD calculation shows an octahedrally coordinated hydration structure of Mg²⁺ with

the Mg²⁺–OH₂ bond length of 200 pm.³⁰⁸ In fact, the distribution of hydration numbers around Mg²⁺ ions is very sharp at CN = 6, although the distribution covers the range 1–6³¹² (Table 15). NMR data also show the hexahydration structure of Mg²⁺.^{313,318,319} The tilt angle of the hydrated water molecules θ is 14°.³⁰⁸

Ca²⁺. The hydration structure of the Ca²⁺ ion may be the 6-coordinated according to most X-ray diffraction data,^{62,101,107,113,117} although some other hydration numbers have been reported. However, molecular dynamics simulations show a much larger value for the hydration number of 9.2–9.6^{116,285} than that obtained by the diffraction methods. Since the hydration number of the first shell of Ca²⁺ is evaluated from the area under the peak ranged from $r = 0$ to $r_{1,\min}$ in the radial distribution curve obtained by the MD calculation, the large hydration number may be obtained due to an asymmetric shape of the first peak of the radial distribution curve. The tilt angle of the hydrated water molecules is estimated to be 26–43°.²⁸⁵

Sr²⁺. The hydration number of Sr²⁺ may be larger than that of Ca²⁺ because of the larger ionic radius of the former than that of the latter. X-ray and neutron diffraction data^{103,115,119,120} give a value more than 6. A result by MD simulations also gives a value of 9.8.³⁰⁹ A value given by an NMR measurement³¹⁷ is even smaller than that of Ca²⁺, which is probably due to an erroneous evaluation of the peak area of the NMR spectrum for such an ion with a fast exchange rate for the solvent substitution reaction.

The Sr²⁺–OH₂ bond length has been determined to be 260–265 pm^{103,119,120,309} by the diffraction and simulation methods.

Ba²⁺. Since barium extensively absorbs X-rays, barium salt solutions for the structural studies by the X-ray diffraction methods are not favorable. Since Ba²⁺ has so many electrons, reliable functions for the cation–anion, cation–water pair potentials are hard to obtain by molecular orbital calculations. Therefore, very few investigations have been done for the hydration structure of Ba²⁺. An X-ray diffraction study shows us the Ba²⁺–H₂O bond length of 290 pm.¹⁰³ The hydration number evaluated by the diffraction work is 9.5,¹⁰³ which accidentally agrees with an NMR data (9.7).³¹⁷

Table 7. Structural Parameters of the Hydration Shell of Oxyanions (XO_n^{2-}) Derived from Diffraction Measurements (See Section III for the Full Definitions of the Abbreviations)

salt	$\text{H}_2\text{O}/\text{salt}$ molar ratio	$r_{\text{XO}(\text{H}_2\text{O})}$, pm	$l_{\text{XO}(\text{H}_2\text{O})}$, pm	$n_{\text{XO}(\text{H}_2\text{O})}$	symmetry	method	model	ref
NO_3^-								
HNO_3	25	325		9	n	X	FN3	67
NH_4NO_3	4.4	350	31	3	n	X	FN3	223
NaNO_3^a	6.1,9.3	314,322	15,28	6	n	X	FN3	89
NaNO_3	7.1	340		1.3,2.4	n	N	fod	224
AgNO_3	14.2	317	27	4.3	n	X	FN3	95
AgNO_3	6.6,4.3	350,340	18,16	11,7.2	n	X	FN3	97
$\text{Zn}(\text{NO}_3)_2$	9.0	344	19	17.7	n	X	SNM	153
$\text{Cd}(\text{NO}_3)_2$	9-54	349	16	8.8	n	X	SNM	225
$\text{Al}(\text{NO}_3)_3$	14.5	339	22	5.9	n	X	SNM	174
$\text{Rh}(\text{NO}_3)_3$	61,145	350	16	8.2	n	X	SNM	226
$\text{Ce}(\text{NO}_3)_3$	25.4	340	28	7.0	n	X	SNM	227
ClO_4^-								
NH_4ClO_4	37	400	51	12.1	n	X	FN3	69
NaClO_4	17.1	360-380		4-5	n	N	fod	228
AgClO_4	10.4	357	50	25.6	n	X	FN3	95
AgClO_4	16.3,3.3	375,370	32,28	7.5,7.9	n	X	FN3	97
$\text{Mg}(\text{ClO}_4)_2$	18	374	31	10.1	n	X	SNM	110
$\text{Sn}(\text{ClO}_4)_2$	16.8	380	5	8	n	X	SNM	164
$\text{Y}(\text{ClO}_4)_3$	40,12.4	380	30	8	n	X	SNM	10
$\text{Rh}(\text{ClO}_4)_3 + \text{HCl}$	277	376	26	12	n	X	SNM	66
$\text{La}(\text{ClO}_4)_3$	12.0	380	30	8	n	X	SNM	10
$\text{Ce}(\text{ClO}_4)_3 + \text{HClO}_4$	38	374	31	10.1	n	X	SNM	110
$\text{Sm}(\text{ClO}_4)_3$	15.2	380	30	8	n	X	SNM	10
$\text{Tb}(\text{ClO}_4)_3$	39.4,13.7	380	30	8	n	X	SNM	10
$\text{Er}(\text{ClO}_4)_3$	12.1	380	30	8	n	X	SNM	10
SO_4^{2-}								
$(\text{NH}_4)_2\text{SO}_4$	15.6	379	24	7.6	n	X	FN1	229
$(\text{NH}_4)_2\text{SO}_4$	15.8	393	30	11.2	n	X	FN3	73
$(\text{NH}_4)_2\text{SO}_4$	14.3	370	20	8	n	X	FN3	230
MgSO_4	20.5	370	22	7.7	n	X	SNM	111
MnSO_4^a	28	382	20	8	n	X	SNM	141
NiSO_4	27.5	381	29	8.1	n	X	SNM	111
$\text{NiSO}_4 + \text{H}_2\text{SO}_4$	48	380	25	7.6	n	X	SNM	111
NiSO_4^a	28	392	10	9.6	n	X	SNM	141
NiSO_4	18,27	379	28	8.2	n	X	SNM	142
$\text{NiSO}_4 + \text{Li}_2\text{SO}_4$	37	380	20	8.2	n	X	SNM	142
CuSO_4	40.4	378	17	8.2	n	X	SNM	150
ZnSO_4	18.6	383	27	8.2	n	X	SNM	231
ZnSO_4	27.1	387	19.3	6.95	n	X	SNM	154
ZnSO_4	100-16.9	383-391	17-28	14.3-7.6	n	X	SNM	155
CdSO_4	17.6	374	28	12	n	X	SNM	160
CdSO_4^b	25	389,383	15,13	6.9,6.0	n	X	SNM	232
$\text{Cr}_2(\text{SO}_4)_3$	18.7	381	21	7.8	n	X	SNM	233
$\text{In}_2(\text{SO}_4)_3$	14.2	389	23	6.4	n	X	SNM	234
SO_3^{2-}								
$(\text{NH}_4)_2\text{SO}_3$	14.3	380	36	9	n	X	FN3	230
$\text{S}_2\text{O}_5^{2-}$								
$(\text{NH}_4)_2\text{S}_2\text{O}_5$	6.1,4.7	376,377	25	9.2,8.9	n	X	FN3	230
SeO_4^{2-}								
$\text{Y}_2(\text{SeO}_4)_3$	69,58.2	395	30	8	n	X	SNM	10
$\text{La}_2(\text{SeO}_4)_3$	76.9,47.0	395	30	8	n	X	SNM	10
$\text{Tb}_2(\text{SeO}_4)_3$	44.3	395	30	8	n	X	SNM	10
$\text{Er}_2(\text{SeO}_4)_3$	68.7,53.1	395	30	8	n	X	SNM	10
CrO_4^{2-}								
Na_2CrO_4	30.7	396	25	12	n	X, N	iso, fod	267
MoO_4^{2-}								
$\text{Na}_2(\text{MoO}_4)_3$	25	406	34	12	n	X	iso	235
WO_4^{2-}								
$\text{Na}_2(\text{WO}_4)_3$	25	406	34	12	n	X	iso	235
PO_4^{3-}								
H_3PO_4	25.1,7.2	373,360	18,16	4 or 8	n	X	FN1	236
H_2PO_4^-								
$\text{Mg}(\text{H}_2\text{PO}_4)_2$	34.0	387	33	8.8	n	X	SNM	237
$\text{Ni}(\text{H}_2\text{PO}_4)_2$	45.6	375	22	4.2	n	X	SNM	238
$\text{Cd}(\text{H}_2\text{PO}_4)_2$	41.7	391	28	4.4	n	X	SNM	238
CH_3CO_2^-								
$\text{Mg}(\text{CH}_3\text{CO}_2)_2$	33.1,14.9	360,370	17,14	4.2,6.1	n	X	SNM	239
$\text{Mn}(\text{CH}_3\text{CO}_2)_2$	33.5	363	19	5.3	n	X	SNM	239

Table 7. (Continued)

salt	H ₂ O/salt molar ratio	$r_{\text{XO}(\text{H}_2\text{O})}$, pm	$l_{\text{XO}(\text{H}_2\text{O})}$, pm	$n_{\text{XO}(\text{H}_2\text{O})}$	symmetry	method	model	ref
			CH ₃ CO ₂ ⁻					
Co(CH ₃ CO ₂) ₂	53.7	360	14	5.5	n	X	SNM	239
Zn(CH ₃ CO ₂) ₂	34.0	352	13	5.2	n	X	SNM	239
Cd(CH ₃ CO ₂) ₂	43.0, 23.0	372, 367	24, 17	4.2, 3.0	n	X	SNM	239

^a Cation-anion contact ion pairs are found. ^b At 9 °C and 62 °C.

Divalent Transition Metal Ions in the First Row. For a long time, the divalent transition metal ions have attracted much attention of traditional coordination chemists, and the ions are still being extensively studied by coordination chemists. The hydration structure of the ions are believed to be regular octahedral except for the Cr²⁺ and Cu²⁺ ions which have d⁴ and d⁹ electron configurations, respectively. These two ions should have a distorted octahedral structure with either elongated or shortened axial bonds perpendicular to the square plane. Investigations for the hydration structure of the divalent transition metal ions have been done by many authors using the visible spectroscopic method, and the octahedral structure predicted by the ligand field theory has been well accepted. However, information about the length of the M²⁺-OH₂ bonds have been scarcely available, because crystals containing hexahydrated metal ions are hardly obtainable and some of the water molecules in the coordination sphere are often replaced with other ligands. Since the water molecules at the apexes of the elongated axis in the distorted octahedral structure of Cr²⁺ and Cu²⁺ are easily replaced with other ligands, no reliable data for the metal-water(ax) bond length have been reported. The diffraction and EXAFS methods have an advantage of determining the bond length of the elongated axis, in principle, provided that the hydrated ions with a distorted octahedron exist in the solution. In the following we will discuss the hydration structure of divalent transition metal ions of the first row in the periodic table.

Ti²⁺. The titanium(II) ion can exist in water, but due to its very strong reducing properties, it is extremely difficult to handle as solution samples containing pure Ti(II) salts. Therefore, no structural data has been reported for Ti²⁺.

V²⁺. The V²⁺ ion is also a strong reducing agent and hard to use as sample solutions for diffraction studies. An attempt appears to have been made by the EXAFS method according to ref 344, in which the V²⁺-H₂O bond length is reported. However, no detailed information, including the composition of the salt used, is given in the literature. Therefore, the structural data given in ref 344 may not be very reliable.

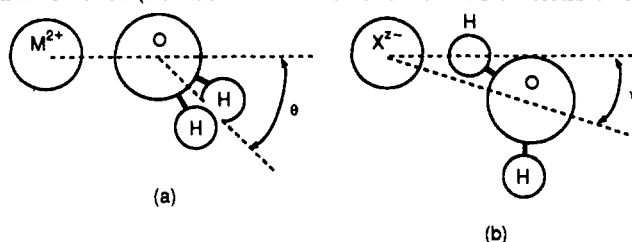
Cr²⁺. The Cr²⁺ ion has 4 d electrons, and thus, the ion is expected to show the Jahn-Teller distortion when the ion has an octahedral structure with a high-spin electron configuration. The structure of the hydrated Cr²⁺ ion is studied by the EXAFS method, and the Cr²⁺-OH₂(equatorial) is reported to be 208 pm.³⁴⁴ The Cr²⁺-H₂O(axial) bonds are not observed in the experiment, although the authors expected the distorted octahedral structure for the Cr²⁺ ion.

Mn²⁺ to Zn²⁺. The structure of hydrated ions from Mn²⁺ to Zn²⁺ has thoroughly been studied by various experimental and theoretical methods. Accumulated experimental data for the static structure of the ions in water have been reviewed by Marcus⁶ and they are

also summarized in Table 2. All the ions have six water molecules in the first coordination sphere, and the M²⁺-H₂O bond length varies from 220 pm in Mn²⁺^{121,123} to 208–210 pm in Zn²⁺^{101,121,154,156–158} passing through the shortest M²⁺-OH₂ bonds in the square plane of the [Cu(H₂O)₆]²⁺ complex having a distorted octahedral structure. The lengths of the M²⁺-OH₂ bond, as well as the dissociation energies of the hydrated water molecules, have recently been calculated by using the local spin density function method for ions from Cr²⁺ to Zn²⁺.³⁴⁵ According to the results the bond lengths and the number of the bonds are as follows: Cr²⁺ [2 × 202.5 pm + 2 × 202.8 pm + 2 × 226.8 pm], Mn²⁺ [6 × 212.1 pm], Fe²⁺ [2 × 207.0 pm + 2 × 207.2 pm + 2 × 207.5 pm], Co²⁺ [2 × 202.8 pm + 2 × 203.8 pm + 2 × 205.6 pm], Ni²⁺ [6 × 200.2 pm], Cu²⁺ [2 × 197.3 pm + 2 × 199.0 pm + 2 × 219.3 pm], and Zn²⁺ [6 × 205.7 pm]. Since the calculations have been done for the isolated [M(H₂O)₆]²⁺ ions, the negative end of the dipoles of the hydrated water molecules orient toward the central ions, which do not fit to the experimental results found by the neutron diffraction measurements^{125,131,133,136,146,240} (Table 8). The trend in the bond length variation of the ions corresponds to the change in the hydration energies of the ions, which is known as the Irving-Williams series and has been explained in terms of the change of the ligand field stabilization energies.¹²¹ The variation of the dissociation energy of a water molecule from the hydration sphere of the ions thus calculated is similar to the experimental²⁰³ and calculated^{121,346} values reported in previous studies. Results for the M²⁺-H₂O bond lengths obtained by simulation calculations slightly disagree with experimental results (Table 8), due probably to incomplete potential functions to describe ion-water interactions. The NMR method is not quite suitable for studies of the hydration structure of the ions, except for Zn²⁺, due to the paramagnetic property of the ions.

Cd²⁺ and Hg²⁺. Cadmium(II) and mercury(II) ions have the regular octahedral structure and the M²⁺-H₂O bond lengths are 229 pm^{101,160} and 233 pm,¹⁶³ respectively. NMR data³¹⁷ (Table 11) give smaller coordination numbers than those found by the diffraction methods, due probably to fast water substitution reaction rates of the ions. No simulation calculation has been undertaken for such ions having a large number of electrons.

Sn²⁺. Sn²⁺ is a peculiar ion, having a less symmetrical hydration structure than other d¹⁰ ions. In the 6-coordinated hydration structure, two kinds of bonds have been observed, one has the bond length of 233–234 pm and the other of 238–290 pm.^{164,165} The asymmetry may arise from the electronic configuration of the ion having 5p² electrons, but since no other ions in the 14 group has been investigated for their hydration structures, we cannot draw a reliable conclusion for the origin of the asymmetric hydration structure of the ion.

Table 8. Structural Parameters of the Orientation of Water Molecules in the First Hydration Shell of Ions Derived from Neutron Diffraction Measurements (See Section III for the Full Definitions of the Abbreviations)

Orientation of water molecule around (a) a cation and (b) an anion

salt	H ₂ O/salt molar ratio	<i>r</i> _{MO} , pm	<i>l</i> _{MO} , pm	<i>n</i> _{MO}	<i>r</i> _{MH} , pm ^a	<i>l</i> _{MH} , pm ^a	<i>n</i> _{MH} ^a	<i>θ</i> or <i>ψ</i> , deg ^b	symmetry	second shell	model	ref
H₃O⁺												
HCl ^c	4-96	252		4				linear	T	n	FN1	63
DCI	55.6	288		4				linear	T	n	FN3	64
Li⁺												
LiCl ^c	3-8.2	195-225	25-31	4	271-273	35-24	8	70	T	n	FN1	74
LiCl	54.3	190		4				54.75	T	n	FN3	76
LiCl	13.9,27.8	208,217	51,25	4					T	n	FN2	77
LiCl	5.6,15.6	195,195		3.3,5.5	250,255			52,40	n	i	fod	78
LiBr	31.7	194		4.5	258		9.2		n	n	fod	85
Cs⁺												
CsCl	53.1	295		8				54.75	n	n	FN3	76
Ca²⁺												
CaCl ₂	12.4	240		5.5	293			51	n	n	fod	114
CaCl ₂	55,20,12	246,239,241		10,7.2,6.4	307,302,304			38,34,34	n	n	fod	115
Fe²⁺												
FeCl ₂ + HCl	52.2	213	28	6	275	36	12.1	32	n	i	fod	125
Ni²⁺												
NiCl ₂	12.6	205		5.8	265			30	n	n	fod	131
NiCl ₂	12.6-645	207-210		5.8-6.8				42-0	n	n	fod	133
NiCl ₂	11.5	207	13	5.8	267	19		40	n	n	fod	136
NiCl ₂	28-550	206		5.9-5.4	268	1.7	12	invar ^d	n	n	fod	137
NiCl ₂ ^e	25	206		5.9	267		11.7		n	n	rdf	138
NiCl ₂ ^f	25	207		6.0	269		11.8		n	n	rdf	138
Ni(ClO ₄) ₂	14.6	207		5.8	267			42	n	n	fod	240
Cu²⁺												
Cu(ClO ₄) ₂ ^g	14.6	197		6	260			36	O	n	fod	146
Zn²⁺												
Zn(CF ₃ SO ₃) ₂	27.8	209	13	5.3	269	16	10.6		n	n	fod	156
Cr³⁺												
Cr(ClO ₄) ₃ ^h	25-27	198	27	5	260	36	11.5,12.0	34	n	n	fod	172
Fe³⁺												
FeCl ₃	52.2	201	32	6	268	40	12.0	20	n	i	fod	125
Fe(NO ₃) ₃ ⁱ	29.9,25.5	201,202		6,4,9	268,268		12,8.3	41	O	i	fod	178
Ln³⁺												
PrCl ₃	14.6	248		10	314			22	n	n	iso	187
NdCl ₃	17.5	248		8.5	313			55	n	n	rdf	189
NdCl ₃	17.5	248	9	8.4	313	17	16.7	24	n	n	fod	190
NdCl ₃	14.6	248		10	314			22	n	n	iso	187
Nd(ClO ₄) ₃	55,165	250,252	30,28 ^j	8.9,8.8	314,315	42,41 ^j			n	n	fod	192
Sm(ClO ₄) ₃	55	246	31 ^j	8.5	311	43 ^j			n	n	fod	192
TbCl ₃	18.4	239		9	308			10	n	n	iso	187
DyCl ₃	21.0	237	15	7.4	304	19		14	n	n	fod	197
DyCl ₃	18.4	239		9	308			10	n	n	iso	187
DyCl ₃	55,165	238	25 ^j	7.8	303	35 ^j			n	n	iso	198
Dy(ClO ₄) ₃	55	239	25 ^j	7.9	303	35 ^j			n	n	iso	198
TmCl ₃	15.6	233		8	302			12	n	n	iso	187
YbCl ₃	15.6	233		8	302			12	n	n	iso	187
Yb(ClO ₄) ₃	55	232	24 ^j	7.8	298	33 ^j			n	n	iso	198
Cl⁻												
DCI	55.6	310		6				bifurc ^k	n	n	FN3	64
LiCl ^c	3-8.2	319-320	19-20	6	226-216	25-24	6	70	T	n	FN1	74
LiCl	54.3	310	6					undet ^l	n	n	FN3	76
LiCl	5.6,15.6	329		5.3,5.9	222				n	n	fod	78
LiCl	5.6,15.6	329,334		5.3,5.9	222,225			0	n	n	fod	206
LiCl	6.0	320		5.4	222.5		5.4		n	n	fod	207
LiCl ^m	6.0	317.5		5.4	222.5		5.4		n	n	fod	207

Table 8. (Continued)

salt	H ₂ O/salt molar ratio	<i>r</i> _{MO} , pm	<i>l</i> _{MO} , pm	<i>n</i> _{MO}	<i>r</i> _{MH} , pm ^a	<i>l</i> _{MH} , pm ^a	<i>n</i> _{MH} ^a	θ or ψ, deg ^b	symmetry	second shell	model	ref
Cl ⁻												
NaCl	54.3	310		6				bifurc ^k	n	n	FN3	87
NaCl	10.4	320		5.5	226			0-10	n	n	fod	206
KCl	53.7	310		6				bifurc ^k	n	n	FN3	87
RbCl	12.7	320		5.8	226			0-10	n	n	fod	206
CsCl	53.1	310		6				undet ⁱ	n	n	FN3	76
CaCl ₂	12.4	325		5.8	225			0	n	n	fod	114
CaCl ₂	12.4	325		5.7	222			0-6	n	n	fod	206
BaCl ₂	50.5	326		6.2	224			0-6	n	n	fod	206
NiCl ₂	12.6	320		5.5				12	n	n	fod	131
NiCl ₂	12.7,18.5	320,325		5.7,5.5	229,223		6-11	0-6	n	n	fod	136
NiCl ₂	11.5	320		5.7	229			7	n	n	fod	136
ZnCl ₂	226-13.9	340-365			225-227		5.1-4.4		n	n	fod	208
NdCl ₃	19.5	345		3.9	229				n	n	fod	213
ErCl ₃	58.5-18.2	320		5.4-5.9					n	n	rdf	199
Br ⁻												
DBr	55.6	321		6				bifurc ^k	O	n	FN3	64

^a H denotes hydrogen or deuterium. ^b θ is used for cations, ψ for anions (see below). ^c The X-ray diffraction method is also applied. ^d invar = orientation of water molecules is invariant and independent of concentrations of the salt. ^e In H₂O. ^f In D₂O. ^g The Jahn-Teller effect is not observed. ^h Three different isotopic mixtures. ⁱ The second sample is heated to 90 °C during the preparation. ^j Full width of half height (FWHH) values. ^k bifurc = water molecules combine with the ion in a bifurcated way. ^l undet = bond angle is not determined. ^m In the glassy state at -148 °C.

Table 9. Structural Parameters of the Incompletely Hydrated First Shell of Metal Complexes [M^IA_m(H₂O)_n]⁺ of Monovalent Cations Derived from Diffraction and EXAFS Measurements (See Section III for the Full Definitions of the Abbreviations)

salt	H ₂ O/salt molar ratio	<i>r</i> _{MO} , pm	<i>l</i> _{MO} , pm	<i>n</i> _{MO}	<i>r</i> _{MA} , pm	<i>l</i> _{MA} , pm	<i>n</i> _{MA}	symmetry	second shell	method	model	ref
Li ⁺												
LiCl	2.0	195		2.3	276		1.5	n	n	N	fod	241
LiCl	3.35	195		2.3	275			n	n	N	fod	242
LiCl	3.0	200		4	280		1	O	n	X, MD	FN3	243
Na ⁺												
NaCl	9.0	241	23	4.6	282	30	0.3	n	n	X	FN3	244
K ⁺												
KCl	12.2	281	13	5.8	315	15	0.6	n	n	X	FN3	244
KCl + MgCl ₂ ^a	12.3,73.6	277	18	3.7	320	17	2.4	n	n	X	FN2	108
KI	8.4	290		1.7	370		1	n	n	X	rdf	93
KF	9.0	280	17	3.3	269	26	2.3	n	n	X	FN3	244
Cs ⁺												
CsCl	5.5-22.2	315		1.9-6.2	330-360		2.7-3.5	n	n	X	rdf	245
CsCl + MgCl ₂ ^a	13.2,41.5	315	29	4.7	339	23	2.0	n	n	X	FN2	108
CsI	22.2	315		8.8-8.9	390-410		1.4-2.4	n	n	X	rdf	245
CsBr	11.1,22.2	315		7.2-8.9	350-390		2.0-2.5	n	n	X	rdf	245
CsI	20	301	18	5.8	388	35	0.8	n	n	X	FN3	83
CsI ^b	20,10	306,302	21,15	4.7,3.0	385,385	36,48	0.8,1.2	n	n	X	FN3	83
CsF	1.7	321	25	3.6	312	33	3.3	n	n	X	FN3	244
Ag ⁺												
AgNO ₃	5-16.8	236-231	6-10	1.9-2.9	315-326		1	n	n	EX	FN3	98
AgClO ₄	3.3	243	16	3	352	20	1	T	a	X	SNM	97
AgNO ₃	4.3	243	14	3	313	21	1	T	a	X	SNM	97

^a The Mg²⁺ ions do not form ion pairs. ^b At 70 °C.

Pb²⁺. The Pb²⁺ ion is not suitable for study by the diffraction method, because it extensively absorbs X-rays. The NMR method may be more adequate because of its diamagnetic property. According to the NMR measurement,³¹⁷ Pb²⁺ has six water molecules in the first coordination sphere as expected.

3. Trivalent Cations

Al³⁺. The Al³⁺ ion is an inert ion and is one of the ions with the strongest ion-water interactions because of its high charge and small ionic radius. The structure of the hydrated Al³⁺ ion is a 6-coordinated one with the Al³⁺-H₂O bond length of 187-190 pm.^{169,173,174} Since

the ion is very inert, splitted NMR signals of ¹⁷O in H₂¹⁷O water are observed, which are the signal from the bulk water in the lower field and that from the hydrated water in the high field, the two peaks being separated by 2330 Hz (430 ppm).³¹⁵ From the area under the peaks, the hydration number of Al³⁺ is calculated to be 6. In most NMR measurements it is difficult to observe separate peaks of the bulk and the hydrated water, but the Al³⁺ case is a typical example for the NMR determination of the hydration structure of ions.

Cr³⁺. The Cr³⁺ ion is an extremely inert ion. The hydration structure of the ion is regular octahedral with

Table 10. Structural Parameters of the Incompletely Hydrated First Shell of Metal Complexes $[M^{II}A_n(H_2O)_n]^{2+}$ of Divalent Cations Derived from Diffraction and EXAFS Measurements (See Section III for the Full Definitions of the Abbreviations)

salt	H ₂ O/salt molar ratio	r_{MO} , pm	l_{MO} , pm	n_{MO}	r_{MA} , pm	l_{MA} , pm	n_{MA}	symmetry	second shell	method	model	ref
Mg²⁺												
Mg(H ₂ PO ₄) ₂	34	211	12.6	6			1.0	O	a	X	SNM	237
Mg(CH ₃ CO ₂) ₂	33.1,14.9	209,219	8.8,14.1	5.2,5.2			0.8,0.8	O	a	X	SNM	239
Ca²⁺												
CaCl ₂ ^a	6.2	244		5.9	275		0.9	n	a	X	FN3	117
CaCl ₂ ^b	6.0	245		5.6	274		1.0	n	a	X	FN3	117
CaCl ₂ ^c	6.2	245		5.3	274		1.4	n	a	X	FN3	117
CaCl ₂ ^d	5.6	244		4.8	275		1.7	n	a	X	FN3	117
CaCl ₂ ^e	4.0	246		3.9	280		2.1	n	a	X	FN3	117
Mn²⁺												
MnCl ₂	9.7,17.3	218.4	10	4.65,4.45	250,250	10,10	1.3,1.5	O	n	X	FN3	246
MnCl ₂	550–11	220	11	6–5.3	249	31		O	a	EX	SNM	247
MnBr ₂	8.3,16.2	218.1	9	5.0,4.8	264,260	10,10	1.1,1.2	O	n	X	FN3	246
Mn(NO ₃) ₂	12.6	219	13	5.4		12	0.6	O	a	X	SNM	248
MnSO ₄	13.2,26.8	222,220	10,12	5.2,5.1		10,13	0.75,0.92	O	a	X	SNM	249
MnSO ₄	28	220	10	5.5	350	11	0.5	O	a	X	SNM	141
Mn(CH ₃ CO ₂) ₂	33.5	220	11	5.2		19	0.8	O	a	X	SNM	239
Fe²⁺												
FeCl ₂	55.5	224	8	5.6	258	18	0.4	O	n	X/	SNM	126
FeBr ₂	17.8,10.3	212	9,7	5.5,5.1	260,262	11,12	0.3,0.7	n	n	X	FN3	250
FeSO ₄	55.5	228	8	5.8	349	26	0.2	O	n	X/	SNM	126
Co²⁺												
CoCl ₂	17.9	210	10	5.5	247	11	0.5	O	a	X	SNM	251
CoCl ₂ + HCl	23.2	214	11	5	235	11	1	O	n	X	FN3	65
CoCl ₂ + LiCl	7.5	210	12	5.5	249	16	1	O	n	X	FN3	182
CoCl ₂ + LiCl	23.1	214	11	5.0	235	11	1	O	n	X	FN3	65
CoCl ₂ + LiCl	8–17	208–209	10–12	5	245–242	13–12	1	O	a	X	SNM	81
CoCl ₂ + NiCl ₂ + 6LiCl	110	210,211	10	5.9,5.7	239,229	14	0.8,1.2	O, n	a	X, EX	SNM	252
CoBr ₂	18.2,10.8	210	8	6.5,3	258	12	0.3,0.6	n	n	X	FN3	250
Co(CH ₃ CO ₂) ₂	53.7	214	11	5.2		21	0.8	O	a	X	SNM	239
Ni²⁺												
NiCl ₂	18	207	9	5.5	244	10	0.5	O	a	X	SNM	251
NiCl ₂	25	206		6.5			0	n	n	EX	FN3	253
NiCl ₂ + HCl ^g	24.6	205.6	7	5.1	247	14		O	a	X	SNM	254
NiCl ₂ + 2LiCl ^h	24.8	206.4	8	4.8	243	13		O	a	X	SNM	254
NiCl ₂ + 3LiCl ⁱ	23.2	207.2	9	4.6	244	12		O	a	X	SNM	254
NiCl ₂ + 4LiCl	25	205		6.0	238		0.7	n	n	EX	FN3	253
NiCl ₂ + 6LiCl	25	205		5.3	238		1.0	n	n	EX	FN3	253
NiCl ₂ + CoCl ₂ + 6LiCl	110	210,206	10	5.9,5.2	239,229	14,–	0.81,0.67	O	a	X, EX	SNM	252
NiBr ₂	9.6–16.5	204–205	8–9	5.7–5.4	258–252	13–12	0.2–0.7	O	n	X	SNM	214
NiBr ₂	24.7	206.5	11	5.7	262	9	0.3	O	a	X	SNM	215
NiBr ₂	11.9,24.7	207.9,206.6	10,8	5.6,5.7	262,261	13,13	0.44,0.29	O	a	X	SNM	216
Ni(en) ₂ (NO ₃) ₂	22.9	210	7,7	2	210	7,4	4.0	O	n	X	FN3	268
Ni(gly) ₂	15.7	208	10	4	209(O),209(N)	11,11	1(O),1(N)	O	n	X	FN3	269
Ni(H ₂ PO ₄) ₂	45.6	203	11	5.25		10	0.75	O	a	X	SNM	238
Cu²⁺ ^j												
CuCl ₂ ^k	10.9	{ 195 –		{ 2.4 –	{ – 243		{ 3.6 –	O	n	X	rdf	255
CuCl ₂ ^k	15.7	{ 195 –		{ 2.7 –	{ – 243		{ 3.3 –	O	n	X	rdf	255
CuCl ₂ ^l	18	{ 195 263	{ 8 16	{ 4 2	{ 225 –	{ 8 –	{ 1.2 –	O	n	X	FN1	251
CuCl ₂	11.6	{ 205 250		{ 2.3 –	{ 256 –		{ 4.2 or 2.8 –	O	n	N	fod	256
CuCl ₂	12.8	196	16	3.4				O	n	N	fod	257
CuCl ₂ + nNH ₃ ^m	18.9–20.5	{ – 233	{ – 10	{ – 2				O	n	X	FN1	258
CuBr ₂	>1000	197						n	n	EX	rdf	217
CuBr ₂	12,100	{ 193 –		{ 3.5 –	{ – 239		{ – 1.5	O	n	EX	FN3	259
CuBr ₂	>100	{ 193 –		{ 7 –	{ – 235		{ – 0.5	n	n	EX	FN3	260
CuBr ₂	sat.	193		3.5	(240)			H	n	EX	FN3	260
CuBr ₂	10.8–53.1	{ 196–199 237–251		{ 2.5–3.7 2	{ 246–241 –		{ 1.3–0.3 –	O	n	X	FN3	261
Cu(NO ₃) ₂	23.5,34.7	{ 200 212,222	13 20	{ 4 2	{ 303,307 –	{ 14,11 –	{ 1.2,1.7 –	O	a	X	SNM	262
Cu(en) ₂ (NO ₃) ₂	28.1	{ – 292		{ – 1.8	{ 194,194 –		{ 7.5,7.5 3.8,3.8	O	n	X	FN3	270

Table 10. (Continued)

salt	H ₂ O/salt molar ratio	r _{MO} , pm	l _{MO} , pm	n _{MO}	r _{MA} , pm	l _{MA} , pm	n _{MA}	symmetry	second shell	method	model	ref
Cu²⁺												
Cu(gly) ₂	39.4	{ 198 229	{ 6.3 9	{ 2 2	199(O),199(N)	6,6	1(O),1(N)	O	n	X	FN3	271
Zn²⁺												
ZnCl ₂ ^h	1.8–6.2	205		0.2–1.7	226–225		3.4–2.4	n	n	X	SNM	263
ZnCl ₂	13.9	209	19	4.1	228	13	1.4	n	n	N	fod	156
ZnCl ₂ + nHCl ^o	21.4	205		2–0	230		2–4	T	n	X	rdf	264
ZnCl ₂	55	206.8	15.9	5.3	224	11.1	1.06	n	n	X	FN1	265
ZnCl ₂ + CdCl ₂	55	205	18	5.8	225.4	5	0.9	n	n	X	FN1	265
ZnBr ₂	7–610	194	10	2.5–7	237	9.5	1.75–0.5	n	n	EX	FN3	260
ZnBr ₂ + 3LiBr ^p	38.4	223	8	2.40	240	13	2.22	n	n	E	FN3	218
ZnBr ₂ + 3LiBr ^p	38.4	221	9	2.42	242	12	2.26	n	n	X	FN3	218
ZnBr ₂ ^{q,r}	10.1	210–202	10	3.0–2.0	239.4–237.3	10	2.03–1.99	n	n	X	SNM	219
ZnBr ₂ ^q	7.57–1.0	210	5	6	236–240	6–11	4.00–1.34	O	n	X	SNM	220
ZnI ₂ ^q	18–55	210	17	6	259–264	7–17	3.4–0.8	O	a	X	SNM	221
ZnI ₂	5,10	210,204	8	2.59,2.3	257.9,258.5	7	1.96,1.92	n	n	X	FN3	222
ZnI ₂ ^s	5	210	8	2.70	258.4	7	2.06	n	n	X	FN3	222
ZnI ₂ ^t	5,10	210,203	8	3.00,3.3	259	7	2.06,2.01	n	n	X	FN3	222
ZnSO ₄ ^u	18.6	210	16	6	313	24	1	O	a	X	SNM	231
Zn(CH ₃ CO ₂) ₂	34	207.4	16	4.6		16	1.44	O	a	X	SNM	239
Zn(gly) ₂	22.1	212	8	4	212(O),212(N)	8	1(O),1(N)	O	n	X	FN3	157
	–	204	2		204(O),204(N)	8	2(O),2(N)	O	n	EX	FN3	273
Zn(α-ala) ₂	43.8	208	8	4	202(O),214(N)	8	2(O)	O	a	X	FN3	158
	34.8	208	8	2	203(O),214(N)	8	2(N)					
Cd²⁺												
CdCl ₂	64,44	237	17,13	4	257	15,14	2	O	n	X	FN1	105
CdCl ₂	55	235.9	7.7	4.4	257.6	8	1.75	n	n	X	FN1	265
CdCl ₂ + ZnCl ₂	55	235.1	7.3	1.9	255.3	11.5	2.17	n	n	X	FN1	265
CdBr ₂	13.2–66.2	218		3	255		2	n	n	EX	rdf	266
CdI ₂	41.0	230		5	280	8.6	1	O	n	X	rdf	272
Cd(NO ₃) ₂	9–54	228	12	5.04	361	16		O	a	X	SNM	226
CdSO ₄	17.6	229		5	348	18		O	a	X	SNM	160
CdSO ₄ ^v	25	232,231	9,8	5.66,5.36	350,346	12–14		O	a	X	SNM	232
Cd(H ₂ PO ₄) ₂	41.7	230	14	5.05		13	0.95	O	a	X	SNM	238
Cd(CH ₃ CO ₂) ₂	43.0,23.0	228,227	10	4.3,3.5		23,20	1.7,2.5	O	a	X	SNM	239

^a At 15 °C. ^b At 33 °C. ^c At 80 °C. ^d At 72 °C. ^e At 120 °C. ^f Mössbauer spectra of frozen solutions are also investigated. ^g 29% [Ni(H₂O)₆]²⁺, 50% [Ni(H₂O)₅Cl]⁺, 21% [Ni(H₂O)₄Cl₂]²⁺ complexes are present. ^h 17% [Ni(H₂O)₆]²⁺, 50% [Ni(H₂O)₅Cl]⁺, 33% [Ni(H₂O)₄Cl₂]²⁺ complexes are present. ⁱ 8% [Ni(H₂O)₆]²⁺, 40% [Ni(H₂O)₅Cl]⁺, 52% [Ni(H₂O)₄Cl₂]²⁺ complexes are present. ^j Parameters in the first and second lines refer to equatorial and axial bonds, respectively. ^k Complexes share ligands in the first hydration shell of the cations. ^l 40% [Cu(H₂O)_{4,eq}(H₂O)_{2,ax}]²⁺, 60% [Cu(H₂O)_{2,eq}Cl_{2,eq}(H₂O)_{2,ax}]²⁺ complexes are present. ^m n = 4.8,5,11.2; [Cu(NH₃)₄(OH₂)₂]²⁺, [Cu(NH₃)₅(OH₂)₂]²⁺, and [Cu(NH₃)₆]²⁺ complexes coexist. ⁿ Extensive ordering is reported up to the second neighbors. ^o n = 0,1,2,3,4. ^p 25% [Zn(H₂O)₆]²⁺, 25% [Zn(H₂O)₅Br]²⁺, 35% [Zn(H₂O)₄Br₂]²⁺, and 15% [ZnBr₄]²⁻ complexes are present. ^q The MO parameters refer to those of the hexaaqua complex. The data given in this table are the averaged one for the mono-, di-, tri-, and tetrahalogeno complexes. ^r Parameters refer to those measured at –40, 25, 40, 80, and 100 °C. ^s Supercooled at –5 °C. ^t In the glassy state at –20 °C. ^u 60% [Zn(H₂O)₆]²⁺, 40% [Zn(H₂O)₅SO₄]²⁻ complexes are probably formed. ^v At 9 °C and 62 °C.

the Cr³⁺–H₂O bond of about 198–200 pm^{166–172} (Table 3).

Fe³⁺. The Fe³⁺ ion has also rather small rate constant for the water substitution reaction due to its strong interaction with hydrated water molecules. The hydration structure of the ion is octahedral with the Fe³⁺–H₂O bond length of 201–205 pm,^{125,175–179} which is slightly longer than the Cr³⁺–H₂O bond. The lengths of the Fe³⁺–H₂O and Cr³⁺–H₂O bonds are slightly shorter than the sum of the radii of the ions (Cr³⁺, 76 pm; Fe³⁺(high spin), 79 pm³⁴¹) and water (140 pm). The hydration energy of Fe³⁺ should be larger than that of Cr³⁺, although the data so far reported do not fit to this consideration.^{203,347} MD simulations also show the hexahydrated structure of Fe³⁺ with the Fe³⁺–H₂O bond length of 203–205 pm,³¹⁰ which fairly well agrees with the experimental result. The tilt angle of the Fe³⁺–O–H bond is 7.7° according to MD simulations.³¹⁰

Rh³⁺. The rhodium(III) ion is an extremely inert ion in water, and the hydrated Rh³⁺ ions cannot be obtained by simple dissolution of rhodium(III) salts in water and must be prepared by a special synthetic way. The hydrated ion is 6-coordinated with the Rh³⁺–H₂O bond

length of 204–206 pm,^{66,68} which is much shorter than the sum of the ionic radius of Rh³⁺ (82 pm³⁴¹) and that of water. The result indicates that the Rh³⁺–H₂O bond has an extensively covalent character.

In³⁺ and Tl³⁺. The In³⁺ ion has an octahedral structure with the In³⁺–H₂O bond length of 215 pm, which is much shorter than the sum of the sizes reported for In³⁺ (94 pm³⁴¹) and water. NMR data also show the 6-coordinated structure of the hydrated In³⁺ ion. The Tl³⁺ ion has also an octahedral structure and the Tl³⁺–H₂O bond length is 223 pm.^{182,183} Again the measured bond length is much shorter than the sum of the sizes of the Tl³⁺ ion (104 pm³⁴¹) and water molecule by 20 pm, the result indicating a significant covalent-type bonding between the ions and water molecules.

Y³⁺ and Lanthanoid Ions, Ln³⁺. The yttrium(III) ion is often compared with the lanthanoid(III) ions in their reactions and structures in solution because of their similar ionic charge and size. In fact, the isomorphous substitution method can be applied to the analysis of the hydration structure of the ions by using the X-ray diffraction method.^{10,180} The Y³⁺ ion is octahydrated, according to the X-ray diffraction meth-

Table 11. Structural Parameters of Incompletely Hydrated First Shell of Metal Complexes $[M^{III}A_m(H_2O)_n]^+$ and $[M^{IV}A_m(H_2O)_n]^2+$ of Tri- and Tetravalent Cations, Respectively, Derived from Diffraction and EXAFS Measurements (See Section III for the Full Definitions of the Abbreviations)

salt	H ₂ O/salt molar ratio	<i>r</i> _{MO} , pm	<i>l</i> _{MO} , pm	<i>n</i> _{MO}	<i>r</i> _{MA} , pm	<i>l</i> _{MA} , pm	<i>n</i> _{MA}	symmetry	second shell	method	model	ref
Cr³⁺												
CrCl ₃ ^a	17.9,26.5	196,198	25,21	4.5,4.9	230,232	10,9	1.5,1.1	O	a	X	SNM	209
CrCl ₃ + HCl ^b	24.5	197	23	5.35	233	9	0.65	O	a	X	SNM	209
Cr ₂ (SO ₄) ₃	18.7	194	10	5.17	318	12	0.83	O	a	X	SNM	233
Fe³⁺												
FeCl ₃		207		4	220		2	O	n	X	rdf	274
FeCl ₃ ^c	6–21.5	194–208	12–15	1.8–4.2	230–237	13–17	3.2–1.8	O	a	X	SNM	210
FeCl ₃ ^d	12–6.7	201–203	9–12	1.7–2.2	221–235	5–10	3.2–3.4	O, T	n	X	FN3	211
FeCl ₃	55	210		6	213			O	n	EX	rdf	124
FeCl ₃ + NaOH ^e	55	199–201	7–10	4.6–6.1	230–231	7–5	1.8–0.3	n	n	EX	rdf	275
Fe(NO ₃) ₃ + NaOH ^e	55	192–208	5.7–2.8	10–7				n	n	EX	rdf	275
Fe ₂ (SO ₄) ₃	14.4–23.8	201–202	7–9	6			1.2–1.0	O	i	X	FN3	276
Y³⁺												
Y ₂ (SeO ₄) ₃	69,58.2	233	10	8.0	375	8,12	0.35,0.60	n	a	X	SNM	10
Rh³⁺												
RhCl ₃ + HCl	141	209	13	3	233	5	3	O	a	X	SNM	66
Rh(NO ₃) ₃ ^f	61,145	202,203	10,6	4		24	2	O	a	X	SNM	226
In³⁺												
InCl ₃	8.8	232	6	5	250	6	2	S ^g	a	X	SNM	212
InBr ₃	9.2	260	6	6	260	6	2	S ^g	a	X	SNM	212
In ₂ (SO ₄) ₃	58.9	216	11	5.12	334	12	0.88	O	a	X	SNM	181
Ln³⁺												
La ₂ (SeO ₄) ₃	76.9	256.0	11	8.0	393	12	0.60	n	n	X	SNM	10
Ce(NO ₃) ₃	25.4	255	12	7.5	344	28	0.9	n	a	X	SNM	227
Ce(ClO ₄) ₃ + HClO ₄	38	257.4	14.6	7.5	359	18	2.09	O	a	X	SNM	110
NdCl ₃ + 3HCl	30	241		7.0	278		1	H	n	X	rdf	188
GdCl ₃ + 3HCl	30	237		6.0	280		2	H	n	X	rdf	195
Tb ₂ (SeO ₄) ₃	44.3	238	11	8.0	378	12	0.6	n	n	X	SNM	10
ErCl ₃	21.5	233	8.4	7.8	265	10	0.25	n	a	X	SNM	11
ErCl ₃ + 7LiCl	55.3	235	7.7	7.8	267	11	0.8	n	a	X	SNM	11
ErBr ₃ + 7LiBr	52.4	235	7	7.9	287	11	0.3	n	a	X	SNM	11
Er(NO ₃) ₃ ^h	52.4–14.9	232–237	6	5.8–3.3	286,278	14,8	0.9–2.2	n	a	X	SNM	277
Er ₂ (SeO ₄) ₃	68.7,53.1	234	10	8.0	375	8,12	0.35,0.6	n	n	X	SNM	10
Th⁴⁺												
ThCl ₄	30	2.48	10	7.0	284	22	1.6	n	n	X	FN3	201
Th(NO ₃) ₄ ^h	49.3–17	245–251	4–10	3.0–7.4	300–310	10	3.5–1.0	n	i	X	FN3	201

^a 20–25% [Cr(H₂O)₆]³⁺, 37–50% [Cr(H₂O)₅Cl]²⁺, 38% [Cr(H₂O)₄Cl₂]⁺, 30% [Cr(H₂O)₃Cl₃] complexes are present. ^b 35% [Cr(H₂O)₆]³⁺, 65% [Cr(H₂O)₅Cl]²⁺ complexes are present. ^c Besides the [Fe(H₂O)₆]³⁺ complex, [Fe(H₂O)₅Cl]²⁺, [Fe(H₂O)₄Cl₂]⁺, [Fe(H₂O)₃Cl₃], and [FeCl₄][–] complexes also coexisted. ^d Only the [Fe(H₂O)₃Cl₃] and [FeCl₄][–] complexes were present. ^e Extended polymerization occurs due to hydrolysis. ^f Hydrated cations are bridged through anions. ^g Bipyramidal structure with the anions in axial positions. ^h Bidentate nitrate complexes are formed.

od,^{10,180} like the heavier lanthanoid ions are. The Y³⁺–H₂O bond length is determined to be 236–237 pm. The hydration number of the Y³⁺ ion measured by NMR is 2.4,³²⁸ which is fairly small compared with the value determined by the diffraction method. The difference may be too large to attribute to experimental uncertainties in both X-ray diffraction and NMR measurements and suggests that two water molecules in the coordination sphere of Y³⁺ may be substituted much more slowly than the other six.

The hydration structure of the lanthanoid(III) ions has been extensively discussed by many authors after the works by Habenschuss and Spedding,^{185,193,196} and the discussions seem to converge to the conclusion that the lighter lanthanoid(III) ions from La³⁺ to Nd³⁺ are nonhydrated and the heavier ions after Gd³⁺ or Tb³⁺ have eight water molecules in the first coordination sphere, and intermediate ions such as Sm³⁺, Eu³⁺ (and probably Gd³⁺, too) have both nona- and octahydrated structures which are in equilibrium. The conclusion has been supported from the Raman spectroscopic measurements³⁴⁸ and EXAFS measurements of the

hydrated structure of the ions in water and in the aqueous glassy state.¹⁹¹

The octa- and nonahydrated structures may be depicted in the way that six water molecules are arranged in a prism or antiprism shape around the ion and the rest two to three water molecules, depending on the sizes of the Ln³⁺ ions, are located at the middle of the prism structure. If we imagine such a structure, slowly exchangeable water molecules found in Y³⁺ by the NMR method may be explainable. In fact, such a small hydration number is observed by the NMR method for Er³⁺ (*n* = 1), which is one of the heavier lanthanoid(III) ions with eight water molecules in the first coordination shell. On the other hand, the hydration number of lighter lanthanoid(III) ions determined by the NMR method is much larger than those found for Y³⁺ and Er³⁺ (Table 11), and the results suggest that the water molecules in the middle part of the prismatically (or antiprismatically) 6-coordinated structure of a lighter lanthanoid(III) ion may be more weakly bound to the central ion than those of the heavier lanthanoid(III) ions so that the six water molecules at

Table 12. Structural Parameters of the Hydration Shell of Monovalent Cations Derived from Radial Distribution Functions Obtained by Computer Simulations (See Section III for the Full Definitions of the Abbreviations)

salt	H ₂ O/salt molar ratio	r _{MO} , pm	n _{MO}	r _{MH} , pm	n _{MH}	θ, deg ^a	water model	method	ref
NH ₄ ⁺									
NH ₄ ⁺	215	290	14				MCY	MC	278
NH ₄ Cl	25	305	8.1	350		15.7	ST2	MD	279
NH ₄ Cl	25	306	8.1				ST2	MD, X	71
Li ⁺									
Li ⁺	200	195	5	259			CI	MC	57
Li ⁺	64	190					HF	MC	280
Li ⁺	215	210	6	270		20–40	MCY	MC	281
Li ⁺	64,125	198	5.3	257	10.6	40	MCY	MD	282
Li ⁺	79	192	4	262	8	55.4	CF	MD	283
Li ⁺	215	213	6				MCY	MC	284
Li ⁺	125	195	4.9	260	10.6	65.8	TIP4P	MC	60
Li ⁺	64	204	6	260	>12	45	TIP4P	MD	285
LiF	50	200	4				HF	MC	286
LiF	100	200	5	260			HF	MC	287
LiF ^b	31	200	<3	350		45	SPC-FP	MC	61
LiCl	10	190–200	4				HF	cluster	58
LiCl	100	200	5	260			HF	MC	288
LiCl	25	206	7.1			49	ST2	MD	289
LiCl	4	211	5.3	280		30	CF	MD	79
LiCl ^b	4	200	5.2	270	10.7	41	BJH	MD	290
LiCl ^b	3	200	4	280	8	0	BJH	MD, X	243
LiI	25	210	7.3			46.4	ST2	MD	289
LiI	25	213	6.1	268	13.1	42.1	ST2	MD	291
LiI	25	213	6.1	267	47		ST2	MD	292
LiI ^c	100	213	6.0				ST2	MD	293
LiI ^d	25	212	6.1	268	15.4		ST2	MD	294
Na ⁺									
Na ⁺	10	230–240	5–6				HF	cluster	58
Na ⁺ ^e	200	233	5.4	300			CI	MC	57
Na ⁺	64	230					HF	MC	280
Na ⁺	200	240						MC	295
Na ⁺	215	235	6	289		20–40	MCY	MC	281
Na ⁺	64,125	229	6.0	295	12	20	MCY	MD	282
Na ⁺ ^e	79	224	6.0	292	12	55.9	CF	MD	283
Na ⁺	215	237	6.0				MCY	MC	284
Na ⁺	125	233	6.0	290	13.2	62.4	TIP4P	MC	60
Na ⁺	64	235	6.2	291	>12.4	43	TIP4P	MD	285
NaCl	25	231	6.6			46.4	ST2	MD	289
NaCl	100	232	7.3				ST2	MD	296
NaCl	25	236	6.0				ST2	MD	297
NaCl	25	230	5.9				CF	MD	298
NaCl	100	230	6.0				MCY	MC	299
NaCl	25	230	5.8	295	13.9	37.5	BJH	MD	300
NaCl/	25	230	6.3	293	16.2	42.2	BJH	MD	300
NaCl	100–7.9	231–230	6.1–4.9				MCY	MC	301
NaClO ₄	25	236	6.5				ST2	MD	302
K ⁺									
K ⁺	10	285	5–7				HF	cluster	58
K ⁺ ^e	200	283	6.8				CI	MC	57
K ⁺	64	280					HF	MC	280
K ⁺	200	265						MC	295
K ⁺	215	271	6.3	319		20–40	MCY	MC	281
K ⁺	64,125	276	7.5	335	15	36	MCY	MD	282
K ⁺ ^e	79	276	7.0	344	14	54.4	CF	MD	283
K ⁺	215	286	6.6				MCY	MC	284
K ⁺	64	286	7.6	332	>15.2	55	TIP4P	MD	285
KCl	25	280	7.8	332	23.4	45.5	ST2	MD	303
Cs ⁺									
CsF	25	310	7.3			56.6	ST2	MD	289
CsF	25	320	7.9	372	23	50.2	ST2	MD	304
CsCl	25	310	8.2			56.6	ST2	MD	289
CsI ^b	20	303	5.8				CF	MD	305
CsI ^{b,g}	20	303	5.3				CF	MD	305
CsI ^{b,h}	10	305	6.0				CF	MD	305

^a The orientational angle of the M–O–H bond (see Figure in Table 8). ^b Ion-pair formation occurs. ^c At 235 °C and 3 kbar pressure.^d The solution is placed between two Lennard-Jones walls of 1231-pm separation. ^e The second shell is indicated or analyzed. ^f At 10 kbar pressure. ^g At 68 °C. ^h At 76 °C.

the corners of the prismatic structure may be detected by the NMR method.

The Ln³⁺–H₂O bond length decreases rather smoothly with the increase in the atomic number and no special

Table 13. Structural Parameters of Hydration Shells of Di- and Trivalent Cations Derived from Radial Distribution Functions Obtained by Computer Simulations (See Section III for the Full Definitions of the Abbreviations)

salt	H ₂ O/salt molar ratio	<i>r</i> _{MO} , pm	<i>n</i> _{MO}	<i>r</i> _{MH} , pm	<i>n</i> _{MH}	θ, deg ^a	water model	method	ref
Be²⁺									
BeCl ₂	50	175	6	249	12.7		BJH	MD	100
BeCl ₂	50	175	4	252			BJH	MD	306
Mg²⁺									
Mg ²⁺ + 37NH ₃	164	205	4.0	270	8.1	0	MCY	MC	307
MgCl ₂	50	200	6.0	275	12.0	14	CF	MD	308
Ca²⁺									
Ca ²⁺	64	254	9.3	313	>18.6	35	TIP4P	MD	285
Ca ²⁺ ^b	64	254	9.6	307	>19.2	43	TIP4P	MD	285
Ca ²⁺ ^c	64	254	9.3	317	>18.6	26	TIP4P	MD	285
CaCl ₂	50	239	9.2	313	18.7	0	CF	MD, X	116
Sr²⁺									
SrCl ₂	50	263	9.8	335	20.1	0	BJH	MD	309
Fe²⁺									
Fe ²⁺ ^d	100	215	6.0	289	6.0		BJH	MD	310
Fe ²⁺ ^e	100	220	6.0	288	6.0		BJH	MD	310
Ni²⁺									
Ni ²⁺	64	217	8.0	276	>16.0	38	TIP4P	MD	285
Zn²⁺									
Zn ²⁺	200	205	7.0	275	14–15	dipolar	MCY	MC	311
Fe³⁺									
Fe ³⁺ ^d	100	203	6.0	281	6.0	7.7	BJH	MD	310
Fe ³⁺ ^e	100	205	6.0	281	6.0	7.7	BJH	MD	310

^a The orientational angle of the M–O–H bond (see Figure in Table 8). ^b At 10 kbar pressure. ^c At 81 °C. ^d In H₂O. ^e In D₂O.

breaking point such as so called “gadolinium break” has been observed.

4. Tetravalent Cations

Sn⁴⁺. Since the Sn⁴⁺ ion is easily hydrolyzed in water, no diffraction experiment has been attempted. NMR measurements carried out in highly acidic solutions show that the ion has six water molecules in the first hydration shell.

Th⁴⁺. Experimental difficulties due to the emission of fluorescence X-rays from Th⁴⁺ ions in the course of the X-ray diffraction measurements must be overcome with suitable corrections. Experiments must be done in highly acidic solutions, because the Th⁴⁺ ions are easily hydrolyzed in water to form various polynuclear complexes. The hydrated Th⁴⁺ ion has about eight water molecules in the first coordination sphere of the ion.²⁰¹ The small hydration number found for a Th(NO₃)₄ solution shows the coordination of an NO₃[−] ion with Th⁴⁺.²⁰⁰ (Table 5). An NMR measurement carried out with H₂¹⁷O also shows a large hydration number of about 10.³³⁵

U⁴⁺. The U⁴⁺ ion is also easily hydrolyzed in water to form polynuclear complexes, and the ion emits fluorescence X-rays upon irradiation under X-ray beams. In spite of these difficulties, an X-ray diffraction study has been done for the structural analysis of the hydrated U⁴⁺ ion. The ion has more than six water molecules (7.9–9.2) and a square antiprism structure has been suggested.²⁰² The U⁴⁺–H₂O bond length has been determined to be 250–251 pm.²⁰²

No monoatomic ion with a charge higher than +4 can exist as a hydrated ion in water.

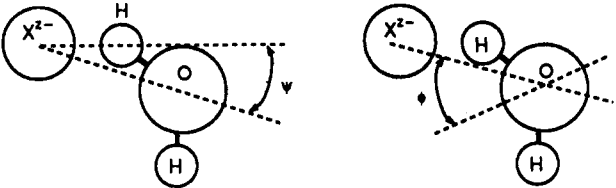
The hydration energies of various cations, as well as anions, have been reviewed by Rosseinsky²⁰³ in this journal.

5. Halide Ions

Water is a moderate donor and a rather strong acceptor solvent, and thus, water is expected to solvate anions more strongly than cations. However, hydration of anions is usually much weaker than that of cations, except for limited cases such as OH[−] and F[−], because most anions have much larger ionic radii than cations. In fact, the hydration enthalpy of F[−] is more negative than that of Na⁺ which has a similar or even smaller ionic radius than F[−].²⁰³ Therefore, information on the hydration structure of anions is not very conclusive compared with that of cations in spite of fairly large number of measurements have been carried out for studies on the hydration of anions.

F[−]. The F[−] ion is a structure-making anion, and it may be coordinated with six water molecules in the first coordination sphere,^{60,70,87,282,283,289,304} although the results so far reported for the hydration structure of F[−] are rather scattered.^{57,69,94,281,284,287} The F–O bond length is determined to be 262–269 pm by the X-ray diffraction method^{69,70,94} (Table 6) and 260–267 pm^{87,281–284,304} by computer simulations (Table 14). A sharp distribution of hydration numbers of F[−]^{60,281} suggests the formation of a well-ordered arrangement of water molecules around F[−] as is expected from its structure-making properties.

Cl[−]. The Cl[−] ion is the most extensively investigated one among anions for the hydration structure and has been studied by various methods. Many X-ray and neutron diffraction measurements show that Cl[−] is hydrated with six water molecules (Tables 6 and 8), but results of computer simulations suggest that the hydration structure around Cl[−] is not so definite and water molecules of such numbers as 1–8^{300,312} or 4–13⁷⁹ seem to surround Cl[−] ions (Table 15). The peak corresponding to the Cl[−]–H₂O interactions found in the radial distribution function is very asymmetric and the

Table 14. Structural Parameters of the Hydration Shell of Anions (X^-) Derived from Radial Distribution Functions Obtained by Computer Simulations (See Section III for the Full Definitions of the Abbreviations)


salt	H ₂ O/salt molar ratio	r_{XO} , pm	n_{XO}	r_{XH} , pm	n_{XH}	ψ or ϕ , deg	water model	method	ref
F⁻									
F ⁻	200		5	168			CI	MC	57
F ⁻	215	260	4.1	168			MCY	MC	281
F ⁻	64,125	267	5.8	173		14	MCY	MD	282
F ⁻	79	264	6	160	6	0 ^a	CF	MD	283
F ⁻	215	263	5				MCY	MC	284
F ⁻	125	260	6.2	165	6.2		TIP4P	MC	60
LiF	100	230	4	130			HF	MC	287
LiF ^b	31	330	—	330			SPC-FP	MC	61
CsF	25	222	6.3			51.7 ^a	ST2	MD	289
CsF	25	264	6.8	165	6.7	53 ^a	ST2	MD	304
Cl⁻									
Cl ⁻	10	340–350	6–7				HF	cluster	58
Cl ⁻	215	325	8.4	225		19	MCY	MC	281
Cl ⁻	64,125	329	7.2	235		17	MCY	MD	282
Cl ⁻	79	328	7.0	232	7.0	5.8	CF	MD	283
Cl ⁻	215	348	8.5				MCY	MC	284
Cl ⁻	125	321	7.4	225	7.0		TIP4P	MC	60
Cl ⁻	64	323	5.6–6.2	229		4	TIP4P	MD	285
Cl ^{-c}	64	323	6.0–6.4	227		6	TIP4P	MD	285
NH ₄ Cl	25	322	8.2	224	7.8	54.5 ^a	ST2	MD	279
NH ₄ Cl	25	320	8.3				ST2	MD, X	71
LiCl	25	268	7.4			54.5 ^a	ST2	MD	289
LiCl	4	322		233			CF	MD	79
LiCl ^b	4	320	8.2	225	6.3	36 ^a	BJH	MC	290
LiCl ^b	3	320	4.9	220		no ^e	BJH	MD, X	243
NaCl	25	266	6.7			49.5 ^a	ST2	MD	289
NaCl	100	270	8.0				ST2	MD	296
NaCl	25	314	6.0				ST2	MD	297
NaCl	25	330	8.0			54.5 ^a	CF	MD	298
NaCl	25	318	7.7	220	6.7	53.5 ^a	BJH	MD	300
NaCl ^c	25	316	9.6	215	7.2	60.1 ^a	BJH	MD	300
NaCl	100–7.9	330	3.1–14.0				MCY	MC	301
KCl	25	316	7.6	220	7.3	54.5 ^a	ST2	MD	303
CsCl	25	266	7.9			58.7 ^a	ST2	MD	289
BeCl ₂	50	312	7.4	225	6.1		BJH	MD	100
MgCl ₂	50	318	7.0	225	6.0	0–11	CF	MD	308
CaCl ₂	50	319	7.9	225	6.7	54.5 ^a	CF	MD, X	116
SrCl ₂	50	318	7.8	222	6.5	54.5 ^a	BJH	MD	309
I⁻									
LiI	25	302	7.3			50.9 ^a	ST2	MD	289
LiI	25	368	8.7	270	6.7	53–90 ^a	ST2	MD	291
LiI ^d	25	364	8.7	271	6.4		ST2	MD	294
CsI ^b	20	364	9.8	314	10.3		CF	MD	305
CsI ^{b,f}	20	369	8.6	311	8.0		CF	MD	305
CsI ^{b,g}	10	365	8.6	310	7.5		CF	MD	305
ClO₄⁻									
NaClO ₄	25	236 ^h	6.5				ST2	MD	302

^a The angle is defined as ϕ instead of ψ of the Figure shown in Table 8. ^b Ion pair is formed. ^c At 10 kbar pressure. ^d The solution is placed between two Lennard-Jones walls of 1231-pm separation. ^e No preferential orientation is found. ^f At 68 °C. ^g At 76 °C. ^h The O–O distance between an oxygen atom in ClO₄⁻ and that in H₂O.

running coordination number has no plateau. Since Cl⁻ is regarded as a structure-breaking ion and rotational and translational correlation times of water molecules around Cl⁻ are even smaller than those of the bulk water, the structural information of the hydration of Cl⁻ is hardly obtained by NMR measurements, and the hydration number of the Cl⁻ ion is often arbitrarily assumed to be 0 in many NMR studies.

The Cl–O bond length is determined to be 310–320 pm. In some cases a much longer bond length has been reported (see Table 6).

The orientation of water molecules around Cl⁻ has been investigated by the neutron diffraction measurements. Most neutron diffraction studies reveal that the tilt angle of the Cl–O–H bond is 0–12°. ^{114,131,136,206} The small angle value has also been obtained in computer simulation studies. ^{281–283,285,308} In some cases bifurcatedly coordinated water molecules to Cl⁻ are reported. ^{64,87}

Br⁻. The hydration number of Br⁻ determined by the X-ray and neutron diffraction methods is 6 for most cases. ^{64,70,84,118,214,215} However, it is obvious from the

Table 15. Characteristic Values for the Distribution of Coordination Numbers (CN) of Ions Estimated from Monte Carlo (MC) and Molecular Dynamics (MD) Simulation Data (See Section III for the Full Definitions of the Abbreviations)

salt	H ₂ O/salt molar ratio	range of CN value	most frequent CN value	frequency, %	water model	method	ref
NH₄⁺							
NH ₄ ⁺ ^a	215	0–4	3	45	MCY	MC	278
Li⁺							
Li ⁺ ^b	215	5–6	6	95	MCY	MC	281
Li ⁺ ^b	125	4–6	5	62	TIP4P	MC	60
LiCl ^c	4	3–6	5	42	CF	MD	79
LiCl ^b	4	3–6	4,5	38	BJH	MD	290
LiCl ^c	4	3–7	6	45	BJH	MD	290
Na⁺							
Na ⁺ ^b	215	5–6	6	95	MCY	MC	281
Na ⁺ ^b	125	5–7	6	95	TIP4P	MC	60
NaCl ^e	25	1–6	6	35	BJH	MD	300
NaCl ^{e,f}	25	1–6	5	25	BJH	MD	300
NaCl ^b	100	4–7	6	60	MCY	MC	301
NaCl ^b	16.5	3–8	5	35	MCY	MC	301
NaCl ^b	7.9	2–7	4–5	30	MCY	MC	301
K⁺							
K ⁺ ^b	215	4–8	6–7	40	MCY	MC	281
Mg²⁺							
MgCl ₂ ^e	50	1–6	6	60	CF	MD	312
Zn²⁺							
Zn ²⁺ ^b	200	4–7	6	53	MCY	MC	311
Zn ²⁺ ^d	200	4–7	7	98	MCY	MC	311
F⁻							
F ⁻ ^b	215	4–6	5	90	MCY	MC	281
F ⁻ ^b	125	6–7	6	90	TIP4P	MC	60
Cl⁻							
Cl ⁻ ^b	215	7–10	8	45	MCY	MC	281
Cl ⁻ ^b	125	6–10	7–8	40	TIP4P	MC	60
LiCl ^c	4	4–13	8	21	CF	MD	79
LiCl ^b	4	3–9	6	36	BJH	MD	290
LiCl ^c	4	6–12	8	31	BJH	MD	290
NaCl ^e	25	1–7	3	30	BJH	MD	300
NaCl ^{e,f}	25	1–8	3	32	BJH	MD	300
MgCl ₂ ^e	50	1–6	2	35	CF	MD	312

^a Definitions of coordination numbers (CN): Integrated over the all pairs with $r_{\text{H(N)}-\text{O}} < 210$ pm. ^b Integrated from $r = 0$ up to the first minimum, $r_{1,\text{min}}$, in $g(r)$. ^c Integrated over the range between the two r_i values where $g(r_i) = 1$. ^d Integrated from $r = 0$ to the absolute minimum, $r_{\text{ab,min}}$, in $g(r)$. ^e Frequency of simultaneous occupation of symmetry sites. ^f At 10 kbar pressure.

discussion given in the case of Cl⁻ that the hydration structure of Br⁻ is not uniform and the number of water molecules around Br⁻ ions may be distributed over a wide range.

The Br–O bond length determined by the diffraction and EXAFS methods is 329–340 pm.^{70,84,118,132,214,216,217} Some values smaller and larger than the range of the hydration number given above are also reported.

I⁻. The hydration structure of the I⁻ ion has been studied rather extensively among those of anions, because it has been used as a good counteranion of various cations, since it scarcely forms ion pairs with hard cations even in concentrated electrolyte solutions. Since the ion is most weakly hydrated among the halide ions, a clear conclusion for the hydration number of the ion may not be obtainable by the diffraction method and a variety of values have been reported (see Table 6). The ambiguity in evaluation of the hydration number arises from difficult extraction of the peak for the I–H₂O interactions from the total radial distribution function obtained by the diffraction method, because the peak may be overlapped with various long-range interatomic interactions in the systems under study. In spite of a large variety of reported hydration numbers of I⁻, the I–O bond length determined by the diffraction measurements converges to values in the

range of 355–370 pm, and values between 360 and 370 pm^{70,82,88,93,190,222} most frequently appear in the literature, because the position of the I–O peak can easily be seen in the radial distribution curve owing to a large scattering factor of iodine. Similar bond lengths have also been reported from computer simulation studies.^{291,294,305} The average hydration number of I⁻ estimated by computer simulations is around 9, but it does not mean that the ion has a definite hydration structure, and the arrangement of water molecules around I⁻ may be disordered very much due to its weak interactions with water molecules.

6. Oxyanions

The hydration structure of oxyanions XO₃^{z-} has been investigated by the diffraction methods and the X–O (within H₂O) distances (noted as $r_{\text{XO(H}_2\text{O)}}$ in Table 7), rmsds, ($l_{\text{XO(H}_2\text{O)}}$) and the numbers of water molecules around the XO₃^{z-} ions ($n_{\text{XO(H}_2\text{O)}}$) have been determined. Some of the oxyanions interact rather strongly with water molecules in solution.

NO₃⁻. Hydration of NO₃⁻ is not very strong and the hydration number $n_{\text{XO(H}_2\text{O)}}$ reported in the literature spreads over a wide range from 1.3²²⁴ to 17.7¹⁵³ (Table 7). If we simply assume that each oxygen atom in the NO₃⁻ ion contacts with 1–2 water molecules, the number

of water molecules around an NO_3^- ion becomes 3 to 6, and therefore, $n_{\text{XO}(\text{H}_2\text{O})} = 1.3$ may be too small. The positively charged N atom in NO_3^- may interact with 1 or 2 water molecules above and/or below the planar triangle structure of the ion. If so, the hydration number of an NO_3^- ion may become a maximum of 8. Therefore, $n_{\text{XO}(\text{H}_2\text{O})} = 17.7$ may be too large. The values 5.9–9.67, 89.97, 174.225–227 seem to be acceptable as the average number of water molecules around an NO_3^- ion.

The N–O(H_2O) distance has been reported to be 314 pm as the minimum⁸⁹ and 350 pm as the maximum.^{97,223,226} Since the N–O bond length in NO_3^- is known to be about 120 pm and the O(NO_3^-)–O(H_2O) distance may be close to 280 pm, the N–O(H_2O) bond length may become to be about 320–350 pm, depending on the N–O–O(H_2O) angle.

ClO_4^- . The regular tetrahedral ClO_4^- ion may be surrounded by 8–12 water molecules if we simply assume that each oxygen atom in the ClO_4^- ion interacts with 2–3 water molecules. Of course, the hydration structure around ClO_4^- may not be so definite as described above, but many of the analyses of radial distribution functions of solutions containing ClO_4^- ions have been done on such a simple and rather unacceptable assumption.^{10,66,164} Some other values between 4²²⁸ and 25.6⁹⁵ have also been reported for the hydration number of ClO_4^- . A computer simulation study³⁰² gives an average hydration number of 6.5 for ClO_4^- (Table 14).

SO_4^{2-} . The SO_4^{2-} ion can strongly combine with water molecules and still keeps some water molecules even in crystals of metal sulfates. According to the results by X-ray diffraction studies of metal sulfate aqueous solutions, an SO_4^{2-} ion is surrounded by about 7^{111,154,229,233,234} to 12^{73,160} water molecules. The S–O(H_2O) length is estimated to be 370–393 pm. Since the S–O bond length in SO_4^{2-} is about 150 pm, the values around 380 pm may be expected to be the S–O(H_2O) length.

SO_3^{2-} and $\text{S}_2\text{O}_5^{2-}$. Intramolecular S–O bond length of the ions may be close to that of SO_4^{2-} , and each oxygen atom in the ions may interact with 1–2 water molecules in solution. An X-ray diffraction study²³⁰ shows the number of water molecules around SO_3^{2-} and $\text{S}_2\text{O}_5^{2-}$ ions to be 9 and 8.9–9.2, respectively.

SeO_4^{2-} . The SeO_4^{2-} ion has a similar structure to SO_4^{2-} , although the length of the Se–O bond (165 pm) is longer than that of the S–O bond. The hydration number of the ion is assumed to be 8 in the structural analysis of the selenates of yttrium(III) and some lanthanoid(III) ions.¹⁰ The value has been consistent with the diffraction data, but some other values, somewhat smaller or larger than that, may also fit to the data. The Se–O(H_2O) length is assumed to be 395 pm from the structural model of $[\text{SeO}_4(\text{H}_2\text{O})_8]^{2-}$.¹⁰

CrO_4^{2-} . The hydration structure of the chromate(VI) ion has not been reported. However, in a recent study with a combined X-ray and neutron diffraction method,²⁶⁷ the CrO_4^{2-} ion was used as the reference ion for the isomorphous substitution of SeO_4^{2-} , and the lengths of 163, 266, and 396 pm were determined for the M–O(MO_4^{2-}), O–O(MO_4^{2-}), and M–O(H_2O) bonds, respectively, where M denotes either Se or Cr. Although the last distance coincides with the previously determined one (395 pm)¹⁰ within the limit of error, the coordination number differs ($n_{\text{O}(\text{MO}_4^{2-})-\text{O}(\text{H}_2\text{O})} = 12^{267}$ instead of 8¹⁰). Therefore, further investigations may be needed for the hydration structure of both anions.

MoO_4^{2-} and WO_4^{2-} . Since MoO_4^{2-} and WO_4^{2-} are isomorphous in their structures, the isomorphous substitution method has been employed in the structural analysis of their sodium salts solutions by means of X-ray diffraction.²³⁵ Therefore, no difference should be found in the hydration structures of the ions. The hydration number of 12 and the metal–O(H_2O) interatomic distance of 406 pm are introduced in the course of the structural analysis of the solutions.

PO_4^{3-} and H_2PO_4^- . The hydration structures of solutions containing H_3PO_4 ²³⁶ and dihydrogen phosphates of divalent metal ions^{237,238} have been studied by means of X-ray diffraction. The P–O(H_2O) distance has been estimated to be 373 and 360 pm for PO_4^{3-} under assumptions of the tetra- and octahydrated structures, respectively, of the ion.²³⁶ The P–O(H_2O) distance in the hydrated H_2PO_4^- ion has been estimated to be 375–391 pm with the hydration number of 4.2–8.8.^{237,238} The hydration structures of the ions are not conclusive, however.

CH_3COO^- . Divalent metal acetate solutions have been investigated by means of X-ray diffraction.²³⁹ The hydration structure of the acetate ion has been estimated by using the second neighbor model around the acetate and metal ions. The number of water molecules around an acetate ion has been evaluated to be 4.2 to 6.1 with the C(CO_2^-)–O(H_2O) distance of 352–372 pm.²³⁹

B. Second Hydration Shell of Ions

Information on the second hydration shell of ions is much poorer than that of the first hydration shell. The quantitative analysis of radial distribution curves in the long r range is difficult and much less reliable. Reliable information in the structure of the second shell may be obtained by the isomorphous substitution method in X-ray diffraction measurements and the isotopic substitution method in neutron diffraction measurements. Of course, such methods cannot be applied to every electrolyte solution. In most works in which some attempts have been done to determine the structure of the second hydration shell of ions, suitable structural models have been introduced. In some other cases fitting procedures between experimental and theoretical $G(r)$ functions have been continued until a more or less satisfactory agreement is obtained between them. The distance between a central ion and water molecules in the second hydration shell, $r_{\text{MO}(2)}$, the rmsd, $l_{\text{MO}(2)}$, and the number of water molecules in the second hydration shell of the ion, $n_{\text{MO}(2)}$, are summarized in Tables 16 and 17. Data in Table 17 are obtained by computer simulations. The $r_{\text{O}(1)-\text{O}(2)}$ and $l_{\text{O}(1)-\text{O}(2)}$ values between water molecules in the first and second hydration shells are also listed in Table 16.

Li^+ . The $r_{\text{MO}(2)}$ value of 441 pm has been evaluated from a model of the octahedral structure of the hydrated Li^+ ion with additional 12 water molecules around the hydrated ion,⁸² in which each water molecule in the first hydration shell is hydrogen-bonded with two water molecules with the C_{3v} arrangement. On the other hand, the water molecules in the first hydration shell of Li^+ is found to have an orientation which is favorable to form three hydrogen bonds with water molecules in the second hydration, the orientation helping to construct a more stable hydration structure than that forms only two hydrogen bonds.^{74,75,78} Therefore, the $n_{\text{MO}(2)}$

Table 16. Structural Parameters of the Second Hydration Shell of Cations Derived from Diffraction Measurements (See Section III for the Full Definitions of the Abbreviations)

salt	H ₂ O/salt molar ratio	$r_{MO(2)}$, pm	$l_{MO(2)}$, pm	$n_{MO(2)}$	$r_{O(1)-O(2)}$, pm	$l_{O(1)-O(2)}$, pm	method	model	ref
Li⁺									
LiI	25	441	13	12	272	10	X, MD	SNM	82
Ag⁺									
AgClO ₄	10.4	444	45	9.5			X	FN3	95
AgNO ₃	14.2	429	45	17.3			X	FN3	95
AgClO ₄	16.3,3.3	440,440	35,28	9.8	285,299 ^a	15,17	X	FN3	97
AgNO ₃	16.6,4.3	436,430	31,45	4.9,5	286,289 ^a	101,5	X	FN3	97
Mg²⁺									
MgCl ₂	27.1,55.5	410,423	68,61	12,12	276,275	1,5	X, MD	SNM	106
MgCl ₂	50	410	5	12	279	2	MD, X	SNM	106
Mg(NO ₃) ₂	10.8,24.8	420,420	60,67	12,12	275,278	7,11	X	SNM	109
Mg(ClO ₄) ₂	18	428	23	12	278	11	X	SNM	110
MgSO ₄	20.5	421	24	12	281	9	X	SNM	111
Mg(H ₂ PO ₄) ₂	34	428	47	9.5	276	11.8	X	FN3	237
Mg(CH ₃ CO ₂) ₂	33.1,14.9	424,415	10,10	12.5,14			X	SNM	111
Ca²⁺									
CaCl ₂	6.0	460		5.9	292		X	SNM	117
CaCl ₂ ^b	6.2	450		5.0	291		X	SNM	117
CaCl ₂ ^c	6.0	460		5.0	294		X	SNM	117
CaCl ₂ ^d	6.2	460		3.8	294		X	SNM	117
CaCl ₂ ^e	5.6	448		2.8	295		X	SNM	117
CaCl ₂ ^f	4.0	454		1.0	293		X	SNM	117
Sr²⁺									
SrCl ₂	26.5,34.6	494,491	28,33	9.3,14.9	287,281	10,9	X	SNM	119
Mn²⁺									
MnCl ₂	550–11	443	33	14–18			EX	SNM	247
Mn(NO ₃) ₂	12.6	425	29	8.9	271	6	X	SNM	248
MnSO ₄	13.2,26.8	417,422	31,29	10.4,9.8	278,274	4,3	X	SNM	249
MnSO ₄	28	434	26	10.7	273	5	X	SNM	141
Mn(CH ₃ CO ₂) ₂	33.5	436	22	10	274	5	X	SNM	239
Fe²⁺									
FeCl ₂	55.5	451	25	12	284	14	X	SNM	126
Fe(ClO ₄) ₂	55.5	430	26	12	287	18	X	SNM	126
FeSO ₄	55.5	443	26	12	285	18	X	SNM	126
Co²⁺									
CoCl ₂	17.9			5.7	275	5	X	SNM	251
CoCl ₂ + LiCl	8–17	428–393	40–27	14.8–10	275–273	1–10	X	SNM	81
CoCl ₂ + NiCl ₂ + 6LiCl	110			7.3	277	1	X, EX	SNM	252
Co(ClO ₄) ₂	15.0	420	29	6.3	279	4	X	SNM	129
Co(CH ₃ CO ₂) ₂	53.7	428	18	10	279	5	X	SNM	239
Ni²⁺									
NiCl ₂	28	399	56	12	272	6	X	SNM	105
NiCl ₂	14	405	32	6.2	268	18	X	SNM	105
NiCl ₂	18			4.1	274	5	X	SNM	251
NiBr ₂	24.7	401	21	10.9	279	9	X	SNM	215
NiBr ₂	11.9,24.7			4.0,10.2	275,280	11,5	X	SNM	218
NiSO ₄	28	426	27	9.2	273	8	X	SNM	141
NiSO ₄	27.5	420	33	12	274	8	X	SNM	111
NiSO ₄ ^u	27	420	31	11.8	274	5	X	SNM	142
NiSO ₄ + H ₂ SO ₄	48	433	30	12	277	10	X	SNM	111
NiSO ₄ + Li ₂ SO ₄	37	428	25	12.1	270	5	X	SNM	142
Ni(H ₂ PO ₄) ₂	45.6	414	15	7.3	270	6	X	SNM	238
NiCl ₂ + HCl	24.6			4.3	276	4	X	SNM	254
NiCl ₂ + 2LiCl	24.8			2.7	273	4	X	SNM	254
NiCl ₂ + 3LiCl	23.2			2.8	272	4	X	SNM	254
Ni(ClO ₄) ₂	15.0	410	21	5.5	277	10	X	SNM	129
Cu²⁺									
Cu(NO ₃) ₂	23.5,34.7	408	41,37	9.1,8.3	272,274	3	X	SNM	262
Cu(ClO ₄) ₂	15.4,25.1	396,395	38,33	11.1,11.6	280,273	13,13	X	SNM	147
CuSO ₄	40.4	420	20	7.6	279	3	X	SNM	150
Zn²⁺									
ZnBr ₂ ^h	10.1	396–395	14	11.8–7.5			X	SNM	219
ZnBr ₂ ⁱ	7.57–1.0	395–410	50	12–14			X	SNM	220
ZnI ₂ ^j	18–55	410–417	34–44	3.7–12.5			X	SNM	221
Zn(NO ₃) ₂	9.0	402	38	10.8	279	31	X	SNM	153
ZnSO ₄	18.6	426	37	12	270	11	X	SNM	113
ZnSO ₄	27.1	424	28	9.9	279.6	2.5	X	SNM	154
ZnSO ₄	100–16.9	421–426	24–40	13.2–7.6	276–280	2–4	X	SNM	155
Zn(CH ₃ CO ₂) ₂	34	423	14	10	269	4	X	SNM	239

Table 16. (Continued)

salt	H ₂ O/salt molar ratio	$r_{\text{MO}(2)}$, pm	$l_{\text{MO}(2)}$, pm	$n_{\text{MO}(2)}$	$r_{\text{O}(1)-\text{O}(2)}$, pm	$l_{\text{O}(1)-\text{O}(2)}$, pm	method	model	ref
Cd²⁺									
Cd(NO ₃) ₂	9–54	431	38	11.9			X	SNM	225
Cd(ClO ₄) ₂	23.0	433	28	12			X	SNM	160
CdSO ₄	17.6	433	28	12			X	SNM	160
CdSO ₄ ⁱ	25	436,437	32,31	11.9,10.3			X	SNM	232
Cd(H ₂ PO ₄) ₂	41.7	433	37	9.3	276	9	X	SNM	238
Cd(CH ₃ CO ₂) ₂	43.0,23.0	441,433	20	8	279,278	7,5	X	SNM	239
Hg²⁺									
Hg(ClO ₄) ₂	19.7	410	76	18.4			X	SNM	161
Sn²⁺									
Sn(ClO ₄) ₂	16.8	440	17	7.2	290	12	X	SNM	164
Al³⁺									
AlCl ₃ ^t	23.8,54.0	402,401	25,33	12,12	269,273	7.5,2	X	SNM	173
Al(NO ₃) ₃	14.5	399	25	12	270	9	X	SNM	174
Al(NO ₃) ₃	100	410–415		12–14			X	rdf	169
Cr³⁺									
CrCl ₃	23.4	420		12	274	5	X	SNM	166
CrCl ₃	55	404	28	12	268	1	X	SNM	167
CrCl ₃	17.9,26.5			7.6,8.3	258,268		X	SNM	209
CrCl ₃ + HCl	24.5			8.3	270	4	X	SNM	209
Cr(NO ₃) ₃	100	420–425		12–14			X	rdf	169
Cr(NO ₃) ₃	55,27	408,406	26,27	12	272,270	6,7	X	SNM	167
Cr(NO ₃) ₃	24.5–50.8			12	276	6	X	SNM	170
Cr(ClO ₄) ₃	25–27			17–19			N	fod	172
Cr ₂ (SO ₄) ₃	18.7	401	30	10	271	7	X	SNM	233
Fe³⁺									
FeCl ₃ ^{l,m}	6–21.5	409–480	20–40	5–11.2	262–277		X	SNM	210
Fe(NO ₃) ₃ ⁿ	22.2,34.7,69			12	270–272		X	SNM	177
Y³⁺									
Y(ClO ₄) ₃	40,12.4	452	20,27	15,9			X	SNM	10
Y ₂ (SeO ₄) ₃	69,58.2	447	21	11			X	SNM	10
Rh³⁺									
RhCl ₃ + HCl	141	411	51	6	270	8	X	SNM	66
Rh(NO ₃) ₃	61,145	408	26	12.6	266,277	5,6	X	SNM	226
Rh(ClO ₄) ₃ + HClO ₄	145	402	21	13.7	269	6	X	SNM	68
Rh(ClO ₄) ₃ + HCl	277	407	22	12	272	8	X	SNM	66
In³⁺									
InCl ₃ ^o	8.8	560	52	8	260	13	X	SNM	212
InBr ₃ ^o	9.2	560	52	8	260	13	X	SNM	212
In ₂ (SO ₄) ₃	14.2	419	31	10.1	267	6	X	SNM	234
Ln³⁺									
La(ClO ₄) ₃	12.0	470	26	13			X	SNM	10
La ₂ (SeO ₄) ₃	76.9	470	22	11			X	SNM	10
Ce(NO ₃) ₃	25.4	456	41	15.5			X	SNM	227
Ce(ClO ₄) ₃ + HClO ₄	38	436	36	19.5			X	SNM	110
Sm(ClO ₄) ₃	15.2	463	24	12			X	SNM	10
Tb(ClO ₄) ₃	39.4,13.7	456,460	20,26	9,14			X	SNM	10
Tb ₂ (SeO ₄) ₃	44.3	450	22	11			X	SNM	10
ErCl ₃	53.9,21.5	451,450	24,22	13.2,12.8			X	SNM	11
ErCl ₃ + 7LiCl	55.3	460	20	11.0			X	SNM	11
ErBr ₃	52.9	449	20	12.0			X	SNM	11
ErBr ₃ + 7LiBr	52.4	450	20	9.0			X	SNM	11
Er(NO ₃) ₃ ^p	2.4–14.9	458–464	28–35	17.0–14.6			X	SNM	277
Er(ClO ₄) ₃	12.1	452	27	15			X	SNM	10
Er(ClO ₄) ₃	49.2	450	26	13			X	SNM	11
Er ₂ (SeO ₄) ₃	68.7,53.1	447	22	11			X	SNM	10
U⁴⁺									
U(ClO ₄) ₄	35.7,31.2	446,447	20,28	8.5,9.6			X	FN3	202

^a The O₍₁₎–O₍₂₎ distance was not distinguishable from the O–O distance in the bulk water. ^b At 15 °C, $n_{\text{O}(1)-\text{O}(2)} = 2.2$. ^c At 33 °C, $n_{\text{O}(1)-\text{O}(2)} = 1.7$. ^d At 80 °C, $n_{\text{O}(1)-\text{O}(2)} = 2.0$. ^e At 72 °C, $n_{\text{O}(1)-\text{O}(2)} = 1.9$. ^f At 120 °C, $n_{\text{O}(1)-\text{O}(2)} = 0.9$. ^g Outer-sphere complexes are formed. ^h Parameters refer to those measured at –40, 25, 40, 80, and 100 °C. ⁱ Parameters refer to those of the hexaaqua complex only, but other complexes are also present in the solutions. ^j At 9 °C and 62 °C. ^k Parameter values of the second shell of cations and those of the first shell of anions are correlated. ^l Parameters refer to those of the hydrated complexes. ^m $n_{\text{O}(1)-\text{O}(2)} = 5–10$. ⁿ $n_{\text{O}(1)-\text{O}(2)} = 4–6$. ^o $n_{\text{O}(1)-\text{O}(2)} = 12$. ^p Oxygen atoms of water molecules in the second shell of cation and those of anion are not distinguishable.

value of 12 may be better explained, in spite of $n_{\text{MO}(1)}$ value of 6 in ref 82, in terms of 3 water molecules bonding to each water molecule in the tetrahedrally hydrated Li⁺ ion, which has been reported by most of the authors

given in references in Table 1. The $r_{\text{O}(1)-\text{O}(2)}$ distance of 272 pm, which is shorter than the water–water intermolecular distance in the bulk, fit the intensity data.

Table 17. Structural Parameters of the Second Hydration Shell of Cations Derived from Radial Distribution Functions Obtained by Computer Simulations (See Section III for the Full Definitions of the Abbreviations)

salt	H ₂ O/salt molar ratio	$r_{\text{MO}(2)}$, pm	$n_{\text{MO}(2)}$	water model	method	ref
Li ⁺	200	400	14.2	CI	MC	57
LiCl	25	450		ST2	MD	289
LiI	25	430		ST2	MD	289
LiI	25	419		ST2	MD	291
LiI	25	441	12	ST2	MD, X	82
Na ⁺	200	450	12.4	CI	MC	57
NaCl	25	450		ST2	MD	289
NaCl	100	444		ST2	MD	296
NaCl	25	447		BJH	MD	300
NaCl ^a	25	480		BJH	MD	300
K ⁺	200	530	17.4	CI	MC	57
KCl	25	460		ST2	MD	303
CsF	25	530		ST2	MD	289
CsF	25	530		ST2	MD	304
CsCl	25	490		ST2	MD	289
NH ₄ Cl	25	506		ST2	MD	279
BeCl ₂	50	373		BJH	MD	100
MgCl ₂ ^b	50	447	12	CF	MD	106
Mg ²⁺ + 37NH ₃	164	430	9	MCY	MD	307
CaCl ₂	50	453		CF	MD, X	116
SrCl ₂	50	500		BJH	MD	309
Zn ²⁺	200	420	16–18	MCY	MC	311

^a At 235 °C and 3 kbar pressure. ^b Analyzed by the SNM method.

Results of MD and MC simulations show the number of water molecules in the second hydration shell of 12–14.^{57,82} with the $r_{\text{MO}(2)}$ value of 400–450 pm.^{57,82,289,291}

Na⁺. The number of water molecules in the second hydration shell of Na⁺ estimated by MD and MC simulations is 12.4,⁵⁷ and the $r_{\text{MO}(2)}$ value is ranged from 441 to 480 pm.^{57,289,296,300} The evaluation of the structural parameters of the second hydration shell of Na⁺ from the radial distribution curve may be difficult.

K⁺. The structure of the second hydration shell of K⁺ may be diffused, because the ion–water interactions of K⁺ is not so strong. An MC simulation calculation reveals that the number of water molecules in the second hydration shell of K⁺ is 17.7 and the $r_{\text{MO}(2)}$ distance is 530 pm.⁵⁷ On the other hand, another MD calculation shows that the $r_{\text{MO}(2)}$ value is 460 pm,³⁰³ which is much shorter than the value obtained by the MC calculation. It may be difficult to conclude now which value is more reliable.

Cs⁺. No value has been proposed for $n_{\text{MO}(2)}$ of Cs⁺. The $r_{\text{MO}(2)}$ value estimated by MD simulations is 490–530 pm.^{289,304}

NH₄⁺. It may be impossible to experimentally determine the second hydration structure of NH₄⁺ by the X-ray diffraction method, because the method can hardly distinguish between oxygen and nitrogen atoms in ammonium salt aqueous solutions. An attempt made by MD simulations for the estimation of the structure of the second hydration structure of NH₄⁺ shows that the N–O(2) distance is 506 pm.²⁷⁹

Ag⁺. The structure of the second hydration shell of Ag⁺ has been explored from the peak shape of the radial distribution curves of silver(I) perchlorate and nitrate solutions.^{95,97} Since the linear structure of the hydrated Ag⁺ ion is not accepted, the values in ref 95 may not be reliable. The Ag⁺–O(2) distance of 430–440 pm and the number of water molecules in the second hydration

shell of Ag⁺ of about 5–9 have been estimated.⁹⁷ The $r_{\text{O}(1)\text{--O}(2)}$ value is about 285 pm.

Be²⁺. The structure of the second hydration shell of Be²⁺ has been investigated by an MD simulation with a modified central force model for water.¹⁰⁰ However, since the result obtained for the first hydration structure of the ion in the study is wrong, which is corrected later³⁰⁶ to fit the experimental result,¹⁰⁰ the information on the second hydration shell may be less reliable.

Mg²⁺. The number of water molecules in the second hydration shell of Mg²⁺ is estimated to be about 12 in most studies^{106,109–111} and the $r_{\text{MO}(2)}$ value is 410–428 pm^{106,109–111,237} according to the results by X-ray diffraction measurements, but the $r_{\text{MO}(2)}$ value estimated by MD simulations is 430–447 pm,^{106,307} which is longer than the experimental value. The O(1)–O(2) distance estimated by the X-ray diffraction studies is 275–281 pm, which is shorter than the water–water distance in the bulk water.

Ca²⁺. The number of water molecules in the second coordination sphere of Ca²⁺ should be larger than that of Be²⁺ and Mg²⁺, because Ca²⁺ has a larger ionic surface than the other two. In fact, the $r_{\text{MO}(2)}$ value of Ca²⁺ (448–460 pm^{116,117}) is larger than those of Be²⁺ and Mg²⁺. Nevertheless, the estimated value of $n_{\text{MO}(2)}$ for Ca²⁺ (1.0–5.9¹¹⁷) is smaller than those found for Be²⁺ and Mg²⁺, and the result may be difficult to be reasonably explained.

Sr²⁺. An X-ray diffraction study shows the result that $r_{\text{MO}(2)}$ is 492–494 pm and $n_{\text{MO}(2)}$ is 9.3–14.9;¹¹⁹ the latter value is much larger than the corresponding value of Ca²⁺. The $r_{\text{MO}(2)}$ distance estimated by an MD simulation is 500 pm.³⁰⁹

Mn²⁺ to Zn²⁺. The structural parameters of the second hydration shell of the divalent transition metal ions in the first row of the periodic table from Mn²⁺ to Zn²⁺, summarized in Table 16, does not show clear conclusions for the structural change of the ions with the atomic number as discussed in section III.A.1. An optimistic observation of the data in Table 16 may draw a conclusion that the $r_{\text{MO}(2)}$ changes in a similar manner to the change in $r_{\text{MO}(1)}$, but the conclusion is not definitive, because the values of $r_{\text{MO}(2)}$ reported are so spread even for a given metal ion and are strongly dependent on the models adopted in the structural analyses.

Cd²⁺, Hg²⁺, and Sn²⁺. It seems to be strange that the $r_{\text{MO}(2)}$ value of Hg²⁺ is smallest¹⁶¹ among the values of the three ions^{160,161,164,225,232,238,239} and even smaller than the values of ions from Mn²⁺ to Zn²⁺. More investigation may be necessary for the $r_{\text{MO}(2)}$ value of Hg²⁺.

Al³⁺, Cr³⁺, and Fe³⁺. The strongly hexahydrated trivalent ions may have a stronger second hydration shell than mono- and divalent ions. Structural models with 12 water molecules in the second hydration shell of the trivalent ions have been adopted by many authors. However, the tilt angle of water molecules in the first hydration shell of Cr³⁺ and Fe³⁺ ions is in favor of the construction of three hydrogen bonds with water molecules in the second hydration shell. Thus, for the evaluation of orientation of water molecules and the $n_{\text{MO}(2)}$ value, more detailed investigations may be needed. The $r_{\text{MO}(2)}$ values may be shortest in Al³⁺ and longest in Fe³⁺, although the difference is not clearly seen from the data in Table 16.

Y^{3+} , Rh^{3+} , In^{3+} , Ln^{3+} , and U^{4+} . In the course of the structural analysis of the first hydration shell of the ions, the structure of the second hydration shell has also been taken into consideration to reduce uncertainties in the structural parameters of the first hydration shell. Therefore, the structural parameters obtained for the second hydration shell are treated as adjustable parameters which may include various kinds of uncertainties in the structure parameters of interatomic interactions except for those of the parameters in the first hydration shell. Thus, we do not intend to discuss the parameter values of the second hydration shell in detail and just summarize the values in Table 16.

C. Influences of Ion-Pair and Complex Formation on Hydration of Ions

When a part of water molecules in the hydration shell of M^{z+} or X^{z-} is replaced with another ligand, say A, the r_{MO} (or r_{XO}), n_{MO} (n_{XO}) and l_{MO} (l_{XO}) values may be influenced by electrostatic, donor-acceptor, and other interactions between M^{z+} or X^{z-} and A. The values of r_{MO} , n_{MO} , and l_{MO} are summarized together with the values of r_{MA} , n_{MA} , and l_{MA} , in Tables 9–11.

Since the structural data obtained by the solution diffraction measurements are much less accurate than those of crystallographic and the frequency data, no clear bond length variations upon the introduction of A (or A's) to the coordination sphere of M^{z+} is seen.

It has been observed that the M^{z+} -H₂O bond length significantly changes when the structure of an octahedrally solvated divalent transition metal ion is changed to a tetrahedral structure at the complex formation reactions with halide ions. In aqueous solutions the complex formation reactions of divalent transition metal ions do not proceed to form highly ligated halogeno complexes, different from nonaqueous systems, and thus, we do not see such variations of the M^{z+} -H₂O bond in the data of Table 10.

When a large ligand is introduced to the coordination sphere of a small metal ion, a structural change also occurs due to a steric hindrance between ligands, although good examples are not given in the tables.

In nonaqueous solutions in which we can choose solvents with various donor-acceptor properties and sizes, we can see such bond length variations upon the complex formation. However, we do not discuss problems in nonaqueous solution systems in this review.

D. Influences of Temperature and Pressure on the Hydration Structure of Ions

This interesting subject has not been well studied because ranges of temperature examined for and pressure applied to aqueous solutions are narrow in structural studies of hydrated ions and complexes. Results so far reported in the literature show that the effects of temperature and pressure on the metal-ligand bond lengths is very small and not detectable within accuracies of the present experimental techniques. Under extremely high temperatures and pressures, aqueous electrolyte solutions may become electrolyte solutions in water under supercritical conditions. It may be very interesting to study structures of hydrated ions in the supercritical conditions.

IV. Dynamic Aspects of Ionic Hydration

Dynamic properties of hydrated ions are more sensitive than structural properties to environmental conditions such as temperature, pressure, and concentration. The isotopic effect which can be neglected in the structural consideration of hydrated ions, becomes significant in some cases. Information on dynamic behavior of hydrated water molecules and the hydrated ions themselves is still rather limited, and in this review we discuss translational and rotational motions including reorientational motions of coordinated water molecules, diffusional motions of hydrated ions and rates of substitution of water molecules in the first hydration sphere with the bulk water. Various techniques have been adopted in studies on dynamic properties of water molecules in the hydration shells and hydrated ions. The NMR method is one of the most powerful and convenient techniques. The quasi-elastic neutron scattering (QENS) method has sometimes been used to investigate dynamics of hydrated water molecules by using protons as the probe. Other relaxation techniques of various kinds have been examined to determine translational and rotational correlation times of water molecules in the hydration shell. The tracer diffusion method is important to determine diffusion coefficients of hydrated ions and water molecules. The rate of solvent substitution reactions, techniques of investigation of fast substitution reactions having been first explored by Eigen (see ref 349 as a review of his work), is an interesting kinetic parameter to understand behavior of water molecules in the hydration shell and the mechanism of water substitution reactions in aqueous solutions. Recently developed MD simulations are very useful to elucidate dynamic properties of water in pure and salt solutions.

A. Self-Diffusion Coefficients of Water Molecules and Ions

Translational, rotational, and reorientational correlation times of pure water are important quantities to the investigation of the behavior of hydrated water molecules, and the corresponding correlation times in the hydration shell are compared with those in pure water. The terms of "structure-making" and "structure-breaking" are originated from the comparison of the correlation times of water molecules in the two different situations. The translational (τ_T) and rotational (τ_R) correlation times are given in Table 19. The dielectric relaxation times (τ_{DE}) of pure water at various temperatures are also given in the table. The reorientational correlation time of water molecules in pure liquid (τ_{RO}) is obtained as $\tau_{RO} = 3\tau_R$, which is correlated with τ_{DE} and should be between $\tau_{DE}/2$ and $2\tau_{DE}/3$. Measured τ_{RO} values are given in Table 19 for comparison.

The self-diffusion coefficient of water in the bulk increases with the increase in temperature. The translational and rotational correlation times of water molecules in the bulk shorten with temperature, as expected from the breaking of hydrogen bonds in water. The shortening of the reorientational (τ_{RO}) and dielectric relaxation (τ_{DE}) times are accompanied by the change in τ_R .

Self-diffusion coefficients experimentally obtained by the quasi-elastic neutron scattering (QENS) method are summarized in Table 20, in which the diffusion

Table 18. The Hydration Number of Cations Determined from the Peak Area (pa) and Chemical Shift (cs) of NMR Spectra (See Section III for the Full Definitions of the Abbreviations)

salt	nucleus	method	hydration number	t, °C	ref	salt	nucleus	method	hydration number	t, °C	ref
HNO ₃	¹ H	cs	2.5 ^a		313	H ⁺					
LiCl	¹ H	cs	3.0 ^a		313	Li ⁺					
NaOH	¹ H	cs	3.5 ^a		313	LiBr	¹ H	cs	3.0 ^a		313
KF	¹ H	cs	3.0 ^a		313	Na ⁺					
RbOH	¹ H	cs	3.5 ^a		313	NaNO ₃	¹ H	cs	3.5 ^a		313
CsCl			3.0		314	K ⁺					
BeCl ₂	¹⁷ O	pa	3.95–4.30	18–32.7	315	KI	¹ H	cs	3.0 ^a		313
BeCl ₂	¹ H	pa	4.0–4.5	–20 to –62	316	Rb ⁺					
Mg(NO ₃) ₂	¹ H	pa	6	–67 to –90	318	Cs ⁺					
Mg(ClO ₄) ₂	¹ H	pa	5.6–6.1	–72 to –82	319	Be ²⁺					
CaCl ₂	¹ H	cs	6.0 ^a		313	Be(NO ₃) ₂	¹ H	pa	4	–20 to 100	317
Ca(NO ₃) ₂	¹ H	cs	6.0 ^a		313	Be(ClO ₄) ₂	¹⁷ O	cs	3.7–3.9	20	35
Sr(NO ₃) ₂	¹ H	pa	5.0	–20 to 100	317	Mg ²⁺					
Ba(NO ₃) ₂	¹ H	pa	5.7	–20 to 100	317	Mg(ClO ₄) ₂	¹ H	pa	6.0	–67 to –90	318
Fe(ClO ₄) ₂	¹⁷ O		5.85		320	Mg(ClO ₄) ₂	¹ H	cs	6.0 ^a		313
CoCl ₂			6		322	Ca ²⁺					
Ni(NO ₃) ₂	¹ H	pa	5.87	–30	324	Ca(ClO ₄) ₂	¹ H	cs	6.0 ^a		313
Ni(ClO ₄) ₂	¹⁷ O	pa	4 or 6	36	325	Sr ²⁺					
Ni(ClO ₄) ₂	¹⁷ O		6		320	Ba ²⁺					
Zn ²⁺	¹ H	pa	6.0		327	Fe ²⁺					
Cd(NO ₃) ₂	¹ H	pa	4.6	–20 to 100	317	Fe(ClO ₄) ₂	¹ H	cs	5.6–5.8	–40 to –80	321
Hg(NO ₃) ₂	¹ H	pa	4.9	–20 to 100	317	Co ²⁺					
Pb(NO ₃) ₂	¹ H	pa	5.7	–20 to 100 ^b	317	Co(ClO ₄) ₂	¹ H	pa	5.9	–38 to –63.7	323
Al(OH) ₃ ^b	²⁷ Al	pa	6.0		329	Ni ²⁺					
AlCl ₃	¹ H	pa	6.1	–29.5	330	Ni(ClO ₄) ₂	¹⁷ O	cs	6	<127	326
AlCl ₃	¹ H	pa	6.0	–47	316	Ni(ClO ₄) ₂	¹ H	cs	4.4–5.4	–30	321
AlCl ₃	¹ H	pa	6.0	–20 to –40	331	Zn ²⁺					
AlCl ₃	¹ H	pa	6.0	–47	332	Zn(ClO ₄) ₂	¹ H	cs	6.4–5.9	–120	321
AlCl ₃	¹⁷ O	pa	6.07–5.82	35	315	Cd ²⁺					
Sc(NO ₃) ₃	¹ H	pa	5.1		327	Hg ²⁺					
Cr(ClO ₄) ₃	¹⁷ O	pa	6.0	20	328	Pb ²⁺					
GaCl ₃	¹ H	pa	5.7	–58	316	Al ³⁺					
Ga(NO ₃) ₃	¹⁷ O	pa	5.9	25	333	AlBr ₃	¹ H	pa	5.6–5.9	–54 to –62	316
Ga(NO ₃) ₃	¹ H	pa	6.1	48	334	Al(NO ₃) ₃	¹ H	pa	6.01	–30 to –55	331
Ga(NO ₃) ₃	¹ H	pa	5.9	2	334	Al(NO ₃) ₃	¹ H	pa	6.0	–40	316
Ga(ClO ₄) ₃	¹⁷ O	cs	6.28	35	335	Al(ClO ₄) ₃	¹ H	pa	6.0	–50	316
Y(NO ₃) ₃			2.4		338	Al(ClO ₄) ₃	¹ H	pa	6.0	–35 to –52	327
In(ClO ₄) ₃	¹ H	pa	5.8–6.0	–89 to –99	316	Sc ³⁺					
						Sc(NO ₃) ₃			3.9		328
						Cr ³⁺					
						Cr(ClO ₄) ₃	¹⁷ O	cs	6.7–6.9	20	35
						Ga ³⁺					
						Ga(ClO ₄) ₃	¹⁷ O	pa	5.89	35	335
						Ga(ClO ₄) ₃			6.0		336
						Ga(ClO ₄) ₃	¹⁷ O	pa	5.9		337
						Ga(ClO ₄) ₃	¹ H	pa	5.8–6.1	–35 to –75	316
						Y ³⁺					
						In ³⁺					

Table 18. (Continued)

salt	nucleus	method	hydration number	<i>t</i> , °C	ref	salt	nucleus	method	hydration number	<i>t</i> , °C	ref
La(ClO ₄) ₃	¹ H	cs	6.0–6.4	–105 to –120	Ln ³⁺ 321	Gd ³⁺	¹ H		8 or 9		339
Ce(ClO ₄) ₃	¹ H	cs	4.5–5.5	–110	321	Er(NO ₃) ₃	¹ H	cs	1.0	–75	321
Sn ⁴⁺	¹ H	pa	6.0		Sn ⁴⁺ 327	SnBr ₄			6		340
SnCl ₄			6		340						
Th ⁴⁺	¹⁷ O	pa	10.0		Th ⁴⁺ 334	Th(ClO ₄) ₄	¹ H	pa	9.1	–100	327
Th(NO ₃) ₄			2.9		338						

^a Estimated value from the concentration and temperature dependences over a broad temperature range. ^b Upon hydrolysis, the predominant species formed are [Al(H₂O)₆]³⁺, [Al(OH)(H₂O)₅]²⁺, [Al₂(OH)₂(H₂O)₈]⁴⁺, [Al₁₃O₄(OH)₂₄(H₂O)₁₂]⁷⁺, and probably [Al₈(OH)₂₀(H₂O)_x]⁴⁺.

Table 19. Self-Diffusion Coefficient *D*, Translational Correlation Time τ_T , Rotational Correlation Time τ_R , Reorientational Correlation Time τ_{RO} , and Dielectric Relaxation Time τ_{DE} of Pure Water at Various Temperatures

<i>t</i> , °C	<i>D</i> , 10 ^{–5} cm ² s ^{–1} (ref 353)	τ_T , ps (ref 30)	τ_R , ps (ref 30)	τ_{RO} , ps (ref 354)	τ_{DE} , ps (ref 354)
0	1.12	11.2	5.2	15.6	17.8
5	1.31	9.6	4.3	12.9	15.0
10	1.54	8.2	3.8	11.4	12.7
15	1.78	7.1	3.3	9.9	10.8
20	2.02	6.2	2.9	8.7	9.55
25	2.3	5.5	2.5	7.5	8.25
30	2.55	4.9	2.2	6.6	7.37
35	2.92	4.3	2.0	6.0	6.60
40	3.23	3.9	1.8	5.4	5.94
45	3.58	3.5	1.7	5.1	5.30
50	3.90	3.2	1.5	4.5	4.84
55	4.20	3.0	1.4	4.2	4.40

coefficients of hydrated (*D_b*) and nonhydrated water molecules (*D_i*) and the average diffusion coefficient (*D_H*) are given, these quantities being related through eqs 16 and 17. However, accuracies of the values determined by MD, QENS, and NMR are still less than those of the values determined by the classical tracer technique. Diffusion coefficients are determinable by using tracers and by the NMR methods. A very thorough and critical review of self-diffusion coefficients have recently been made by Mills et al.³⁵⁰ A part of the data which can be compared with those by QENS are also given in Table 20.

Self-diffusion coefficients of water molecules in pure solvent (*D^w*), in the hydration shell of cations (*D^{w+}*) and anion (*D^{w–}*), together with self-diffusion coefficients of hydrated cations (*D⁺*) and anions (*D[–]*) themselves, determined by MD simulations are summarized in Table 21. The data experimentally obtained are shown in the same table for comparison. Since the origins of the data are sometimes different from those given in Table 20, the values in Tables 20 and 21 are occasionally different. In general, an agreement between MD and experimental results is satisfactory. Times elapsed for the simulation calculations are also given in the table to see how long the simulations have been carried out. The data may be important to judge the reliability of the results. Experimental results are compared with the simulation results when the data are available.

B. Rotational Correlation Time of Hydrated Water Molecules

Rotational correlation times of water molecules in the hydration shell of ions can be determined by the

NMR method. Intensive work has been devoted to the relaxation studies on aqueous solutions by the NMR method. A review published by Hertz³⁵¹ is worth citing as an important one. In Table 22 the rotational correlation times τ_R^* , given as a time of rotation of a vector from a proton in a hydrated water molecule to the center of an ion, and the rotational correlation times τ_R^+ and τ_R^- of the dipolar axis of water molecules around cations and anions, respectively, are given, together with hydration numbers of the ions assumed in the works. For paramagnetic ions such as transition metal ions, proton relaxation times burden that τ_R^{**} can only be determined instead of τ_R^* . Here τ_R^{**} is defined as

$$(1/\tau_R^{**}) = (1/\tau_R^*) + (1/\tau_{RES}^i) \quad (33)$$

where τ_{RES}^i is the residence time of water molecules in the hydration shell of ion *i*. Therefore, the residence time τ_{RES}^i must be known to obtain τ_R^* . Most cations, however, do not strictly follow the dipole–dipole mechanism expressed by eq 33, except for the cases such as Cu²⁺ and Gd³⁺. Since the τ_R^* indicates the rotational correlation time of ion–proton vector, the rotational relaxation time of water molecules in the hydration shell can be obtained, in the strict sense, only for ions such as Al³⁺ and Cr³⁺, which very strongly combine with water molecules, and thus, the rotation of the ion–proton vector can be regarded as the rotation of a water molecule itself.

For systems containing diamagnetic ions the assumption of the rigid body of solvated ions should be rejected. The average rotational correlation time τ_R^w of water molecules in a given system is measured and is separated into values of individual τ_R^+ and τ_R^- after extrapolation of the τ_R^w values to 0 concentration. The τ_R^+ and τ_R^- values, the rotational correlation times of water molecules around a cation and an anion, respectively, without specification of bond vector, are usually given in the literature as the ratio τ_R^+/τ_R^0 or τ_R^-/τ_R^0 , where τ_R^0 denotes the rotational correlation time of pure water in the system, which is given to be 2.5×10^{-12} s at 25 °C. At the separation of the τ_R^w value into τ_R^+ and τ_R^- , the hydration numbers of the cation and anion must be known. In Table 22 the τ_R^+ and τ_R^- values so far reported are summarized.

The values of τ_R^+ for Li⁺ and Na⁺ are larger than τ_R^0 and the τ_R^+ values of other alkali metal ions are even smaller than τ_R^0 . The former are called the structure-making ions and the latter the structure-breaking ones. Rotational motions of water molecules are enhanced around structure-breaking cations due to the breaking

Table 20. Translational Self-Diffusion Coefficients Determined by the QENS Method for Ions

salt	H ₂ O/salt	<i>t</i> , °C	<i>D</i> , 10 ⁻⁵ cm ² s ⁻¹					ref
			<i>D_b</i>	<i>D_t</i>	<i>D_H</i>	<i>D_{tracer}</i>	<i>D_{NMR}</i>	
LiCl	11				1.30	1.22 ^a	1.23 ^b	19
CsF	19.5				1.69		1.62 ^c	19
CsCl	19.5				2.57	2.38 ^d	2.61 ^c	19
CsI	32.6				2.60		2.54 ^e	19
MgCl ₂	27.8				1.05		1.17 ^b	19
MgCl ₂	19.5				0.76		0.81 ^b	19
CaCl ₂	27.8				1.40	1.36 ^d	1.36 ^b	19
CaCl ₂	18.5				1.00	1.04 ^d	1.02 ^b	19
NiCl ₂	55.5				1.68	1.72 ^a		19
NiCl ₂	37.0				1.49	1.39 ^a		19
NiCl ₂	27.8				1.16	1.07 ^a		19
NiCl ₂	18.5				0.75	0.74 ^a		19
NiCl ₂	27.8	27	0.45		1.44		1.72 ^a	19
Ni(NO ₃) ₂	27.8	19.7	0.35		1.16			355
Ni(ClO ₄) ₂	27.8	27	0.46		1.60			355
CuCl ₂	27.8	2.3			0.65			355
CuCl ₂	18.5	4.2			0.49			355
Cu(ClO ₄) ₂	27.8	2.2			0.68			355
Cu(ClO ₄) ₂	18.5	5.0			0.51			355
Cu(ClO ₄) ₂	18.5	28.8			1.11			355
CuCl ₂ ^{f,g}	27.8	5	0.26	0.79	0.65		0.71 ^h	355
CuCl ₂ ^{f,g}	18.5	5	0.20	0.58	0.49		0.50 ^h	355
Cu(ClO ₄) ₂ ^{f,g}	27.8	5	0.26	0.82	0.68		0.74 ^h	355
Cu(ClO ₄) ₂ ^{f,g}	18.5	5	0.20	0.60	0.51		0.51 ^h	355
Cu(ClO ₄) ₂ ^{f,g}	18.5	25	0.34	1.19	1.11		1.01 ^h	355
ZnCl ₂	28.3	28	0.49	1.52	1.30		1.52 ⁱ	355
Zn(ClO ₄) ₂	28.0	26	0.44	1.12	0.93		1.24 ⁱ	355
Zn(ClO ₄) ₂ ^f	21.5	28.6	0.47	1.50	1.44		1.73 ^j	355
Cr(ClO ₄) ₃	31.0	26	0.22	0.97	0.82	0.87		356
Fe(NO ₃) ₃	27.8	19	0.14	0.64	0.53	0.52		357
Fe(ClO ₄) ₃ ^k	27.8	28	0.17	0.77	0.63	0.68		357
Al(ClO ₄) ₃	27.8	19	0.15	0.72	0.60	0.53		357
Ga(ClO ₄) ₃ ^k	23.5	28	0.21	0.84	0.68	0.65		357
NdCl ₃	55.5	17.6	0.41	1.14				355
NdCl ₃	27.8	24.5	0.30	0.89				355
Dy(ClO ₄) ₃ ^l	38.3	26	0.43	1.25	1.08			357
Dy(ClO ₄) ₃ ^l	38.3	38	0.48	1.67	1.42			357

^a Reference 358. ^b Reference 359. ^c Reference 360. ^d Reference 361. ^e Reference 362. ^f *D_i* = *D_b* is assumed. ^g Hydration number *n_i* = 4 is assumed. ^h Reference 353. ⁱ Reference 413. ^j Reference 424. ^k *n_i* = 6 is assumed. However, due to the hydrolysis of the metal ion, *n_i* may be reduced to about 5. ^l *n_i* = 8 is assumed.

of hydrogen bonds between hydrated and bulk water molecules. Similar trends are seen in halide ions. τ_{R^-} of F⁻ is larger than τ_{R^0} , and thus, $\tau_{R^-}/\tau_{R^0} > 1$, while the values for Cl⁻, Br⁻, and I⁻ are less than unity. The τ_{R^+} values of divalent and trivalent cations are larger than τ_{R^0} , as expected from the strong hydration structure of the ions. The τ_{R^-} value of SO₄²⁻ is larger, while that of ClO₄⁻ is smaller than τ_{R^0} . The results show that the hydration of SO₄²⁻ is strong, while ClO₄⁻ breaks the water structure by the ion-water interaction. The τ_{R^-} value of BF₄⁻ is obtained to be almost equal to τ_{R^0} when the hydration number of the ions is assumed to be 0.

In Table 23 rotational correlation times $\tau_{R,D}$ and $\tau_{R,OH}$ are listed, which are determined by using proton-, deuteron-, and ¹⁷O-waters. $\tau_{R,D}$ is defined as the correlation time of rotation of a position vector at D in D₂O in the hydration shell of ions, and $\tau_{R,OH}$ is that of rotation of an O-H axis connecting in a water molecule. These values are determined by the NMR method. The isotope effect between ¹H and ²H (D) has been seen. The $\tau_{R,H}$ (τ_{R^0} in the preceding section) is determined to be 2.5×10^{-12} s, while $\tau_{R,D}^0$ is 1.95×10^{-12} s. The isotope effect of water should be reflected to the rotational correlation time of ions, $\tau_{R,D}^i$. The $\tau_{R,D}^i$ values are very close to the $\tau_{R,OH}^i$, the rotational correlation time of O-H bond in the hydrated water of the ion *i* (*i* = + for cations and *i* = - for anions). Both $\tau_{R,D}^i$ and

$\tau_{R,OH}^i$ decrease with an increase in the ionic radius in the series of alkali metal ions, and $\tau_{R,D}^+$ and $\tau_{R,OH}^+$ of alkali metal ions are close to the τ_{R^+} values in Table 22. The same situation is seen for halide ions.

C. Reorientational Time of Hydrated Water Molecules

MD simulations reveal molecular movements of water in the hydration shell at the molecular level. The reorientational ($\tau_{RO,X}^i$) times of hydrated water molecules are summarized in Table 24 for rather limited systems. The reorientational time of the dipole (μ) of a water molecule, which is denoted as $\tau_{RO,\mu}^i$ for water molecules around an ion *i* (*i* = + for cation and *i* = - for anion; the reorientational time of pure water or water in the bulk is denoted with the superscript 0 in Table 24) may reflect the strength of the ion-water bond in the hydration shell of ions. The reorientation times of the H-H axis in a water molecule ($\tau_{RO,HH}^i$) around ions *i* are close to the values of $\tau_{RO,\mu}^i$. The reorientational anisotropy of hydrated water molecules can be seen from the different values between $\tau_{RO,\mu}^i$ and $\tau_{RO,HH}^i$.

Neon is regarded as a Lennard-Jones solute. The reorientational time of water molecules around neon is close to that of Li⁺ and larger than those of NH₄⁺ and

Table 21. Self-Diffusion Coefficients Determined by MD Simulations for Cations (D^+), Anions (D^-), Solvent Water (D^w), and Water Molecules in the Hydration Shell of the Cations (D^{w+}) and Anions (D^{w-}) and in the Bulk Water (D^{w0}) at 25 °C ($10^{-5} \text{ cm}^2 \text{ s}^{-1}$)^a

salt	H ₂ O/salt	D^+	D^-	D^w	D^{w+}	D^{w-}	D^{w0}	simulation time, ps	water model	ref(s)
NH ₄ Cl	25	1.0 (1.58)	1.3 (2.66)	2.80	2.90 (2.78)	2.98	2.72	3.5	ST2	363 353,364
Li ⁺ ^b	64,125	0.3 (0.60)						30	MCY	282 365
Li ⁺ ^c	64,125	1.8 (3.10)						30	MCY	282 365
LiCl	3	0.20 (0.21)	0.17 (0.21)	0.35 (0.41)				7.5	BJH	366 367
LiCl	4	0.70	0.90	0.96				2.4	CF	79
LiI	25	0.7 (1.0)	1.40 (1.47)	2.48 (2.35)	1.33	2.67	2.85	10	ST2	368 362
Na ⁺ ^d	64,125	1.0 (0.91)						30	MCY	282 365
NaCl	25	0.82 (1.12)	1.08 (1.60)	1.60 (1.92)	0.90	1.51	1.86	5	BJH	300 365,369
NaCl ^e	25	0.55 (1.30)	1.25 (1.85)	1.51 (1.60)	0.89	1.44	1.76	5	BJH	300 365,369
K ⁺ ^f	64,125	2.8 (0.86)						30	MCY	282 365
KCl	25	1.1 (1.50)	1.1 (1.85)	2.60 (1.86)	2.40	2.50	2.70	8.7	ST2	370 371,372
SrCl ₂	50	0.6	1.2		0.9	1.4	1.4	4	BJH	309
F ⁻ ^b	64,125		0.9 (0.86)					30	MCY	282 365
Cl ⁻ ^g	64,125		2.3 (1.60)					30	MCY	282 365
HS ^h	107	2.91		3.46				70	ST2	373

^a Values in parentheses are those experimentally obtained. ^b At 5 °C. ^c At 95 °C. ^d At 9 °C. ^e At 30 °C and 10 kbar pressure. ^f At 1 °C. ^g At 14 °C. ^h Lennard-Jones (Hard Sphere) solute at 30 °C.

I⁻, the result suggesting the hydrophobic structure-making effect around neon atoms. A similar trend can also be seen for the rotational correlation times of $\tau_{R^{LJ}}$ for neon.

The rotational correlation (τ_{R,X^i}) times of the dipole ($X = \mu$) and proton-proton ($X = HH$) vectors of water molecules in the first hydration shell of cations ($i = +$), anions ($i = -$), and bulk water ($i = 0$) have been investigated by MD simulations, and the results are summarized in Table 24. The rotational anisotropy of water molecules around the ions examined is not conclusive.

D. Residence Time of Water Molecules in the First Hydration Shell of Ions

A question how long water molecules stay in the hydration shell is interesting, but is very difficult to answer. Molecular dynamics simulations may reply to the question to some extent. The residence time τ_{RES} is, of course, different from the rate of solvent substitution process of ions, the data being summarized in the last table. The residence times (τ_{RES}^i) of water molecules in the first hydration shell of cations and anions and at a given position in the bulk ($i = +, -,$ and 0, respectively) are listed in Table 25.

The dynamic hydration number n_{hyd}^i is newly defined as follows:

$$n_{hyd}^i = n^i \exp(-\tau_{RES}^0 / \tau_{RES}^i) \quad (34)$$

where n^i denotes the static hydration number of a cation ($i = +$) and an anion ($i = -$). τ_{RES}^0 and τ_{RES}^i stand for the residence times of water molecules in the bulk and in the hydration shell of ions, respectively.²⁸² From

Table 22. Rotational Correlation Times τ_R^* , τ_R^+ , and τ_R^- for Some Paramagnetic and Diamagnetic Ions Obtained by the NMR Method at 25 °C

ion	nucleus	τ_R^* , ps	$\tau_R^+, \tau_R^-,^a$ ps	ref
Li ⁺	⁷ Li	12	4.5	374
Li ⁺	¹ H		7.3	375
Li ⁺	¹ H		5.8	375
Na ⁺	¹ H		4.5	375
Na ⁺	¹ H		4.0	375
K ⁺	¹ H		2.3	375
Rb ⁺	¹ H		1.5	362
Cs ⁺	¹ H		1.3	362
Cs ⁺	¹ H		1.8	362
Mg ²⁺	¹ H		13.0	375
Ca ²⁺	¹ H		8.8	362
Ca ²⁺	¹ H		7.3	362
Sr ²⁺	¹ H		6.5	362
Ba ²⁺	¹ H		5.5	362
V ²⁺	¹ H	21		376
Mn ²⁺	¹ H	31		376
Mn ²⁺	¹ H	31		377
Mn ²⁺	¹ H	32		378
Cu ²⁺	¹ H	25		378
Cu ²⁺	¹⁷ O	29.5		351
Cr ³⁺	¹ H	45		378
Cr ³⁺	¹ H	83		376
Al ³⁺	²⁷ Al	53	44	374
Gd ³⁺	¹ H	20		376
F ⁻	¹ H		5.8	362
F ⁻	¹⁹ F	11–17		360
Cl ⁻	¹ H		2.3	362
Cl ⁻	¹ H		2.3	362
Br ⁻	¹ H		1.5	362
Br ⁻	¹ H		1.8	362
I ⁻	¹ H		1.0	375
SO ₄ ²⁻	¹ H		4.3	375
ClO ₄ ⁻	¹ H		1.3	375
BF ₄ ⁻	¹⁹ F		2.4	360

^a Recalculated from the τ_R^i/τ_R^0 ratios with $\tau_R^0 = 2.5 \times 10^{-12} \text{ s}$ for pure water at 25 °C.

Table 23. Rotational Correlation Times $\tau_{R,D}^i$ and $\tau_{R,OH}^i$ for Ions Obtained by the NMR Method at 25 °C

ion	salt	H ₂ O/salt	nucleus	$\tau_{R,D}^i$, ps	$\tau_{R,OH}^i$, ps	ref
Li ⁺ ^a	LiCl	14.0	¹ H, ² H, ¹⁷ O	4.1	4.6	379
Li ⁺ ^a	LiCl	30.3	¹ H, ² H, ¹⁷ O	3.9	3.7	379
Li ⁺ ^b	LiCl	14.0	¹ H, ² H, ¹⁷ O	5.0	5.0	379
Li ⁺ ^b	LiCl	30.3	¹ H, ² H, ¹⁷ O	3.0	3.0	379
Li ⁺ ^a	LiBr	270–55	¹ H, ¹⁷ O	4.53	4.54	380
Li ⁺ ^c	LiBr	270–55	¹ H, ¹⁷ O	4.83	4.81	380
Li ⁺ ^d	LiBr	270–55	² H, ¹⁷ O	4.72		381
Na ⁺ ^a	NaCl	13.9	¹ H, ² H, ¹⁷ O	3.1	3.5	379
Na ⁺ ^b	NaCl	13.9	¹ H, ² H, ¹⁷ O	3.7	3.7	379
Na ⁺ ^a	NaBr	270–55	¹ H, ¹⁷ O	3.36	3.34	380
Na ⁺ ^b	NaBr	270–55	¹ H, ¹⁷ O	3.58	3.54	380
Na ⁺ ^d	NaBr	270–55	² H, ¹⁷ O	3.49		381
K ⁺ ^a	KCl	13.9	¹ H, ² H, ¹⁷ O	1.8	1.7	379
K ⁺ ^b	KCl	13.9	¹ H, ² H, ¹⁷ O	1.6	1.6	379
K ⁺ ^a	KCl	270–55	¹ H, ¹⁷ O	1.64	1.63	380
K ⁺ ^b	KCl	270–55	¹ H, ¹⁷ O	1.75	1.73	380
K ⁺ ^d	KCl	270–55	² H, ¹⁷ O	1.96		381
Cs ⁺ ^a	CsBr	270–55	¹ H, ¹⁷ O	1.52	1.50	380
Cs ⁺ ^b	CsBr	270–55	¹ H, ¹⁷ O	1.62	1.59	380
Cs ⁺ ^d	CsBr	270–55	² H, ¹⁷ O	1.67		381
Mg ²⁺ ^a	MgCl ₂	13.9–55.5	¹ H, ² H, ¹⁷ O	2.02	1.96	382
Mg ²⁺ ^b	MgCl ₂	13.9–55.5	¹ H, ² H, ¹⁷ O	1.94	1.94	382
F ⁻ ^a	KF	13.9	¹ H, ² H, ¹⁷ O	3.9	4.7	379
F ⁻ ^b	KF	13.9	¹ H, ² H, ¹⁷ O	5.3	5.3	379
F ⁻	KF	270–55	² H, ¹⁷ O	6.47		383
Cl ⁻	KCl	270–55	² H, ¹⁷ O	1.70		383
Br ⁻	KBr	270–55	² H, ¹⁷ O	1.33		383
I ⁻	KI	270–55	² H, ¹⁷ O	0.90		383

^a The intramolecular relaxation rates are calculated by assuming that the O–H bond length is same as that in pure water. ^b The rotational isotropy is taken into account. The bond lengths in a water molecule are slightly changed. ^c The intramolecular relaxation rates are calculated with OH distance longer than that in pure water. ^d In D₂O.

Table 24. Reorientational Characteristics of Water Molecules Determined by the MD Simulation Method: Reorientation Times $\tau_{RO,X}^i$ and Rotational Correlation Times $\tau_{R,X}^i$ of Dipole Vector ($X = \mu$) and of Proton–Proton Vector ($X = HH$) of the Water Molecules in the First Hydration Shells of Cations ($i = +$), Anions ($i = -$), and in the Bulk ($i = 0$) at 25 °C (10^{-12} s)

salt	H ₂ O/salt	$\tau_{RO,\mu}^+$	$\tau_{RO,\mu}^-$	$\tau_{RO,\mu}^0$	$\tau_{RO,HH}^+$	$\tau_{RO,HH}^-$	$\tau_{RO,HH}^0$	$\tau_{R,\mu}^+$	$\tau_{R,\mu}^-$	$\tau_{R,\mu}^0$	$\tau_{R,HH}^+$	$\tau_{R,HH}^-$	$\tau_{R,HH}^0$	simulation time, ps	water model	ref
NH ₄ Cl	25	4.6	7.9	5.8				1.7	2.4	1.6	2.1	2.0	1.4	3.5	ST2	363
LiI	25	6.8	4.6	4.4	4.5	3.3	3.1	2.5	1.5	1.3	2.4	1.4	1.5	10	ST2	368
Ne ^a	107	6.59		3.82	4.03		3.42	2.55		1.61	2.65		2.12	5.4	ST2	384

^a A Lennard-Jones solute (neon) at 30 °C.

Table 25. Residence Times of Water Molecules in the First Hydration Shells of the Cations τ_{RES}^+ and Anions τ_{RES}^- and in the Bulk τ_{RES}^0 , and Dynamic Hydration Numbers n_{hyd}^+ , n_{hyd}^- for Cations and Anions, Respectively, Determined by the MD Simulation Method at 25 °C

salt	H ₂ O/salt	τ_{RES}^+ , ps	τ_{RES}^- , ps	τ_{RES}^0 , ps	n_{hyd}^+	n_{hyd}^-	simulation time, ps	water model	ref
Li ⁺ ^a	64,125	33.3		4.8	4.6		30	MCY	282
Li ⁺ ^b	64,125	6.0					30	MCY	282
LiI	25	25	5				10	ST2	368
Na ⁺ ^c	64,125	9.9		3.8	3.8		30	MCY	282
NaCl	25	long	3.8				1.4	CF	298
K ⁺ ^d	64,125	4.8		4.0	2.9		30	MCY	282
F ⁻ ^e	64,125		20.3	5.5		4.6	30	MCY	282
Cl ⁻ ^e	64,125		4.5	4.1		2.6	30	MCY	282
Ne ^f	107		4.8	4.8			5.4	ST2	384

^a At 5 °C. ^b At 95 °C. ^c At 9 °C. ^d At 1 °C. ^e At 14 °C. ^f A Lennard-Jones solute (neon) at 30 °C.

the definition, the dynamic hydration number is 0 when the residence time of hydrated water molecules is very small compared with that in the bulk and increases with the increase in the residence time of water molecules to approach the static hydration number n^i . The dynamic hydration number may be an interesting quantity to discuss dynamic behavior of hydrated water molecules around ions, but the usefulness of the quantity is not yet well established in solution chemistry.

The residence times of oxygen and hydrogen atoms

in the hydration shell are usually different, because a proton can move faster than an oxygen atom to the next water molecule in the second hydration shell through a hydrogen bond. Therefore, the residence time of protons should be shorter than that of oxygen atoms. The residence time of an oxygen atom is regarded as the residence time of hydrated water molecules. Various methods have been used to determine the residence times of proton and oxygen atoms in hydrated water molecules. The results are summarized in Table 26.

Table 26. Residence Time of Oxygens $\tau_{\text{RES}}^{\text{O}}$ or Protons $\tau_{\text{RES}}^{\text{P}}$ for Water Molecules in the First Hydration Shells of Ions Determined by Various Methods at 25 °C (See Sections III and IV for the Full Definitions of the Abbreviations)

ion	salt	$\tau_{\text{RES}}^{\text{O}}, \text{s}$	$\tau_{\text{RES}}^{\text{P}}, \text{s}$	method	ref
Li ⁺	LiI	2.5×10^{-12}	$\sim 3 \times 10^{-11}$	MD	368
Li ⁺				NMR	351
Li ⁺				QENS	355
K ⁺	Be(ClO ₄) ₂	$<10^{-10}$	$\leq 10^{-10}$	QENS	415
Cs ⁺				QENS	355
Be ²⁺				NMR	315
Mg ²⁺	MnSO ₄	$\geq 3 \times 10^{-4}$	$\geq 5 \times 10^{-9}$	QENS	355
Mg ²⁺				NMR	415
Mg ²⁺				NMR	415
Ca ²⁺	Fe(NH ₄) ₂ (SO ₄) ₂	$\sim 10^{-5}$	$\leq 10^{-10}$	QENS	355
Ca ²⁺				NMR	415
Mn ²⁺				NMR	385
Fe ²⁺	CoSO ₄	3.2×10^{-8}	$\sim 10^{-6}$	NMR	385
Fe ²⁺				NMR	385
Co ²⁺				NMR	385
Ni ²⁺	Ni(NO ₃) ₂	8.8×10^{-7}	$\geq 5 \times 10^{-9}$	QENS	355
Ni ²⁺				NMR	385
Ni ²⁺				NMR	415
Ni ²⁺	Ni(ClO ₄) ₂	3.7×10^{-5}	$\sim 10^{-6}$	NMR	386
Ni ²⁺				NMR	387
Ni ²⁺				NMR	387
Cu ²⁺	Cu(NO ₃) ₂	3×10^{-6}	3.3×10^{-5}	NMR	387
Cu ²⁺				NMR	385
Cu ²⁺				NMR	385
Zn ²⁺		1×10^{-4}	$\leq 10^{-10}$	QENS	355
Ti ³⁺				QENS	388
Ti ³⁺				NMR	389
V ³⁺		6×10^{-5}	$>10^{-10}$	NMR	390
V ³⁺				NMR	390
V ³⁺				NMR	391
Cr ³⁺		1.8×10^5 to 2.2×10^5	2×10^{-6}	NMR	351
Cr ³⁺				QENS	356
Cr ³⁺				QENS	356
Cr ³⁺	Cr(ClO ₄) ₃	5×10^{-5}	$\geq 5 \times 10^{-9}$	NMR	387
Cr ³⁺				NMR	387
Cr ³⁺				NMR	387
Fe ³⁺	Fe(ClO ₄) ₃	6×10^{-3}	$\geq 5 \times 10^{-9}$	QENS	357
Fe ³⁺				NMR	389
Fe ³⁺				NMR	392
Fe ³⁺		6×10^{-3}	$\geq 5 \times 10^{-9}$	NMR	393
Fe ³⁺				NMR	393
Fe ³⁺				NMR	393
Co ³⁺	AlCl ₃	10^5	2×10^{-3}	NMR	394
Co ³⁺				NMR	394
Co ³⁺				NMR	394
Al ³⁺		1	2×10^{-3}	NMR	394
Al ³⁺				NMR	395
Al ³⁺				NMR	395
Al ³⁺		6.0	$\geq 5 \times 10^{-9}$	NMR	389
Al ³⁺				NMR	389
Al ³⁺				NMR	396
Al ³⁺		0.78	$\geq 5 \times 10^{-9}$	QENS	357
Al ³⁺				QENS	357
Al ³⁺				QENS	357
Ga ³⁺		5.5×10^{-4}	$\geq 5 \times 10^{-9}$	NMR	389
Ga ³⁺				NMR	389
Ga ³⁺				NMR	389
Nd ³⁺		1.3×10^{-8} to 3.9×10^{-8}	$>10^{-10}$	QENS	355
Nd ³⁺				QENS	355
Nd ³⁺				QENS	355
Tb ³⁺		1.4×10^{-8} to 4.8×10^{-8}	$>10^{-10}$	NMR	397
Tb ³⁺				NMR	397
Tb ³⁺				NMR	397
Dy ³⁺		3.1×10^{-8} to 5.9×10^{-8}	$>10^{-10}$	NMR	397
Dy ³⁺				NMR	397
Dy ³⁺				NMR	397
Dy ³⁺		3.2×10^{-8} to 7.1×10^{-8}	$>10^{-10}$	NMR	397
Dy ³⁺				NMR	397
Dy ³⁺				NMR	397
Ho ³⁺		1.6×10^{-8} to 9.1×10^{-8}	$>10^{-10}$	QENS	357
Ho ³⁺				QENS	357
Ho ³⁺				QENS	357
Ho ³⁺		1.8×10^{-8} to 1.1×10^{-7}	$>10^{-10}$	NMR	397
Ho ³⁺				NMR	397
Ho ³⁺				NMR	397
Er ³⁺		7.4×10^{-9} to 1.5×10^{-7}	$>10^{-10}$	NMR	397
Er ³⁺				NMR	397
Er ³⁺				NMR	397
Er ³⁺		7.7×10^{-9} to 1.9×10^{-7}	$>10^{-10}$	NMR	397
Er ³⁺				NMR	397
Er ³⁺				NMR	397
Tm ³⁺		1.5×10^{-7} to 2.5×10^{-7}	$>10^{-10}$	NMR	397
Tm ³⁺				NMR	397
Tm ³⁺				NMR	397
Tm ³⁺		1.6×10^{-7} to 3.0×10^{-7}	$>10^{-10}$	NMR	397
Tm ³⁺				NMR	397
Tm ³⁺				NMR	397
F ⁻	NaCl	3.8×10^{-12}	$\leq 10^{-10}$	QENS	355
Cl ⁻				MD	298
Cl ⁻				QENS	355
I ⁻	LiI	5×10^{-11}	$\leq 10^{-10}$	MD	368
I ⁻				QENS	355
I ⁻				QENS	355
ClO ₄ ⁻			$\leq 10^{-10}$	QENS	355

E. Rates of Water Substitution Reactions of Ions

In the last table, Table 27, kinetic parameters for water substitution reactions of various hydrated ions

are summarized. The geometries and the static hydration number (n) of the hydrated ions taken into consideration of the water substitution reactions are also shown in the table, which are not absolutely necessary to discuss the thermodynamic quantities, but the geometries and the hydration numbers are important to discuss the reaction mechanisms from the thermodynamic quantities of activation state of the reaction. The rates (k), and enthalpies (ΔH^\ddagger), entropies (ΔS^\ddagger), and volumes (ΔV^\ddagger) of activation are listed in the table. It is supposed that a positive value of the entropy of activation and a negative value of the volume of activation indicate the associative mechanism, and the reverse shows the dissociative mechanism at the substitution reaction of hydrated water molecules. From the criteria, reaction mechanisms of the solvent substitution reactions are proposed for various cases. However, it should be noted that no sound theoretical base has been established to say that the negative (positive) entropy of activation or the negative (positive) activation volume indicates the associative (dissociative) mechanism. The criteria might be reasonable as long as the bond length in the hydrated ion, and thus the radius of the spherical shape of the hydrated ion, were preserved during the solvent substitution process. These requirements may hardly be fulfilled in most cases. Reliable theoretical considerations should be done to discuss reaction mechanisms from the kinetic parameters.

Rate constants of solvent substitution reactions decrease with increasing ionic radii of alkali metal and alkaline earth metal ions due to the decrease in the ion-water interaction energy. The irregularity of the rate constants of transition metal ions has been explained in terms of the stabilization of activated complexes by using the ligand field theory.³⁵²

Ruthenium(II,III), palladium(II), and platinum(II) ions are very inert, which may be compared with chromium(III).

V. Concluding Remarks

Structural studies of hydrated ions seem to be established by the development of the diffraction techniques and simulation procedures. Of course, more reliable and precise measurements will be done in the future for the static structures of hydrated ions. The methods are extended to nonaqueous solutions. Structures of various complexes formed in solution have also been determined by the diffraction methods, and the bond length variations with solvents and composition of complexes have been discussed in the field of solution chemistry. However, studies on dynamic properties of ions and water molecules in the bulk and the hydration sphere have not been performed as much as those on static properties and appears to be an important subject for more intensive investigation in the beginning with the 1990s. Reaction mechanisms of solvent substitution reactions and complex formation reactions will be discussed in terms of behavior of individual ions and molecules with time. Thermodynamics may still provide a sound base in solution chemistry, but thermodynamic properties must be connected with molecular behavior of each species in solution. According to recent MD investigations, the water structure is not so rigid as seen in pictures drawn in various texts and water molecules are very quickly moving at every moment.

Table 27. The Assumed Geometry and Hydration Number n for the $[M(H_2O)_n]^{z+}$ Ion, the Rate Constant k at 25 °C, the Enthalpy ΔH^\ddagger , Entropy ΔS^\ddagger , and Volume of Activation ΔV^\ddagger

ion	salt	geometry	n	k , s ⁻¹	ΔH^\ddagger , kJ mol ⁻¹	ΔS^\ddagger , J K ⁻¹ mol ⁻¹	ΔV^\ddagger , cm ³ mol ⁻¹	proposed mechanism ^a	ref(s)
Be ²⁺		T	4	730	59.2	8.4	-13.6	A	24
V ²⁺		O	6	87	61.8	-0.4	-4.1	I _a	398
Mn ²⁺	MnSO ₄	O	6	3.1×10^7	33.9	12.2			385
Mn ²⁺		O	6	2.2×10^7	32.2	3.8			399
Mn ²⁺	Mn(ClO ₄) ₂	O	6	2.1×10^7	32.9	5.7	-5.4	I _a	400
Fe ²⁺		O	6	3.2×10^6	32.2	-12.5			385
Fe ²⁺	Fe(ClO ₄) ₂	O	6	4.39×10^6	41.4	21.2	3.8	I _a -I _d	400
Co ²⁺	CoSO ₄	O	6	1.35×10^6	33.4	-17.4			385
Co ²⁺	-	O	6	2.38×10^6	43.5	22.1			401
Co ²⁺	-	O	6	2.45×10^6	49.7	44.3			402
Co ²⁺	Co(ClO ₄) ₂	O	6	3.18×10^6	46.9	37.2	6.1	I _a -I _d	400
Ni ²⁺	Ni(NO ₃) ₂	O	6	2.7×10^4	48.5	2.5			385
Ni ²⁺	Ni(ClO ₄) ₂	O	6		58.1	41.8			326
Ni ²⁺	Ni(ClO ₄) ₂	O	6	3.14×10^4	56.8	32.2			403
Ni ²⁺	Ni(ClO ₄) ₂	O	6	3.37×10^4	52.3	17.2	7.1	I _d	404
Cu ²⁺	Cu(NO ₃) ₂	O	4	1×10^4	192	-16.8			385
			2	2×10^8	87.8				
Ru ²⁺		O	6	1.8×10^{-2}	87.8	16.1	-0.4	I	24
Pd ²⁺	Pd(ClO ₄) ₂	Sp ^b	4	560	49.5	-26	-2.2	I _a or A	405
Pt ²⁺	Pt(ClO ₄) ₂	Sp ^b	4	3.9×10^{-4}	89.7	-9	-4.6	I _a or A	24,405
Pt ²⁺	Pt(ClO ₄) ₂		4	5.8×10^{-4}	100	29		I _d	406
Al ³⁺	AlCl ₃		6	0.17	113	117			389
Al ³⁺	Al(ClO ₄) ₃	O	6	1.29	84.7	41.6	5.7	I _d	396
Ga ³⁺	Ga(ClO ₄) ₃	O	6	400	67.1	30.1	5.0	I _d	407
Ti ³⁺		O	6	1.8×10^5	43.4	1.2	-12.1	I _a or A	407
V ³⁺	V(CF ₃ SO ₃) ₃	O	6	500	49.4	-27.8	-8.9	I _a	408
V ³⁺	VCl ₃		6	1.67×10^3	25.9	-96			408
Cr ³⁺		O	6	2.4×10^{-6}	108.6	11.6	-9.6	I _a	409
Fe ³⁺	Fe(ClO ₄) ₃	O	6	167	77.3	57.7			392
Fe ³⁺	Fe(ClO ₄) ₃	O	6	160	64.0	12.1		I _a	393
Fe ³⁺		O	6	160	64.0	12.1	-5.4	I _a	24
Fe ³⁺	Fe(ClO ₄) ₃	O	6	6.8×10^4	40.3	80	-5.4	I _a	410
Ru ³⁺		O	6	3.5×10^{-6}	89.8	-48.3	-8.3	I _a	24
Rh ³⁺		O	6	2.2×10^{-9}	131.2	29.3	-4.2	I _a	24
Gd ³⁺	Gd(ClO ₄) ₃		9	10.6×10^8	12.0	-31.9		I _a	411
Gd ³⁺	Gd(ClO ₄) ₃		8	11.9×10^8	12.0	-30.9		I _a	192
Tb ³⁺	Tb(ClO ₄) ₃		9	4.96×10^8	12.08	-37.9	-5.7	I _a	411
Tb ³⁺	Tb(ClO ₄) ₃		8	5.58×10^8	12.1	-36.9	-5.7	I _a	412
Dy ³⁺	Dy(ClO ₄) ₃		9	3.86×10^8	16.57	-25.0	-6.0	I _a	411
Dy ³⁺	Dy(ClO ₄) ₃		8	4.34×10^8	16.6	-24.0	-6.0	I _a	412
Ho ³⁺	Ho(ClO ₄) ₃		9	1.91×10^8	16.36	-31.5	-6.6	I _a	411
Ho ³⁺	Ho(ClO ₄) ₃		8	2.14×10^8	16.4	-30.5	-6.6	I _a	412
Er ³⁺	Er(ClO ₄) ₃		9	1.18×10^8	18.37	-28.8	-6.9	I _a	411
Er ³⁺	Er(ClO ₄) ₃		8	1.33×10^8	18.4	-27.8	-6.9	I _a	412
Tm ³⁺	Tm(ClO ₄) ₃		9	0.81×10^8	22.68	-17.4	-6.0	I _a	411
Tm ³⁺	Tm(ClO ₄) ₃		8	0.47×10^8	22.7	-16.4	-6.0	I _a	412
Yb ³⁺	Yb(ClO ₄) ₃		9	0.41×10^8	23.29	-21.0		I _a	411
Yb ³⁺	Yb(ClO ₄) ₃		8	0.47×10^8	23.3	-21.0		I _a	192

^a A, associative; D, dissociative; I, interchange; I_a, associative interchange; I_d, dissociative interchange. ^b Square planar.

This behavior of water molecules is well understood by chemists, but such pictures drawn from dynamic properties of ions and water molecules do not coincide well with structural pictures which are too much static in the drawings. The difference in the two kinds of pictures are so different that our understandings of solution are still confused. Besides studies under equilibrium conditions, studies on nonequilibrium processes in complex formation reactions have scarcely been investigated so far. Dynamic studies of ions and water molecules in solution may be a first step of investigation of nonequilibrium processes in solution. Therefore, the studies on dynamic processes of ions and water molecules should be investigated more extensively. No information is available for the structure of activated complexes. Discussions on the associative (A-) and dissociative (D-) mechanisms for solvent substitution reactions shown in Table 26 should disappear when we could see the structure of the activated complexes of $[M(H_2O)_{n-1}]^{z+}$ of $[M(H_2O)_{n+1}]^{z+}$ in the

solution. Some attempts have been started to determine structures of reaction intermediates in solution by the EXAFS method combined with a stopped-flow technique,⁴¹⁷ but the goal to the direct structural analysis of activated complexes in solution is still far.

Acknowledgments. One of the authors (T.R.) is greatly indebted to the Institute for Molecular Science, Okazaki, for the invitation as a guest scientist, within the frame of the invitation he could contribute to the preparation of this review.

VI. References

- (1) Conway, B. E. *Ionic Hydration in Chemistry and Biophysics, Studies in Physical and Theoretical Chemistry 12*; Elsevier: Amsterdam, 1981.
- (2) Marcus, Y. *Ion Solvation*; Wiley: Chichester, UK, 1986.
- (3) Burgess, J. *Metal Ions in Solution*; Ellis Horwood: New York, 1978.
- (4) Ohtaki, H. *Yoeki Kagaku (Solution Chemistry)*; Shokabo: Tokyo, 1985 (in Japanese); *Ion no Suiwa (Ionic Hydration)*; Kyoritsu Shuppan Publ.: Tokyo, 1990; (in Japanese).

- (5) Magini, M.; Licheri, G.; Paschina, G.; Piccaluga, G.; Pinna, G. *X-Ray Diffraction of Ions in Aqueous Solutions: Hydration and Complex Formation*; CRC Press: Boca Raton, FL, 1988.
- (6) Marcus, Y. *Chem. Rev.* **1988**, *88*, 1475.
- (7) Bjerrum, N. *Kgl. Danske Videnskab. Selskab.* **1926**, *7*, 9.
- (8) *International Tables for X-Ray Crystallography*; The Kynoch Press: England, 1974; Vols. 3 and 4.
- (9) Debye, P.; Menke, H. *Phys. Z.* **1930**, *31*, 797.
- (10) Johansson, G.; Wakita, H. *Inorg. Chem.* **1985**, *24*, 3047.
- (11) Johansson, G.; Yokoyama, H. *Inorg. Chem.* **1990**, *29*, 2460.
- (12) Enderby, J. E.; Neilson, G. W. *Adv. Phys.* **1980**, *29*, 323.
- (13) Enderby, J. E.; Neilson, G. W. *Rep. Prog. Phys.* **1981**, *44*, 38.
- (14) Herdman, G. J.; Neilson, G. W. *Adv. Phys.* **1990**, *46*, 165.
- (15) Pálkás, G.; Kálmán, E.; Kovács, P. *Mol. Phys.* **1977**, *34*, 525.
- (16) Dorosh, A. K.; Skryshevskii, A. F. *Russ. J. Struct. Chem.* **1966**, *8*, 300.
- (17) Marques, M. A.; Marques, M. I. D. B. *Proc. N. Ned. Akad. Wet., Part B* **1974**, *77*, 286.
- (18) Zeldler, M. D. *Electrochim. Acta* **1988**, *33*, 1195.
- (19) Hewish, N. A.; Enderby, J. E.; Howells, W. S. *J. Phys. C: Solid State Phys.* **1983**, *16*, 1777.
- (20) Lee, P. A.; Citrin, P. H.; Eisenberger, P.; Kincaid, B. M. *Rev. Mod. Phys.* **1981**, *53*, 769.
- (21) Hinton, J. F.; Amis, E. S. *Chem. Rev.* **1967**, *67*, 367.
- (22) Hunt, J. P. *Coord. Chem. Rev.* **1971**, *7*, 1.
- (23) Lang, E. W.; Lüdemann, H.-D. In *NMR Basic Principles and Progress*; Springer: Berlin, 1990; Vol. 24, p 129.
- (24) Merbach, A. E.; Akitt, J. W. In *NMR Basic Principles and Progress*, Springer: Berlin, 1990; Vol. 24, p 191.
- (25) Volino, F. In *Microscopic Structure and Dynamics of Liquids*; Plenum: New York, 1977; p 221.
- (26) Abragam, A. *The Principles of Magnetic Resonance*; Oxford University Press: Oxford, 1960.
- (27) Schlichter, C. P. *Principles of Magnetic Resonance*; Harper and Row: New York, 1963.
- (28) Farrar, T. C.; Becker, E. D. *Pulse and Fourier Transform NMR*; Academic: New York, 1971.
- (29) Hertz, H. G. In *Molecular Motions in Liquids*; Lascombe, J., Ed.; Reidel Publ. Co.: Dordrecht, The Netherlands, 1974; p 337.
- (30) von Goldammer, E. In *Modern Aspects of Electrochemistry*; Bockris, J. O'M., Conway, B. E., Eds.; Plenum: New York, 1975; No. 10, p 1.
- (31) Covington, A. K.; Newman, K. E. In *Modern Aspects of Electrochemistry*; Bockris, J. O'M., Conway, B. E., Eds.; Plenum: New York, 1977; No. 12, p 41.
- (32) Ebsworth, E. A. V.; Rankin, D. W. H.; Craddock, S. In *Structural Methods in Inorganic Chemistry*; Blackwell: Palo Alto, 1987; p 28 and references quoted therein.
- (33) Kula, R. J.; Rabenstein, D. L.; Reed, G. H. *Anal. Chem.* **1965**, *37*, 1783.
- (34) Jackson, J. A.; Lemons, J. F.; Taube, H. *J. Chem. Phys.* **1960**, *32*, 553.
- (35) Alei, M.; Jackson, J. A. *J. Chem. Phys.* **1964**, *41*, 3402.
- (36) Irish, D. E.; Broker, M. H. *Adv. Raman Infra Red Spectrosc.* **1976**, *2*, 212.
- (37) Detrich, J.; Corongiu, G.; Clementi, E. *Int. J. Quant. Chem.* **1984**, *18*, 701.
- (38) Ewald, P. P. *Ann. Phys.* **1921**, *64*, 253.
- (39) Barker, J. A.; Watts, R. O. *Chem. Phys. Lett.* **1969**, *3*, 144.
- (40) Street, W. B.; Tildesley, D. J.; Saville, G. *ACS Symp. Ser.* **1978**, *86*, 144.
- (41) Wood, W. W.; Erpenbeck, J. J. *Ann. Rev. Phys. Chem.* **1976**, *27*, 319.
- (42) Fumi, F. G.; Tosi, M. P. *J. Phys. Chem. Solids* **1964**, *25*, 31. Tosi, M. P.; Fumi, F. G. *J. Phys. Chem. Solids* **1964**, *25*, 45.
- (43) Bjerrum, N. *Kungl. Dansk. Videnskab. Selskab. Mat.-Fys. Medd.* **1951**, *27*, 1.
- (44) Ben-Naim, A.; Stillinger, F. H. In *Water and Aqueous Solutions*; Horne, R. A., Ed.; Wiley-Interscience: New York, 1972; p 295.
- (45) Stillinger, F. H.; Rahman, A. *J. Chem. Phys.* **1974**, *60*, 1545.
- (46) Rowlinson, J. S. *Trans. Faraday Soc.* **1951**, *47*, 120.
- (47) Matsuoka, O.; Clementi, E.; Yoshimine, M. *J. Chem. Phys.* **1976**, *64*, 1351.
- (48) Stillinger, F. H.; Rahman, A. *J. Chem. Phys.* **1978**, *68*, 666.
- (49) Bopp, P.; Jancsó, G.; Heinzinger, K. *Chem. Phys. Lett.* **1983**, *98*, 129.
- (50) Bopp, P. In *The Physics and Chemistry of Aqueous Ionic Solutions*, NATO ASI Series, Vol. C205; Kluwer: Dordrecht, 1987; p 217.
- (51) Heinzinger, K.; Pálkás, G. In *Interactions of Water in Ionic and Nonionic Hydrates*; Springer: Berlin, 1987; p 1.
- (52) Heinzinger, K. In *Computer Modelling of Fluids, Polymers and Solids*; Kluwer Academic Publ.: Dordrecht, 1990; p 357.
- (53) Metropolis, N.; Rosenbluth, A. W.; Rosenbluth, M. N.; Teller, A. H.; Teller, E. *J. Chem. Phys.* **1953**, *21*, 1087.
- (54) Beveridge, D. L.; Mezei, M.; Mehrotra, P. K.; Marchese, F. T.; Rahvi-Shanker, G.; Vasu, T.; Swaminathan, S. In *Molecular-Based Studies of Fluids*; Haile, J. M., Mansoori, G. A., Eds.; The American Chemical Society: Washington, DC, 1983.
- (55) McGreevy, R. L.; Pusztai, L. *Mol. Simul.* **1988**, *1*, 359.
- (56) Howe, M. A. *J. Phys.: Condens. Matter* **1990**, *2*, 741.
- (57) Clementi, E.; Barsotti, R. *Chem. Phys. Lett.* **1978**, *59*, 21.
- (58) Kistenmacher, H.; Popkie, H.; Clementi, E. *J. Chem. Phys.* **1974**, *61*, 799.
- (59) Jorgensen, W. L.; Chandrasekhar, J.; Madura, J. D.; Impey, R. W.; Klein, M. L. *J. Chem. Phys.* **1983**, *78*, 926.
- (60) Chandrasekhar, J.; Spellmeyer, D. C.; Jorgensen, W. L. *J. Am. Chem. Soc.* **1984**, *106*, 903.
- (61) Zhu, S.-B.; Robinson, G. W. *Z. Naturforsch.* **1991**, *A46*, 221.
- (62) Eck, C. L. van P. van; Mendel, H.; Boog, W. *Discuss. Faraday Soc.* **1957**, *24*, 200; 235.
- (63) Triolo, R.; Narten, A. H. *J. Chem. Phys.* **1975**, *63*, 3624.
- (64) Ohtomo, N.; Arakawa, K.; Takeuchi, M.; Yamaguchi, T.; Ohtaki, H. *Bull. Chem. Soc. Jpn.* **1981**, *54*, 1314.
- (65) Lee, H.-G.; Matsumoto, Y.; Yamaguchi, T.; Ohtaki, H. *Bull. Chem. Soc. Jpn.* **1983**, *56*, 443.
- (66) Caminiti, R.; Atzei, D.; Cucca, P.; Squintu, F.; Bongiovanni, G. *Z. Naturforsch.* **1985**, *A40*, 1319.
- (67) Valeev, A. H.; Smirnov, P. R.; Trostin, V. N.; Krestov, G. A. *Zh. Fiz. Khim.* **1988**, *42*, 352.
- (68) Caminiti, R.; Cucca, P. *Chem. Phys. Lett.* **1984**, *108*, 51.
- (69) Terekhova, D. S.; Ryss, A. I.; Radchenko, I. V. *J. Struct. Chem.* **1969**, *10*, 807.
- (70) Narten, A. H. *J. Chem. Phys.* **1970**, *74*, 765.
- (71) Pálkás, G.; Radnai, T.; Szász, Gy. I.; Heinzinger, K. *J. Chem. Phys.* **1981**, *74*, 3522.
- (72) Hewish, N. A.; Neilson, G. W. *Chem. Phys. Lett.* **1981**, *84*, 425.
- (73) Musinu, A.; Paschina, G.; Pinna, G. *Chem. Phys. Lett.* **1981**, *80*, 163.
- (74) Narten, A. H.; Vaslow, F.; Levy, H. A. *J. Chem. Phys.* **1973**, *58*, 5017.
- (75) Licheri, G.; Piccaluga, G.; Pinna, G. *J. Appl. Crystallogr.* **1973**, *6*, 392.
- (76) Ohtomo, N.; Arakawa, K. *Bull. Chem. Soc. Jpn.* **1979**, *52*, 2755.
- (77) Pálkás, G.; Radnai, T.; Hajdu, H. *Z. Naturforsch.* **1980**, *A35*, 107.
- (78) Newsome, J. R.; Neilson, G. W.; Enderby, J. E. *J. Phys. C: Solid State Phys.* **1980**, *13*, L923.
- (79) Okada, I.; Kitsuno, Y.; Lee, H.-G.; Ohtaki, H. *Stud. Phys. Theor. Chem.* **1983**, *27*, 81.
- (80) Paschina, G.; Piccaluga, G.; Pinna, G.; Magini, M. *Chem. Phys. Lett.* **1983**, *98*, 157.
- (81) Musinu, A.; Paschina, G.; Piccaluga, G.; Magini, M. *J. Chem. Phys.* **1984**, *80*, 2772.
- (82) Radnai, T.; Pálkás, G.; Szász, Gy. I.; Heinzinger, K. *Z. Naturforsch.* **1981**, *A36*, 1076.
- (83) Tamura, Y.; Yamaguchi, T.; Okada, I.; Ohtaki, H. *Z. Naturforsch.* **1987**, *A42*, 367.
- (84) Licheri, G.; Piccaluga, G.; Pinna, G. *Chem. Phys. Lett.* **1975**, *35*, 119.
- (85) Cartailleur, T.; Kunz, W.; Turq, P.; Bellissent-Funel, M.-C. *J. Phys.: Condens. Matter* **1991**, *3*, 9511.
- (86) Caminiti, R.; Licheri, G.; Piccaluga, G.; Pinna, G. *Rend. Semin. Fac. Sci. Univ. Cagliari* **1977**, *XLVI*, Suppl. 19.
- (87) Ohtomo, N.; Arakawa, K. *Bull. Chem. Soc. Jpn.* **1980**, *53*, 1789.
- (88) Maeda, M.; Ohtaki, H. *Bull. Chem. Soc. Jpn.* **1975**, *48*, 3755.
- (89) Caminiti, R.; Licheri, G.; Paschina, G.; Piccaluga, G.; Pinna, G. *J. Chem. Phys.* **1980**, *72*, 4522.
- (90) Brady, G. W.; Krause, T. J. *J. Chem. Phys.* **1957**, *27*, 304.
- (91) Brady, G. W. *J. Chem. Phys.* **1958**, *28*, 464.
- (92) Neilson, G. W.; Skipper, N. *Chem. Phys. Lett.* **1985**, *114*, 35.
- (93) Fishkis, M. Ya.; Soboleva, T. E. *Zh. Strukt. Khim.* **1974**, *15*, 186.
- (94) Bertagnolli, H.; Weidner, J.-U.; Zimmermann, H. W. *Ber. Bunsen-Ges. Phys. Chem.* **1974**, *78*, 2.
- (95) Maeda, M.; Maegawa, Y.; Yamaguchi, T.; Ohtaki, H. *Bull. Chem. Soc. Jpn.* **1979**, *52*, 2545.
- (96) Yamaguchi, T.; Lindquist, O.; Boyce, J. B.; Claeson, T. In *EXAFS and Near Edge Structure III*; Hodgson, K. O., Hedman, B., Penner-Hahn, J. E., Eds.; Springer-Verlag: Berlin, 1985; p 417.
- (97) Yamaguchi, T.; Johansson, G.; Holmberg, B.; Maeda, M.; Ohtaki, H. *Acta Chem. Scand.* **1984**, *A38*, 437.
- (98) Yamaguchi, T.; Lindquist, O.; Boyce, J. B.; Claeson, T. *Acta Chem. Scand.* **1984**, *A38*, 423.
- (99) Sandström, M.; Neilson, G. W.; Johansson, G.; Yamaguchi, T. *J. Phys. C: Solid State Phys.* **1985**, *18*, L1115.
- (100) Yamaguchi, T.; Ohtaki, H.; Spohr, E.; Pálkás, G.; Heinzinger, K.; Probst, M. M. *Z. Naturforsch.* **1986**, *A41*, 1175.
- (101) Bol, W.; Gerrits, G. J. A.; van Panthaleon van Eck, C. L. *J. Appl. Crystallogr.* **1970**, *3*, 486.
- (102) Dorosh, A. K.; Skryshevskii, A. F. *J. Struct. Chem.* **1964**, *5*, 842.
- (103) Albright, J. N. *J. Chem. Phys.* **1972**, *56*, 3783.
- (104) Caminiti, R.; Licheri, G.; Piccaluga, G.; Pinna, G. *J. Appl. Crystallogr.* **1979**, *12*, 34.
- (105) Caminiti, R.; Licheri, G.; Paschina, G.; Piccaluga, G.; Pinna, G. *Z. Naturforsch.* **1980**, *A35*, 1361.
- (106) Pálkás, G.; Radnai, T.; Dietz, W.; Szász, Gy. I.; Heinzinger, K. *Z. Naturforsch.* **1982**, *A37*, 1049.
- (107) Caminiti, R.; Licheri, G.; Piccaluga, G.; Pinna, G. *Chem. Phys. Lett.* **1977**, *47*, 275.
- (108) Waizumi, K.; Tamura, Y.; Masuda, H.; Ohtaki, H. *Z. Naturforsch.* **1991**, *A46*, 307.
- (109) Caminiti, R.; Licheri, G.; Piccaluga, G.; Pinna, G. *Chem. Phys. Lett.* **1979**, *61*, 45.

- (110) Caminiti, R.; Cerioni, G.; Crisponi, G.; Cucca, P. Z. *Naturforsch.* **1988**, *A43*, 317.
- (111) Caminiti, R. *Chem. Phys. Lett.* **1982**, *88*, 103.
- (112) Ryss, A. I.; Radchenko, I. V. *J. Struct. Chem.* **1965**, *6*, 422.
- (113) Licheri, G.; Piccaluga, G.; Pinna, G. *J. Chem. Phys.* **1976**, *64*, 2437.
- (114) Cummings, S.; Enderby, J. E.; Howe, R. A. *J. Phys. C: Solid State Phys.* **1980**, *13*, 1.
- (115) Hewish, N. A.; Neilson, G. W.; Enderby, J. E. *Nature* **1982**, *297*, 138.
- (116) Probst, M. M.; Radnai, T.; Heinzinger, K.; Bopp, P.; Rode, B. M. *J. Phys. Chem.* **1985**, *89*, 753.
- (117) Yamaguchi, T.; Hayashi, S.; Ohtaki, H. *Inorg. Chem.* **1989**, *28*, 2434.
- (118) Licheri, G.; Piccaluga, G.; Pinna, G. *J. Chem. Phys.* **1975**, *63*, 4412.
- (119) Caminiti, R.; Musinu, A.; Paschina, G.; Pinna, G. *J. Appl. Crystallogr.* **1982**, *15*, 482.
- (120) Neilson, G. W.; Broadbent, R. D. *Chem. Phys. Lett.* **1990**, *167*, 429.
- (121) Ohtaki, H.; Yamaguchi, T.; Maeda, M. *Bull. Chem. Soc. Jpn.* **1976**, *49*, 701.
- (122) Sham, T. K.; Hastings, J. B.; Perlman, M. L. *Chem. Phys. Lett.* **1981**, *83*, 391.
- (123) Shapovalov, I. M.; Radchenko, I. V. *J. Struct. Chem.* **1971**, *12*, 705.
- (124) Apted, M. J.; Waychunas, G. A.; Brown, G. E. *Geochim. Cosmochim. Acta* **1985**, *49*, 2081.
- (125) Herdman, G. J.; Neilson, G. W. *J. Phys.: Condens. Matter* **1992**, *4*, 649.
- (126) Kálmán, E.; Radnai, T.; Pálkás, G.; Hajdu, F.; Vértés, A. *Electrochim. Acta* **1988**, *33*, 1223.
- (127) Wertz, D. L.; Kruh, R. F. *Inorg. Chem.* **1970**, *9*, 595.
- (128) Sandström, D. R.; Stults, B. R.; Greegor, R. B. In *EXAFS Spectroscopy*; Teo, B. K., Joy, D. C., Eds.; Plenum: New York, 1981.
- (129) Magini, M.; Giubileo, G. *Gazz. Chim. Ital.* **1981**, *111*, 449.
- (130) Shapovalov, I. M.; Radchenko, I. V.; Lesovitskaya, M. K. *J. Struct. Chem.* **1972**, *13*, 121.
- (131) Soper, A. K.; Neilson, G. W.; Enderby, J. E.; Howe, R. A. *J. Phys. C: Solid State Phys.* **1977**, *10*, 1793.
- (132) Caminiti, G.; Licheri, G.; Piccaluga, G.; Pinna, G. *Faraday Disc. Chem. Soc.* **1978**, *64*, 62.
- (133) Neilson, G. W.; Enderby, J. E. *J. Phys. C: Solid State Phys.* **1978**, *11*, L625.
- (134) Sandström, D. R. *J. Chem. Phys.* **1979**, *71*, 2381.
- (135) Licheri, G.; Paschina, G.; Piccaluga, G.; Pinna, G.; Vlaic, G. *Chem. Phys. Lett.* **1981**, *83*, 384.
- (136) Neilson, G. W.; Enderby, J. E. *Proc. R. Soc. Lond.* **1983**, *A390*, 353.
- (137) Powell, D. H.; Neilson, G. W. *J. Phys.: Condens. Matter* **1990**, *2*, 3871.
- (138) Powell, D. H.; Neilson, G. W.; Enderby, J. E. *J. Phys.: Condens. Matter* **1989**, *1*, 8721.
- (139) Sandström, D. R.; Dodgen, H. W.; Lytle, F. W. *J. Chem. Phys.* **1977**, *67*, 473.
- (140) Licheri, G.; Pinna, G.; Navarra, G.; Vlaic, G. *Z. Naturforsch.* **1983**, *A38*, 559.
- (141) Licheri, G.; Paschina, G.; Piccaluga, G.; Pinna, G. *J. Chem. Phys.* **1984**, *81*, 6059.
- (142) Caminiti, R. *J. Chem. Phys.* **1986**, *84*, 3336.
- (143) Salmon, P. S.; Neilson, G. W. *J. Phys.: Condens. Matter* **1989**, *1*, 5291.
- (144) Beagley, B.; Eriksson, A.; Lindgren, J.; Persson, I.; Pettersson, L. G. M.; Sandström, M.; Wahlgren, U.; White, E. W. *J. Phys.: Condens. Matter* **1989**, *1*, 2395.
- (145) Ohtaki, H.; Maeda, M. *Bull. Chem. Soc. Jpn.* **1974**, *47*, 2197.
- (146) Neilson, G. W.; Newsome, J. R.; Sandström, M. *J. Chem. Soc., Faraday Trans. 2* **1981**, *77*, 1245.
- (147) Magini, M. *Inorg. Chem.* **1982**, *21*, 1535.
- (148) Nomura, M.; Yamaguchi, T. *J. Phys. Chem.* **1988**, *92*, 6157.
- (149) Fishkis, M. Ya.; Zhmak, V. A. *J. Struct. Chem.* **1974**, *15*, 1.
- (150) Musinu, A.; Paschina, G.; Piccaluga, G.; Magini, M. *Inorg. Chem.* **1983**, *22*, 1184.
- (151) Sano, M.; Maruo, T.; Yamatera, H. *Bull. Chem. Soc. Jpn.* **1983**, *56*, 3287.
- (152) Matsubara, E.; Waseda, Y. *J. Phys. C: Condens. Matter* **1989**, *1*, 8575.
- (153) Dagnall, S. P.; Hague, D. N.; Towl, A. D. C. *J. Chem. Soc., Faraday Trans. 2* **1982**, *78*, 2161.
- (154) Musinu, A.; Paschina, G.; Piccaluga, G.; Magini, M. *J. Appl. Crystallogr.* **1982**, *15*, 621.
- (155) Licheri, G.; Paschina, G.; Piccaluga, G.; Pinna, G. *Z. Naturforsch.* **1982**, *A37*, 1205.
- (156) Powell, D. H.; Gullidge, P. M. N.; Neilson, G. W. *Mol. Phys.* **1990**, *71*, 1107.
- (157) Ozutsumi, K.; Ohtaki, H. *Bull. Chem. Soc. Jpn.* **1985**, *58*, 1651.
- (158) Radnai, T.; Inoue, K.; Ohtaki, H. *Bull. Chem. Soc. Jpn.* **1990**, *63*, 3420.
- (159) Ohtaki, H.; Maeda, M.; Ito, S. *Bull. Chem. Soc. Jpn.* **1974**, *47*, 2217.
- (160) Caminiti, R.; Johansson, G. *Acta Chem. Scand.* **1981**, *A35*, 373.
- (161) Johansson, G. *Acta Chem. Scand.* **1971**, *25*, 2787.
- (162) Sandström, M.; Persson, I.; Arhland, S. *Acta Chem. Scand.* **1978**, *A32*, 607.
- (163) van Eck, C. L. Van P.; Wolters, H. B. M.; Jaspers, W. J. M. *Recl. Trav. Chim. Pays-Bas* **1956**, *75*, 802.
- (164) Yamaguchi, T.; Lindquist, O.; Claeson, T.; Boyce, J. B. *Chem. Phys. Lett.* **1982**, *93*, 528.
- (165) Johansson, G.; Ohtaki, H. *Acta Chem. Scand.* **1973**, *27*, 643.
- (166) Caminiti, R.; Licheri, G.; Piccaluga, G.; Pinna, G. *J. Chem. Phys.* **1976**, *65*, 3134.
- (167) Caminiti, R.; Licheri, G.; Piccaluga, G.; Pinna, G. *J. Chem. Phys.* **1978**, *69*, 1.
- (168) Cristini, A.; Licheri, G.; Piccaluga, G.; Pinna, G. *Chem. Phys. Lett.* **1974**, *24*, 289.
- (169) Bol, W.; Welzen, T. *Chem. Phys. Lett.* **1977**, *49*, 189.
- (170) Caminiti, R.; Licheri, G.; Piccaluga, G.; Pinna, G. *Chem. Phys.* **1977**, *19*, 371.
- (171) Sham, T. K.; Hastings, J. B.; Perlman, M. L. *J. Am. Chem. Soc.* **1980**, *102*, 5904.
- (172) Broadbent, R. D.; Neilson, G. W.; Sandström, M. *J. Phys.: Condens. Matter* **1992**, *4*, 639.
- (173) Caminiti, R.; Licheri, G.; Piccaluga, G.; Pinna, G.; Radnai, T. *J. Chem. Phys.* **1979**, *71*, 2473.
- (174) Caminiti, R.; Radnai, T. *Z. Naturforsch.* **1980**, *A35*, 1368.
- (175) Piccaluga, G. *Z. Naturforsch.* **1982**, *A37*, 154.
- (176) Magini, M.; Caminiti, R. *J. Inorg. Nucl. Chem.* **1977**, *39*, 91.
- (177) Caminiti, R.; Magini, M. *Chem. Phys. Lett.* **1979**, *61*, 40.
- (178) Herdman, G. J.; Neilson, G. W. *J. Phys.: Condens. Matter* **1992**, *4*, 627.
- (179) Magini, M. *J. Inorg. Nucl. Chem.* **1977**, *40*, 43.
- (180) Johansson, G.; Niinitso, L.; Wakita, H. *Acta Chem. Scand.* **1985**, *A39*, 359.
- (181) Maeda, M.; Ohtaki, H. *Bull. Chem. Soc. Jpn.* **1977**, *50*, 1893.
- (182) Glaser, J. *Acta Crystallogr.* **1978**, *A34*, S197.
- (183) Glaser, J.; Johansson, G. *Acta Chem. Scand.* **1982**, *A36*, 125.
- (184) Smith, L. S.; Wertz, D. L. *J. Am. Chem. Soc.* **1975**, *97*, 2365.
- (185) Habenschuss, H.; Spedding, F. H. *J. Chem. Phys.* **1979**, *70*, 3758.
- (186) Smith, L. S.; Wertz, D. L. *J. Inorg. Nucl. Chem.* **1977**, *39*, 95.
- (187) Yamaguchi, T.; Tanaka, S.; Wakita, H.; Misawa, M.; Okada, I.; Soper, A. K.; Howells, S. W. *Z. Naturforsch.* **1991**, *A46*, 84.
- (188) Steele, M. L.; Wertz, D. L. *Inorg. Chem.* **1977**, *16*, 1225.
- (189) Narten, A. H.; Hahn, R. L. *Science* **1982**, *217*, 1249.
- (190) Narten, A. H.; Hahn, R. L. *J. Phys. Chem.* **1983**, *87*, 3193.
- (191) Yamaguchi, T.; Nomura, M.; Wakita, H.; Ohtaki, H. *J. Chem. Phys.* **1988**, *89*, 5153.
- (192) Helm, J.; Merbach, A. E. *Eur. J. Solid State Inorg. Chem.* **1991**, *28*, 245.
- (193) Habenschuss, H.; Spedding, F. H. *J. Chem. Phys.* **1980**, *73*, 442.
- (194) Ryss, A. I.; Lesovitskaya, M. K.; Shapovalov, I. M. *VINITI* **1976**, *856*; *Chem. Abstr.* **1978**, *89*, 95116.
- (195) Steele, M. L.; Wertz, D. L. *J. Am. Chem. Soc.* **1976**, *98*, 4424.
- (196) Habenschuss, H.; Spedding, F. H. *J. Chem. Phys.* **1979**, *70*, 2797.
- (197) Annis, B. K.; Hahn, R. L.; Narten, A. H. *J. Chem. Phys.* **1985**, *82*, 2086.
- (198) Cossy, C.; Barnes, A. C.; Enderby, J. E. *J. Chem. Phys.* **1989**, *90*, 3254.
- (199) Brady, G. W. *J. Chem. Phys.* **1960**, *33*, 1079.
- (200) Magini, M.; Cabrini, A.; Scibona, G.; Johansson, G.; Sandström, M. *Acta Chem. Scand.* **1976**, *A30*, 437.
- (201) Johansson, G.; Magini, M.; Ohtaki, H. *J. Solution Chem.* **1991**, *20*, 775.
- (202) Pöce, S.; Johansson, G. *Acta Chem. Scand.* **1973**, *27*, 2146.
- (203) Rosseinsky, D. R. *Chem. Rev.* **1965**, *65*, 467.
- (204) Lee, S. C.; Kaplow, R. *Science* **1970**, *169*, 477.
- (205) Wertz, D. L. *J. Solution Chem.* **1972**, *1*, 489.
- (206) Cummings, S.; Enderby, J. E.; Neilson, G. W.; Newsome, J. R.; Howe, R. A.; Howells, W. S.; Soper, A. K. *Nature* **1980**, *287*, 714.
- (207) Jal, J. F.; Soper, A. K.; Carmona, P.; Dupuy, J. *J. Phys.: Condens. Matter* **1991**, *3*, 551.
- (208) Powell, D. H.; Barnes, A. C.; Enderby, J. E.; Neilson, G. W.; Salmon, P. S. *Faraday Discuss. Chem. Soc.* **1988**, *85*, 137.
- (209) Magini, M. *J. Chem. Phys.* **1980**, *73*, 2499.
- (210) Magini, M.; Radnai, T. *J. Chem. Phys.* **1979**, *71*, 4255.
- (211) Magini, M. *J. Chem. Phys.* **1982**, *76*, 1111.
- (212) De Barros Marques, M. I.; Cabaco, M. I.; Sousa Oliveira, M. A.; Alves Marques, M. *Chem. Phys. Lett.* **1982**, *91*, 222.
- (213) Biggin, S.; Enderby, J. E.; Hahn, R. L.; Narten, A. H. *J. Phys. Chem.* **1984**, *88*, 3634.
- (214) Wakita, H.; Ichihashi, M.; Mibuchi, T.; Masuda, I. *Bull. Chem. Soc. Jpn.* **1982**, *55*, 817.
- (215) Caminiti, R.; Cucca, P. *Chem. Phys. Lett.* **1982**, *89*, 110.
- (216) Magini, M.; DeMoraes, M.; Licheri, G.; Piccaluga, G. *J. Chem. Phys.* **1985**, *83*, 5797.
- (217) Eisenberger, P.; Kincaid, B. M. *Chem. Phys. Lett.* **1975**, *36*, 134.
- (218) Kálmán, E.; Serke, I.; Pálkás, G.; Johansson, G.; Kabisch, G.; Maeda, M.; Ohtaki, H. *Z. Naturforsch.* **1983**, *A38*, 225.
- (219) Takamuku, T.; Ihara, M.; Yamaguchi, T.; Wakita, H. *Z. Naturforsch.* **1992**, *A47*, 485.
- (220) Goggin, P. L.; Johansson, G.; Maeda, M.; Wakita, H. *Acta Chem. Scand.* **1984**, *A38*, 625.
- (221) Wakita, H.; Johansson, G.; Sandström, M.; Goggin, P. L.; Ohtaki, H. *J. Solution Chem.* **1991**, *20*, 643.
- (222) Takamuku, T.; Yamaguchi, T.; Wakita, H. *J. Phys. Chem.* **1991**, *95*, 10098.
- (223) Caminiti, G.; Licheri, G.; Piccaluga, G.; Pinna, G. *J. Chem. Phys.* **1978**, *68*, 1967.

- (224) Neilson, G. W.; Enderby, J. E. *J. Phys. C: Solid State Phys.* **1982**, *15*, 2347.
- (225) Caminiti, R.; Cucca, P.; Radnai, T. *J. Phys. Chem.* **1984**, *88*, 2382.
- (226) Caminiti, R.; Atzei, D.; Cucca, P.; Anedda, A.; Bongiovanni, G. *J. Phys. Chem.* **1986**, *90*, 238.
- (227) Caminiti, R.; Cucca, P.; D'Andrea, A. *Z. Naturforsch.* **1983**, *A38*, 533.
- (228) Neilson, G. W.; Schiöberg, D.; Luck, W. A. P. *Chem. Phys. Lett.* **1985**, *122*, 475.
- (229) Caminiti, R.; Paschina, G.; Pinna, G.; Magini, M. *Chem. Phys. Lett.* **1979**, *64*, 391.
- (230) Yamaguchi, T.; Lindquist, O. *Acta Chem. Scand.* **1982**, *A36*, 377.
- (231) Radnai, T.; Pálkás, G.; Caminiti, R. *Z. Naturforsch.* **1982**, *A37*, 1247.
- (232) Caminiti, R. *Z. Naturforsch.* **1981**, *A36*, 1062.
- (233) Caminiti, R. *Chem. Phys. Lett.* **1982**, *86*, 214.
- (234) Caminiti, R.; Paschina, G. *Chem. Phys. Lett.* **1981**, *82*, 487.
- (235) Johansson, G.; Caminiti, R. *Z. Naturforsch.* **1986**, *A41*, 1325.
- (236) Caminiti, R.; Cucca, P.; Atzei, D. *J. Phys. Chem.* **1985**, *89*, 1457.
- (237) Caminiti, R. *J. Mol. Liquids* **1984**, *28*, 191.
- (238) Caminiti, R. *J. Chem. Phys.* **1982**, *77*, 5682.
- (239) Caminiti, R.; Cucca, P.; Monduzzi, M.; Saba, G.; Crisponi, G. *J. Chem. Phys.* **1984**, *81*, 543.
- (240) Newsome, J. R.; Neilson, G. W.; Enderby, J. E.; Sandström, M. *Chem. Phys. Lett.* **1981**, *82*, 399.
- (241) Ichikawa, K.; Kameda, Y.; Matsumoto, T.; Misawa, M. *J. Phys. C: Solid State Phys.* **1984**, *17*, L725.
- (242) Copestake, A. P.; Neilson, G. W.; Enderby, J. E. *J. Phys. C: Solid State Phys.* **1985**, *18*, 4211.
- (243) Tanaka, K.; Ogita, N.; Tamura, Y.; Okada, I.; Ohtaki, H.; Pálkás, G.; Spohr, E.; Heinzinger, K. *Z. Naturforsch.* **1987**, *A42*, 29.
- (244) Ohtaki, H.; Fukushima, N. *J. Solution Chem.* **1991**, *21*, 23.
- (245) Lawrence, R. M.; Kruh, R. F. *J. Chem. Phys.* **1967**, *47*, 4758.
- (246) Tajiri, Y.; Ichihashi, M.; Mibuchi, T.; Wakita, H. *Bull. Chem. Soc. Jpn.* **1986**, *59*, 1155.
- (247) Beagley, B.; McAuliffe, C. A.; Smith, S. P. B.; White, E. W. *J. Phys.: Condens. Matter* **1991**, *3*, 7919.
- (248) Caminiti, R.; Cucca, G.; Pintori, T. *Chem. Phys.* **1984**, *88*, 155.
- (249) Caminiti, R.; Marongiu, G.; Paschina, G. *Z. Naturforsch.* **1982**, *A37*, 581.
- (250) Ichihashi, M.; Wakita, H.; Masuda, I. *J. Solution Chem.* **1984**, *13*, 505.
- (251) Magini, M. *J. Chem. Phys.* **1981**, *74*, 2523.
- (252) Corrias, A.; Musinu, A.; Pinna, G. *Chem. Phys. Lett.* **1985**, *120*, 295.
- (253) Licheri, G.; Paschina, G.; Piccaluga, G.; Pinna, G. *J. Chem. Phys.* **1983**, *79*, 2168.
- (254) Magini, M.; Paschina, G.; Piccaluga, G. *J. Chem. Phys.* **1982**, *76*, 1116.
- (255) Bell, J. R.; Tyvoll, J. L.; Wertz, D. L. *J. Am. Chem. Soc.* **1973**, *95*, 1456.
- (256) Neilson, G. W. *J. Phys. C: Solid State Phys.* **1982**, *15*, L233.
- (257) Salmon, P. S.; Neilson, G. W.; Enderby, J. E. *J. Phys. C: Solid State Phys.* **1988**, *21*, 1335.
- (258) Yamaguchi, T.; Ohtaki, H. *Bull. Chem. Soc. Jpn.* **1979**, *52*, 415.
- (259) Fontaine, A.; Lagarde, P.; Raoux, D.; Fontana, M. P.; Maisano, G.; Migliardo, P.; Wanderlingh, F. *Phys. Rev. Lett.* **1978**, *41*, 504.
- (260) Lagarde, P.; Fontaine, A.; Raoux, D.; Sadoc, A.; Migliardo, P. *J. Chem. Phys.* **1980**, *72*, 3061.
- (261) Ichihashi, M.; Wakita, H.; Mibuchi, T.; Masuda, I. *Bull. Chem. Soc. Jpn.* **1982**, *55*, 3160.
- (262) Licheri, G.; Musinu, A.; Paschina, G.; Piccaluga, G.; Sedda, A. F. *J. Chem. Phys.* **1984**, *80*, 5308.
- (263) Yamaguchi, T.; Hayashi, S.; Ohtaki, H. *J. Phys. Chem.* **1989**, *93*, 2620.
- (264) Wertz, D. L.; Bell, J. R. *J. Inorg. Nucl. Chem.* **1973**, *35*, 861.
- (265) Paschina, G.; Piccaluga, G.; Pinna, G.; Magini, M. *J. Chem. Phys.* **1983**, *78*, 5745.
- (266) Sadoc, A.; Lagarde, P.; Vlaic, G. *J. Phys. C: Solid State Phys.* **1985**, *18*, 23.
- (267) Caminiti, R.; Cilloco, F.; Felici, R. *Mol. Phys.* **1992**, *76*, 681.
- (268) Fujita, T.; Ohtaki, H. *Bull. Chem. Soc. Jpn.* **1982**, *55*, 455.
- (269) Ozutsumi, K.; Ohtaki, H. *Bull. Chem. Soc. Jpn.* **1983**, *56*, 3635.
- (270) Fujita, T.; Ohtaki, H. *Bull. Chem. Soc. Jpn.* **1983**, *56*, 3276.
- (271) Ozutsumi, K.; Ohtaki, H. *Bull. Chem. Soc. Jpn.* **1984**, *57*, 2605.
- (272) Tsurumi, M.; Maeda, M.; Ohtaki, H. *Denki Kagaku* **1977**, *45*, 367.
- (273) Ozutsumi, K.; Yamaguchi, T.; Ohtaki, H.; Tohji, K.; Udagawa, Y. *Bull. Chem. Soc. Jpn.* **1985**, *58*, 2786.
- (274) Lind, M. D. *J. Chem. Phys.* **1967**, *46*, 2010.
- (275) Combes, J. M.; Manceau, A.; Calas, G.; Bottero, J. Y. *Geochim. Cosmochim. Acta* **1989**, *53*, 583.
- (276) Magini, M. *J. Chem. Phys.* **1979**, *70*, 317.
- (277) Yokoyama, H.; Johansson, G. *Acta Chem. Scand.* **1990**, *44*, 567.
- (278) Noto, R.; Martorana, V.; Migliore, M.; Fornili, S. L. *Z. Naturforsch.* **1991**, *A46*, 107.
- (279) Szász, Gy. I.; Heinzinger, K. *Z. Naturforsch.* **1979**, *A34*, 840.
- (280) Ergin, Yu. V.; Koop, O. Ya.; Khrapko, A. M. *Zh. Fiz. Khim.* **1979**, *53*, 2109.
- (281) Mezei, M.; Beveridge, D. L. *J. Chem. Phys.* **1981**, *74*, 6902.
- (282) Impey, R. W.; Maden, P. A.; McDonald, I. R. *J. Phys. Chem.* **1983**, *87*, 5071.
- (283) Nguyen, H. L.; Adelman, S. A. *J. Chem. Phys.* **1984**, *81*, 4564.
- (284) Marchese, F. T.; Beveridge, D. L. *J. Am. Chem. Soc.* **1984**, *106*, 3713.
- (285) Bounds, D. G. *Mol. Phys.* **1985**, *54*, 1335.
- (286) Watts, R. O.; Clementi, E.; Fromm, J. *J. Chem. Phys.* **1974**, *61*, 2550.
- (287) Fromm, J.; Clementi, E.; Watts, R. O. *J. Chem. Phys.* **1975**, *62*, 1388.
- (288) Watts, R. O. *Mol. Phys.* **1976**, *32*, 659.
- (289) Heinzinger, K.; Vogel, P. C. *Z. Naturforsch.* **1976**, *A31*, 463.
- (290) Bopp, P.; Okada, I.; Ohtaki, H.; Heinzinger, K. *Z. Naturforsch.* **1985**, *A40*, 116.
- (291) Szász, Gy. I.; Heinzinger, K.; Riede, W. O. *Z. Naturforsch.* **1981**, *A36*, 1067.
- (292) Szász, Gy. I.; Heinzinger, K.; Pálkás, G. *Chem. Phys. Lett.* **1981**, *78*, 194.
- (293) Szász, Gy. I.; Heinzinger, K. *Earth Planet. Sci. Lett.* **1982**, *64*, 163.
- (294) Spohr, E.; Heinzinger, K. *J. Chem. Phys.* **1986**, *84*, 2304.
- (295) Malenkov, G. G.; Dyakonova, L. P.; Brizhik, L. S. *VINITI* **1980**, 346.
- (296) Vogel, P. C.; Heinzinger, K. *Z. Naturforsch.* **1976**, *A31*, 476.
- (297) Pálkás, G.; Riede, W. O.; Heinzinger, K. *Z. Naturforsch.* **1977**, *A32*, 1137.
- (298) Bopp, P.; Dietz, W.; Heinzinger, K. *Z. Naturforsch.* **1979**, *A34*, 1424.
- (299) Limtakrul, J. P.; Rode, B. M. *Monatsch. Chem.* **1985**, *116*, 1377.
- (300) Jancsó, G.; Heinzinger, K.; Bopp, P. *Z. Naturforsch.* **1985**, *A40*, 1235.
- (301) Schwendinger, M. G.; Rode, B. M. *Chem. Phys. Lett.* **1989**, *155*, 527.
- (302) Heinje, G.; Luck, W. A. P.; Heinzinger, K. *J. Phys. Chem.* **1987**, *91*, 331.
- (303) Migliore, M.; Fornili, S. L.; Spohr, E.; Pálkás, G.; Heinzinger, K. *Z. Naturforsch.* **1986**, *A41*, 826.
- (304) Szász, Gy. I.; Heinzinger, K. *Z. Naturforsch.* **1983**, *A38*, 214.
- (305) Tamura, Y.; Ohtaki, H.; Okada, I. *Z. Naturforsch.* **1991**, *A46*, 1083.
- (306) Probst, M. M.; Spohr, E.; Heinzinger, K. *Chem. Phys. Lett.* **1989**, *161*, 405.
- (307) Kheawarikul, S.; Hannongbua, S. V.; Rode, B. M. *Z. Naturforsch.* **1991**, *A46*, 111.
- (308) Szász, Gy. I.; Dietz, W.; Heinzinger, K.; Pálkás, G.; Radnai, T. *Chem. Phys. Lett.* **1982**, *92*, 388.
- (309) Spohr, E.; Pálkás, G.; Heinzinger, K.; Bopp, P.; Probst, M. M. *J. Phys. Chem.* **1988**, *92*, 6754.
- (310) Kneifel, C. L.; Friedman, H. L.; Newton, M. D. *Z. Naturforsch.* **1989**, *A44*, 385.
- (311) Yongyos, Y. P.; Kokpol, S.; Rode, B. M. *Chem. Phys.* **1991**, *156*, 403.
- (312) Dietz, W.; Riede, W. O.; Heinzinger, K. *Z. Naturforsch.* **1982**, *A37*, 1038.
- (313) Vargin, J.; Knapp, P. S.; Flint, W. L.; Anton, A.; Highberger, G.; Malinowski, E. R. *J. Chem. Phys.* **1971**, *54*, 178.
- (314) Creekmore, R. W.; Reilley, C. N. *J. Phys. Chem.* **1969**, *73*, 1563.
- (315) Connick, R. E.; Fiat, D. N. *J. Phys. Chem.* **1963**, *39*, 1349.
- (316) Fratiello, A.; Lee, R. E.; Nishida, V. M.; Schuster, R. E. *J. Chem. Phys.* **1968**, *48*, 3705.
- (317) Swift, T. J.; Sayre, W. G. *J. Chem. Phys.* **1966**, *44*, 3567.
- (318) Matwiyoff, N. A.; Taube, H. *J. Am. Chem. Soc.* **1968**, *90*, 2796.
- (319) Jörgensen, C. K. *Acta Chem. Scand.* **1957**, *11*, 399.
- (320) Chmelnik, A. M.; Fiat, D. N. *J. Phys. Chem.* **1971**, *93*, 2875.
- (321) Fratiello, A.; Kubo, V.; Peak, S.; Sanchez, B.; Schuster, R. E. *Inorg. Chem.* **1971**, *10*, 2552.
- (322) Zeltmann, A. H.; Matwiyoff, N. A.; Morgan, L. O. *J. Phys. Chem.* **1968**, *72*, 121.
- (323) Matwiyoff, N. A.; Darley, P. E. *J. Phys. Chem.* **1968**, *72*, 2659.
- (324) Swift, T. J.; Weinberger, G. P. *J. Am. Chem. Soc.* **1968**, *90*, 2023.
- (325) Connick, R. E.; Fiat, D. *J. Chem. Phys.* **1966**, *44*, 4103.
- (326) Neely, J. W.; Connick, R. E. *J. Am. Chem. Soc.* **1972**, *94*, 3519.
- (327) Fratiello, A.; Lee, R. E.; Schuster, R. E. *Inorg. Chem.* **1970**, *9*, 391.
- (328) Alei, M. *Inorg. Chem.* **1964**, *3*, 44.
- (329) Akitt, J. W.; Greenwood, N. N.; Khandelwal, B. L.; Lester, G. D. *J. Chem. Soc., Dalton Trans.* **1972**, 604.
- (330) Takahashi, A. *J. Phys. Soc. Jpn.* **1968**, *24*, 657.
- (331) Matwiyoff, N. A.; Darely, P. E.; Movius, W. G. *Inorg. Chem.* **1968**, *7*, 2173.
- (332) Fratiello, A.; Schuster, R. E. *J. Phys. Soc. Jpn.* **1967**, *47*, 1554.
- (333) Swift, T. J.; Fritz, O. G.; Stephenson, T. A. *J. Chem. Phys.* **1967**, *46*, 406.
- (334) Watanabe, I.; Yamagata, Y. *J. Chem. Phys.* **1967**, *46*, 407.
- (335) Fiat, D.; Connick, R. E. *J. Am. Chem. Soc.* **1966**, *88*, 4754.
- (336) Fratiello, A.; Lee, R. E.; Schuster, R. E. *Inorg. Chem.* **1970**, *9*, 82.
- (337) Glass, G. E.; Schwabacher, W. B.; Tobias, R. S. *Inorg. Chem.* **1968**, *7*, 2471.
- (338) Fratiello, A.; Lee, R. E.; Nishida, V. M.; Schuster, R. E. *J. Chem. Phys.* **1969**, *50*, 3624.
- (339) Morgan, L. O. *J. Chem. Phys.* **1963**, *38*, 2788.
- (340) Fratiello, A.; Kubo, V.; Schuster, R. E.; Davis, D. D. *Inorg. Chem.* **1971**, *10*, 744.
- (341) Shannon, R. D.; Prewitt, C. T. *Acta Crystallogr.* **1969**, *B25*, 925.
- Shannon, R. D. *Acta Crystallogr.* **1976**, *A32*, 751.

- (342) Bauschlicher, C. W., Jr.; Langhoff, S. R.; Partridge, H.; Rice, J. E.; Komornicki, A. *J. Chem. Phys.* **1991**, *95*, 5142.
- (343) Hashimoto, K.; Yoda, N.; Iwata, S. *Chem. Phys.* **1987**, *116*, 193.
- (344) Miyanaga, T.; Watanabe, I.; Ikeda, S. *Chem. Lett.* **1988**, 1073.
- (345) Waizumi, K.; Ohtaki, H.; Masuda, H.; Fukushima, N.; Watanabe, Y. *Chem. Lett.* **1992**, 1489.
- (346) Sano, M.; Yamatera, H. *In Ions and Molecules in Solution*; Tanaka, N., Ohtaki, H., Tamamushi, R., Eds.; Elsevier: Amsterdam, 1983; p 109.
- (347) Randales, J. E. B. *Trans. Faraday Soc.* **1956**, *52*, 1573.
- (348) Kanno, H.; Hiraishi, J. *Chem. Phys. Lett.* **1980**, *75*, 553.
- (349) Eigen, M. *Pure Appl. Chem.* **1963**, *6*, 97.
- (350) Mills, R.; Lobo, V. M. *Self-Diffusion in Electrolyte Solutions*; Elsevier: Amsterdam, 1989.
- (351) Hertz, H. G. In *Water—A Comprehensive Treatise*; Franks, F., Ed.; Plenum: New York, 1973; Vol. 6, p 301.
- (352) Basolo, F.; Pearson, R. G. *Mechanisms of Inorganic Reactions*, 2nd ed.; John Wiley & Sons, Inc.: New York, 1967.
- (353) Mills, R. *J. Phys. Chem.* **1973**, *77*, 685.
- (354) Eisenberg, D.; Kauzmann, F. *Structure and Properties of Water*; Clarendon Press: Oxford, 1969.
- (355) Salmon, P. S.; Howells, W. S.; Mills, R. *J. Phys. C: Solid State Phys.* **1987**, *20*, 5727.
- (356) Salmon, P. S.; Herdman, G. J.; Lindgren, J.; Read, M. C.; Sandström, M. *J. Phys.: Condens. Matter* **1989**, *1*, 3459.
- (357) Herdman, G. J.; Salmon, P. S. *J. Am. Chem. Soc.* **1991**, *113*, 2930.
- (358) Stokes, P. H.; Phang, S.; Mills, R. *J. Chem. Solids* **1979**, *8*, 489.
- (359) McCall, D. W.; Douglass, D. C. *J. Phys. Chem.* **1965**, *69*, 2001.
- (360) Hertz, H. G.; Keller, G.; Versmold, H. *Ber. Bunsen-Ges. Phys. Chem.* **1969**, *73*, 549.
- (361) Fortes, J.-M.; Mercer, H.; Molenat, J. *J. Chim. Phys.* **1974**, *71*, 164.
- (362) Endom, L.; Hertz, H. G.; Thül, B.; Zeidler, M. D. *Ber. Bunsen-Ges. Phys. Chem.* **1967**, *71*, 1008.
- (363) Szász, Gy. I.; Riede, W. O.; Heinzinger, K. *Z. Naturforsch.* **1979**, *A34*, 1083.
- (364) Emelyanov, M. I.; Agisher, A. Sh. *Zh. Strukt. Khim.* **1964**, *5*, 670.
- (365) Robinson, R. A.; Stokes, R. H. *Electrolyte Solutions*; Butterworths: London, 1955.
- (366) Tamura, Y.; Tanaka, K.; Spohr, E.; Heinzinger, K. *Z. Naturforsch.* **1988**, *A43*, 1103.
- (367) Tanaka, K.; Nomura, M. *J. Chem. Soc., Faraday Trans. 1* **1987**, *83*, 1779.
- (368) Szász, Gy.; Heinzinger, K. *J. Chem. Phys.* **1983**, *79*, 3467.
- (369) Tanaka, K. *J. Chem. Soc., Faraday Trans. 1* **1975**, *71*, 1127.
- (370) Migliore, M.; Fornili, S. L.; Spohr, E.; Heinzinger, K. *Z. Naturforsch.* **1987**, *A42*, 227.
- (371) Hertz, H. G.; Holz, M.; Mills, R. *J. Chem. Phys.* **1974**, *71*, 1356.
- (372) Hertz, H. G.; Mills, R. *J. Chim. Phys.* **1976**, *73*, 499.
- (373) Rapaport, D. C.; Sheraga, H. A. *J. Phys. Chem.* **1982**, *86*, 873.
- (374) Hertz, H. G.; Tutsch, R.; Versmid, H. *Ber. Bunsen-Ges. Phys. Chem.* **1971**, *75*, 1177.
- (375) Engel, G.; Hertz, H. G. *Ber. Bunsen-Ges. Phys. Chem.* **1968**, *72*, 807.
- (376) Bloembergen, N.; Morgan, L. O. *J. Chem. Phys.* **1961**, *34*, 842.
- (377) Pfeifer, H. *Z. Naturforsch.* **1962**, *A17*, 279.
- (378) Hausser, R.; Noack, F. *Z. Phys.* **1964**, *182*, 93.
- (379) Van der Maarel, J. R. C.; Lankhorst, D.; De Bleijser, J.; Leyte, J. C. *J. Phys. Chem.* **1986**, *90*, 1470.
- (380) Shimizu, A.; Taniguchi, Y. *Bull. Chem. Soc. Jpn.* **1991**, *64*, 221.
- (381) Shimizu, A.; Taniguchi, Y. *Bull. Chem. Soc. Jpn.* **1990**, *63*, 1572.
- (382) Struis, R. P. W. J.; De Bleijser, J.; Leyte, J. C. *J. Phys. Chem.* **1987**, *91*, 1639.
- (383) Shimizu, A.; Taniguchi, Y. *Bull. Chem. Soc. Jpn.* **1991**, *64*, 1613.
- (384) Geiger, A.; Rahman, A.; Stillinger, F. H. *J. Chem. Phys.* **1979**, *70*, 263.
- (385) Swift, T. J.; Connick, R. E. *J. Chem. Phys.* **1962**, *37*, 307.
- (386) Hunt, J. P.; Friedman, H. L. *Prog. Inorg. Chem.* **1983**, *30*, 359.
- (387) Luz, Z.; Shulman, R. G. *J. Chem. Phys.* **1965**, *43*, 3750.
- (388) Salmon, P. S.; Bellisent-Funel, M.-C.; Herdman, G. J. *J. Phys.: Condens. Matter* **1990**, *2*, 4297.
- (389) Fiat, D.; Connick, R. E. *J. Am. Chem. Soc.* **1968**, *90*, 608.
- (390) Chmelnik, A. M.; Fiat, D. N. *J. Magn. Reson.* **1972**, *8*, 325.
- (391) Hunt, J.; Plane, R. A. *J. Am. Chem. Soc.* **1954**, *76*, 5960.
- (392) Dodgen, H. W.; Liu, G.; Hunt, J. P. *Inorg. Chem.* **1981**, *20*, 1002.
- (393) Grant, M.; Jordan, R. B. *Inorg. Chem.* **1981**, *20*, 55.
- (394) Rutenberg, A. C.; Taube, H. *J. Chem. Phys.* **1952**, *20*, 825.
- (395) Takahashi, A. *J. Phys. Soc. Jpn.* **1970**, *28*, 207.
- (396) Hugi-Cleary, D.; Helm, L.; Merbach, A. E. *Helv. Chim. Acta* **1985**, *68*, 545.
- (397) Reuben, J.; Fiat, D. *J. Chem. Phys.* **1969**, *51*, 4918.
- (398) Merbach, A. E. *Pure Appl. Chem.* **1987**, *59*, 161.
- (399) Zetter, M. S.; Lo, G. Y.-S.; Dodgen, H. W.; Hunt, J. P. *J. Am. Chem. Soc.* **1978**, *100*, 4430.
- (400) Ducommun, Y.; Newman, K. E.; Merbach, A. E. *Inorg. Chem.* **1980**, *19*, 3696.
- (401) Chmelnik, A. M.; Fiat, D. N. *J. Chem. Phys.* **1967**, *47*, 3986.
- (402) Zeltmann, A. H.; Matwiyoff, N. A.; Morgan, L. O. *J. Phys. Chem.* **1969**, *73*, 2689.
- (403) Bechtold, D. B.; Liu, G.; Dodgen, H. W.; Hunt, J. P. *J. Phys. Chem.* **1978**, *82*, 333.
- (404) Ducommun, Y.; Earl, W. L.; Merbach, A. E. *Inorg. Chem.* **1979**, *18*, 2754.
- (405) Helm, L.; Elding, L. I.; Merbach, A. E. *Inorg. Chem.* **1985**, *24*, 1719.
- (406) Gröning, Ö.; Drakenberg, T.; Elding, L. I. *Inorg. Chem.* **1982**, *21*, 1820.
- (407) Hugi-Cleary, D.; Helm, L.; Merbach, A. E. *J. Am. Chem. Soc.* **1987**, *107*, 4444.
- (408) Hugi, A. D.; Helm, L.; Merbach, A. E. *Helv. Chim. Acta* **1985**, *68*, 508.
- (409) Xu, F.-C.; Krouse, H. R.; Swaddle, T. W. *Inorg. Chem.* **1985**, *24*, 267.
- (410) Swaddle, T. W.; Merbach, A. E. *Inorg. Chem.* **1981**, *20*, 4212.
- (411) Cossy, C.; Helm, L.; Merbach, A. E. *Inorg. Chem.* **1988**, *27*, 1973.
- (412) Cossy, C.; Helm, L.; Merbach, A. E. *Inorg. Chem.* **1989**, *28*, 2699.
- (413) Price, W. E.; Woolf, L. A.; Harris, K. R. *J. Phys. Chem.* **1990**, *94*, 5109.
- (414) Weingärtner, H.; Müller, K. J.; Hertz, H. G.; Edge, A. V. J.; Mills, R. *J. Phys. Chem.* **1984**, *88*, 2173.
- (415) Friedman, H. L. *Chim. Scripta* **1985**, *25*, 42.
- (416) Private communication.
- (417) Ohtaki, H.; Funahashi, S.; Inada, Y.; Nakajima, K.; Tabata, M.; Ozutsumi, K. To be published.